Chapter 1
The Standard Model of Disc Accretion

Galina Lipunova, Konstantin Malanchev, and Nikolay Shakura

Abstract Accretion discs are powerful energy factories in our Universe. They effectively transform the potential energy of gravitational interaction to emission, thereby unraveling the physics of distant objects. This is possible due to the presence of viscosity, driven by turbulent motions in accretion discs. In this chapter, we describe the equations for disc accretion in the framework of the standard model. We outline basic elements of the theory of turbulent viscosity and the emergence of the α-parameter. We further describe the radial and vertical structure of thin stationary accretion discs, and present analytical solutions to the basic equation of the evolution of a viscous accretion disc for both an infinite disc and for a disc in a binary system. Finally, we present a numerical method to solve the equations of disc evolution and vertical structure simultaneously.

1.1 Introduction

The theory of disc accretion has tremendously broad applications in astrophysics—it is used to study for example bright objects at a wide spectral range in our own Galaxy, the luminous centres of other active galaxies, relativistic jets from compact objects, protostars and the formation of planetary systems, and to explain the most luminous sources of the universe, the gamma-ray bursts.

G. Lipunova (✉)
Sternberg Astronomical Institute, Lomonosov Moscow State University, Moscow, Russia
e-mail: galja@sai.msu.ru

K. Malanchev
Sternberg Astronomical Institute, Lomonosov Moscow State University, Moscow, Russia
e-mail: malanchev@sai.msu.ru

National Research University Higher School of Economics, Moscow, Russia

N. Shakura
Sternberg Astronomical Institute, Lomonosov Moscow State University, Moscow, Russia

Kazan Federal University, Kazan, Russia

N. Shakura (ed.), *Accretion Flows in Astrophysics*, Astrophysics and Space Science Library 454, https://doi.org/10.1007/978-3-319-93009-1_1

The bases for the theory of standard disc accretion are found in the papers by Shakura (1973) and Shakura and Sunyaev (1973). Other important early works include the papers by Gorbatskii (1965), Lynden-Bell (1969), and Pringle and Rees (1972). The development of the theories for the various processes connected to disc accretion can be found in the textbooks by Kato et al. (1998), Frank et al. (2002) and in the overview by Abramowicz and Fragile (2013). Galactic discs, discs in close binaries and in protoplanetary systems are discussed in the textbook by Morozov and Khoperskov (2005). Bisikalo et al. (2013) studied the gas dynamics of mass-transfer in close binary systems. A short and comprehensive overview of standard disc accretion, including aspects of discs in dwarf and X-ray novae, can be found in Lasota (2015).

In this chapter we consider the basic properties of stationary and non-stationary discs in the framework of the standard model of disc accretion, touching only lightly upon relativistic effects. We derive the basic equations describing non-radial infall of matter in astrophysical situations, where the effects of viscous stresses lead to heating of the matter and subsequent emission of thermal energy that can be observed by astronomical instruments from enormous distances.

Discs are formed around stars as a result of matter with non-zero angular momentum being captured by the star's gravitational field. The matter may originate from the interstellar medium or be transferred from a close companion star. If the matter is rotating in approximately a single plane, the structure is called an accretion disc. As a result of transfer of angular momentum the matter moves towards the central object and thereby releases its gravitational energy. This energy is transferred to kinetic energy, increasing towards the centre, and to thermal energy of the plasma. If the thermal energy can be emitted effectively, the disc is relatively thin.

We here consider geometrically thin 'flat' accretion discs. In a geometrically thin disc, the half-thickness in the direction perpendicular to the disc plane is much smaller than the distance to the centre at a given point in the disc. If a geometrically thin disc has an optical depth much exceeding unity ($\tau \gg 1$) in the direction perpendicular to the disc plane, the equations of energy balance can be written in a rather simple form. In this case the photons are absorbed and dissipated or scattered many times before they leave the disc and we can assume local thermodynamic equilibrium. In a geometrically thin disc we may also neglect radial advection (the transfer of heat with matter moving radially). The condition of local thermodynamic equilibrium suggests equal temperature of electrons and ions in the plasma. Moreover, the standard models do not take into account mass loss from the disc surface: the matter leaves the disc only through its inner boundary. In reality, or rather in the current largely consistent picture of accretion discs, these conditions are satisfied at distances far from the disc centre.

It is important to note that the accretion process is driven by viscosity caused by turbulent motions of the matter in the disc. The characteristic time scale for changes in the radial structure of the disc is called the viscous time scale. The viscous time scale is related to the radial motion of matter in the disc. In the framework of the standard equations for accretion discs, discussed in this section, the characteristic viscous time scale $\tau_{\rm vis}$ is much longer than the dynamic time scale $\tau_{\rm dyn}$, set by the orbital velocity of matter in the disc. The viscous time scale is also much longer

than the 'hydrostatic' time scale $\tau_{\rm hyd}$, on which the thickness of the disc changes with pressure, and much longer than the 'thermal' time scale $\tau_{\rm th}$, that is, the time for a given patch of the disc to radiate the stored thermal energy and to change the temperature:

$$\tau_{\rm vis} \gg \tau_{\rm dyn}\,; \quad \tau_{\rm vis} \gg \tau_{\rm hyd}\,; \quad \tau_{\rm vis} \gg \tau_{\rm th}\,.$$

As in stars, the disc equilibrium structure depends on its luminosity. For a wide range of accretion rates, the disc luminosity is proportional to the rate with which matter flows into the disc. There is, however, a critical luminosity close to which radiation pressure starts to play a decisive role for the formation of the disc structure. This is the Eddington luminosity limit. Like in stars, the Eddington luminosity is determined from the balance between the forces of radiation pressure and gravitational forces acting on the proton. In the case of spherical symmetry:

$$L_{\rm Edd} = \frac{4\,\pi\,c\,G\,M\,m_{\rm p}}{\sigma_{\rm T}} \approx 1.25 \times 10^{38}\,\frac{M}{M_\odot}\,{\rm erg/s}\,. \tag{1.1}$$

We use the following notations: the universal gravitational constant G, the mass of the central body M, the mass of the Sun $M_\odot \approx 2 \times 10^{33}\,{\rm g}$, the proton mass $m_{\rm p}$, the Thomson cross section for electron scattering $\sigma_{\rm T}$. Using the expression for the effective luminosity in the accretion process $L = \eta_{\rm accr}\,\dot{M}\,c^2$, we obtain the critical accretion rate in the disc:

$$\dot{M}_{\rm Edd} = \frac{4\,\pi\,G\,M}{c\,\eta_{\rm accr}\,\kappa_{\rm T}} \approx 1.4 \times 10^{18}\,\frac{M}{M_\odot}\,{\rm g/s}\,,$$

where we have set the energy conversion efficiency of accretion $\eta_{\rm accr} = 0.1$ ($\eta_{\rm accr} = 1/12$ in the Newtonian metric for a disc with the inner boundary at radius $6\,G\,M/c^2$), and the Thomson cross section per gram $\kappa_{\rm T} \approx 0.4\,{\rm cm^2/g}$. In disc models the accretion rate is often normalised to this value. However, it is only an approximate evaluation of the accretion rate, above which the disc becomes thick. The thin disc approximation is no longer valid in a region, the radius of which is proportional to the accretion rate, and this region may experience outflow of material from the disc surface.

Various disc instabilities may arise at accretion rates lower than the critical one. For example, at temperatures and densities corresponding to the conditions for recombination of ions in the plasma, thermal instability arises which results in a change in the vertical structure of the disc on thermal time scales (Meyer and Meyer-Hofmeister 1981). In particular, this instability leads to outbursts in dwarf novae. Close to the disc centre, if the radiation pressure exceeds the gas pressure, viscous and thermal instabilities arise (Lightman and Eardley 1974; Shibazaki and Hōshi 1975; Shakura and Sunyaev 1976). Nevertheless, there exists a wide range of accretion rates at which the structure of the accretion disc can be treated as quasi stationary.

1.2 Disc Equations

When examining geometrically thin discs, it is convenient to work in cylindrical coordinates (r, φ, z). We assume that accretion discs are axially symmetric. This leads to the disappearance of all derivatives with respect to φ. For thick discs or for a study of the structure of outflowing matter, spherical coordinates should be used.

1.2.1 Important Note

In the standard theory of disc accretion, as we outline it here following Shakura and Sunyaev (1973), the viscous stress tensor is frequently written as a physically positive value. In Chap. 1 this value appears under notation $w^{\mathrm{t}}_{r\varphi} = -w_{r\varphi}$.

1.2.2 Continuity Equation

The continuity equation in cylindrical coordinates in the axial symmetric case takes the form:

$$\frac{\partial \rho}{\partial t} + \frac{1}{r}\frac{\partial}{\partial r}(\rho\, v_r\, r) + \frac{\partial}{\partial z}(\rho\, v_z) = 0\,. \tag{1.2}$$

1.2.3 Equations of Motion

The equations of motion in cylindrical coordinates in the axial symmetric case are written as:

$$\frac{\partial v_r}{\partial t} + v_r\frac{\partial v_r}{\partial r} + v_z\frac{\partial v_r}{\partial z} - \frac{v_\varphi^2}{r} = -\frac{\partial \Phi}{\partial r} - \frac{1}{\rho}\frac{\partial P}{\partial r} + N_r, \tag{1.3}$$

$$\frac{\partial v_\varphi}{\partial t} + v_r\frac{\partial v_\varphi}{\partial r} + v_z\frac{\partial v_\varphi}{\partial z} + \frac{v_r v_\varphi}{r} = N_\varphi, \tag{1.4}$$

$$\frac{\partial v_z}{\partial t} + v_r\frac{\partial v_z}{\partial r} + v_z\frac{\partial v_z}{\partial z} = -\frac{\partial \Phi}{\partial z} - \frac{1}{\rho}\frac{\partial P}{\partial z} + N_z, \tag{1.5}$$

where Φ is the gravitational potential, P is the pressure, and N_r, N_φ, and N_z are the components of the viscous force $\boldsymbol{N}$ per unit mass. We write the components of $\boldsymbol{N}$ in

the case of axial symmetry as:

$$\rho N_r = \frac{1}{r}\frac{\partial}{\partial r}(r w_{rr}) - \frac{w_{\varphi\varphi}}{r} + \frac{\partial w_{rz}}{\partial z}, \tag{1.6}$$

$$\rho N_\varphi = \frac{1}{r^2}\frac{\partial}{\partial r}(r^2 w_{\varphi r}) + \frac{\partial w_{\varphi z}}{\partial z}, \tag{1.7}$$

$$\rho N_z = \frac{1}{r}\frac{\partial}{\partial r}(r w_{zr}) + \frac{\partial w_{zz}}{\partial z}, \tag{1.8}$$

where w_{ik} are the components of the viscous stress tensor. We write these components:

$$w_{rr} = 2\eta\frac{\partial v_r}{\partial r} + \left(\zeta - \frac{2}{3}\eta\right)\operatorname{div}\boldsymbol{v}, \tag{1.9}$$

$$w_{r\varphi} = w_{\varphi r} = \eta\left[r\frac{\partial}{\partial r}\left(\frac{v_\varphi}{r}\right)\right], \tag{1.10}$$

$$w_{rz} = w_{zr} = \eta\left(\frac{\partial v_z}{\partial r} + \frac{\partial v_r}{\partial z}\right), \tag{1.11}$$

$$w_{\varphi\varphi} = 2\eta\frac{v_r}{r} + \left(\zeta - \frac{2}{3}\eta\right)\operatorname{div}\boldsymbol{v}, \tag{1.12}$$

$$w_{\varphi z} = w_{z\varphi} = \eta\frac{\partial v_\varphi}{\partial z}, \tag{1.13}$$

$$w_{zz} = 2\eta\frac{\partial v_z}{\partial z} + \left(\zeta - \frac{2}{3}\eta\right)\operatorname{div}\boldsymbol{v}\,, \tag{1.14}$$

where

$$\operatorname{div}\boldsymbol{v} = \frac{1}{r}\frac{\partial}{\partial r}(r v_r) + \frac{\partial v_z}{\partial z}.$$

Here η is the dynamic coefficient of the shear viscosity due to the relative motion of different layers of the flow, and ζ is the second viscosity (Landau and Lifshitz 1959). In the following, we will omit the effects of second viscosity.

For thin accretion discs, the only significant component of the viscous stress tensor is $w_{r\varphi}$. As a result we have that

$$\rho N_\varphi = \frac{1}{r^2}\frac{\partial}{\partial r}(r^2 w_{r\varphi}), \tag{1.15}$$

$$w_{r\varphi} = \eta r\frac{\partial}{\partial r}\frac{v_\varphi}{r} = \eta r\frac{\partial\omega}{\partial r}, \tag{1.16}$$

where $\omega = v_\varphi/r$ is the angular velocity of matter in the disc.

We will consider thin stationary discs for which the partial derivatives with respect to time in the equation of motion (1.3)–(1.5) become zero. For such discs the most important terms in Eq. (1.3) are v_φ^2/r and the gravitational potential gradient. For a Newtonian gravitational potential $\Phi = -GM/r$, neglecting the self-gravitation of the disc, we obtain Kepler's law:

$$\omega_\mathrm{K} = \sqrt{\frac{GM}{r^3}}. \tag{1.17}$$

In this case the radial component of the friction force and the pressure gradient are negligible comparing to the gravitational force from the central body.

In the direction perpendicular to the disc plane, hydrostatic equilibrium is established, in which the vertical gravity component is balanced by the vertical pressure gradient. From (1.5) we have:

$$-\frac{1}{\rho}\frac{\partial P}{\partial z} = \frac{G\,M}{r^3}\,z\,. \tag{1.18}$$

1.2.4 Energy Conservation Equation

The energy conservation equation for the general case is written in the following way (Landau and Lifshitz 1959; Kato et al. 2008):

$$\frac{\partial E}{\partial t} + \mathrm{div}\Big[(E+P)\,\boldsymbol{v} - (\boldsymbol{v}\,w_{ik}) + \boldsymbol{F}_\mathrm{th}\Big] = \rho\epsilon_\mathrm{mass}\,, \tag{1.19}$$

where $E = \rho\,(e + v^2/2 + \Phi)$ is the sum of the thermal, kinetic and potential energy per unit volume. Its change over time is a result of the energy flux arising due to motion of the medium, the work of pressure and viscosity forces, and other possible energy flows. In a thin plane disc, the energy flux connected to viscous forces is radial and equals $(-v_\varphi\,w_{r\varphi})$. The vector $\boldsymbol{F}_\mathrm{th}$ contains other types of thermal energy flows: radiative, conductive and convective. In a thin disc the main contribution is given by F_z, which includes the radiative flux transferring energy to the radiating disc surface. In general, there could be other heating or cooling mechanisms operating within a unit volume (for example, nuclear reactions, Joule dissipation or radiative cooling of the optically thin medium). The rate of such heating or cooling per unit mass is ϵ_mass.

1.2.5 Energy Dissipation

Let us consider the change of kinetic energy in the flow expressing the total velocity derivative with the help of the Navier-Stokes equation (Eqs. (1.3)–(1.5)):

$$\frac{\mathrm{d}}{\mathrm{d}t}\left(\frac{v^2}{2}\right) = \boldsymbol{v}\left(-\nabla\Phi - \frac{1}{\rho}\nabla P + \boldsymbol{N}\right). \tag{1.20}$$

Subtracting this equation from the equation for the total energy conversion (1.19) and using the first law of thermodynamics

$$T\,\mathrm{d}s = \mathrm{d}e + P\,\mathrm{d}\left(\frac{1}{\rho}\right),$$

where s is the specific entropy, we arrive at the following equation for the thermal balance:

$$\rho\, T\,\frac{\mathrm{d}s}{\mathrm{d}t} = \varepsilon + \rho\,\epsilon_{\mathrm{mass}} - \mathrm{div}\boldsymbol{F}_{\mathrm{th}}\,, \tag{1.21}$$

for a gravitational potential Φ constant in time, where

$$\varepsilon = w_{ik}\frac{\partial v_i}{\partial x_k} \tag{1.22}$$

is the dissipated energy per unit volume per unit time due to viscosity (summation over indices).

In cylindrical coordinates for an axisymmetric flow:

$$\varepsilon = \eta\left[4\left(\frac{\partial v_r}{\partial r}\right)^2 + 2\left(\frac{\partial v_z}{\partial z}\right)^2 + \left(\frac{\partial v_\varphi}{\partial r} - \frac{v_\varphi}{r}\right)^2 + \left(\frac{\partial v_\varphi}{\partial z}\right)^2 + \right.$$
$$\left. + \left(\frac{\partial v_z}{\partial r} + \frac{\partial v_r}{\partial z}\right)^2\right] - \frac{2}{3}\eta\left(\frac{\partial v_r r}{r\partial r} + \frac{\partial v_z}{\partial z}\right)^2. \tag{1.23}$$

In thin accretion discs, v_φ dominates significantly over other velocity terms. We note that v_φ does not change with z in a thin disc. Thus, the dominant component in the energy dissipation has the form:

$$\varepsilon = w_{r\varphi}\left(\frac{\partial v_\varphi}{\partial r} - \frac{v_\varphi}{r}\right) = \eta\left(\frac{\partial v_\varphi}{\partial r} - \frac{v_\varphi}{r}\right)^2 = \eta\, r^2\left(\frac{\partial \omega}{\partial r}\right)^2. \tag{1.24}$$

1.2.6 Energy Source in the Disc

The main source of energy which dissipates in the disc due to friction, and which in principle can be radiated, is the released potential energy as the matter moves progressively closer to the gravitating body. Let us illustrate this for a thin Keplerian disc.

With the help of expressions (1.7), (1.10) and (1.24), it can be shown that the identity

$$\rho\, v_\varphi\, N_\varphi + \varepsilon\, = \frac{1}{r}\,\frac{\partial}{\partial r}(r\, v_\varphi\, w_{r\varphi})\,. \tag{1.25}$$

holds in a thin disc.

To write down $\rho\, v_\varphi\, N_\varphi$, we use (1.20). Let the mass of the central object and its gravitational potential be constant in time. We have:

$$\rho\, v_r\, \frac{\partial}{\partial r}\Big(\frac{v^2}{2} + \Phi\Big) = \frac{1}{r}\frac{\partial (r\, v_\varphi\, w_{r\varphi})}{\partial r} - \varepsilon. \tag{1.26}$$

Here, we omit the term $v_r\, \partial P/\partial r$, which is small compared to the other terms, i.e. we neglect the work performed by pressure forces in a Keplerian disc.

And thus, the energy from the gravitational interaction extracted as the matter moves in the disc progressively towards the centre is transformed to kinetic energy of orbital motion, then redistributed in the disc due to viscous forces transferring angular momentum, and finally spent on heating of the disc (Lynden-Bell and Pringle 1974; Shakura and Sunyaev 1976).

1.3 Viscosity in Accretion Discs

The key hypothesis in models for accretion discs is the turbulent nature of their viscosity (Shakura 1973; Shakura and Sunyaev 1973; Zeldovich 1981; Fridman 1989; Dubrulle 1993; Balbus and Hawley 1998; Richard and Zahn 1999; Bisnovatyi-Kogan and Lovelace 2001; Marov and Kolesnichenko 2011). The values of the coefficients of molecular viscosity obtained from studies of the properties of liquids and gases cannot explain the observed properties of astrophysical discs. The required rate of transfer of mass towards the disc centre and the accompanying outward transfer of momentum can be explained only for very high values of viscosity in the disc matter, exceeding the molecular viscosity by several orders of magnitude. Turbulent motions of the matter may lead to significant stresses $w_{r\varphi}$ in the disc. In addition, the Reynolds number for accretion discs is very large and this in itself may serve as a basis for development of turbulence regardless of the specific mechanisms for it occurrence.

Differential rotation in Keplerian gaseous discs is considered the basic source of their turbulence. The angular momentum transfer by small-scale magnetic fields in accretion discs was suggested in Shakura and Sunyaev (1973). In the late 1950s and early 1960s, Velikhov (1959) and Chandrasekhar (1960) discovered the MHD-instability in shear flows with angular velocity falling outwards in the existence of a seed poloidal magnetic field. The importance of this instability for accretion discs was shown in the calculations by Balbus and Hawley (see the reviews by Balbus and Hawley (1991, 1998)). Disc accretion with the presence of magnetic fields was studied by many authors (see, for example, Eardley and Lightman 1975; Galeev et al. 1979; Coroniti 1981; Tout and Pringle 1992; Brandenburg et al. 1996).

At the present stage of development of theories of accretion discs, there is no full consensus regarding how to express viscous stresses in a viscous flow. Most authors describe the action of a small scale viscosity by a phenomenological α-prescription (Shakura 1973; Shakura and Sunyaev 1973).

In Sect. 1.2 it was assumed that the derived equations describe the average large-scale motions in the gas. Turbulence arises as a result of transfer of part of the energy of the large-scale motions to random perturbations on smaller scales. In general, such chaotic perturbations in the flow have a very complicated structure and an individual description does not seem possible. Numerical solutions to the associated non-linear equations cannot be achieved at present due to the unreasonably large computational power needed for such a task, and an analytical solution to the general spatially-unbounded problem with smooth initial conditions have not been found either. A solution to the Navier-Stokes equations is one of the seven Millennium Goals announced in 2000 by the Clay Mathematical Institute. In applied problems, methods based on various approximations are mainly used, for example the Reynolds method of averaging or large-eddy simulations (Deardorff 1970).

1.3.1 The Reynolds Equations and the Reynolds Tensor

Reynolds suggested a decomposition of the hydrodynamic fields in the real medium into two components: an average field and a fluctuating (chaotic) field, followed by an averaging of the equations. For example, for the velocity components we assume $v_i = \overline{v_i} + v_i'$, for the pressure $p = \overline{p} + p'$, etc. The average fields are always smooth and slowly changing. The fluctuating fields are chaotic in both space and time. Note that elsewhere in this chapter, we will use ρ without a bar for the local averaged density of the turbulized matter.

Averaging the Navier-Stokes equations according to the rules suggested by Reynolds leads to equations of motion for the average quantities—the Reynolds equations. The method of averaging is not very important. It may be over time, in space, or it may be a theoretical average over a statistical ensemble of various hydrodynamic flows with common boundary conditions (Monin and Yaglom 1971). Average quantities over space and time converge to theoretic-probabilistic mean

values if the random process is stationary and spatially homogeneous. The second condition is always a mathematical idealization. In practice, we can only talk about homogeneity in some limited space and time domain. The general condition for convergence of the values that are averaged over space and time to probabilistic mean values is the condition of ergodicity.

Let us write down the Navier-Stokes equation in tensor notation:

$$\rho \left(\frac{\partial v_i}{\partial t} + v_k \frac{\partial v_i}{\partial x_k} \right) = f_i - \frac{\partial \left(P \, \delta_{ik} \right)}{\partial x_k} + \frac{\partial w_{ik}}{\partial x_k} , \tag{1.27}$$

where f_i are the components of an external force acting on a unit volume of matter.

For an incompressible fluid ($\rho = const$) we use the equalities

$$\frac{\partial v_k}{\partial x_k} = 0 \qquad \text{and} \qquad \frac{\partial \left(v_i \, v_k \right)}{\partial x_k} = v_k \frac{\partial v_i}{\partial x_k} ,$$

in particular, replacing the second term on the left in (1.27) with $\partial (v_i \, v_k)/\partial x_k$.

We perform averaging according to the Reynolds rules (Monin and Yaglom 1971, their chapter 2), part of which looks like the following:

$$\overline{f'} = 0 , \quad \overline{\frac{\partial f}{\partial x}} = \frac{\partial \overline{f}}{\partial x} , \quad \overline{v_i \cdot v_k} = \overline{v_i} \cdot \overline{v_k} + \overline{v_i' \cdot v_k'} .$$

The average mass transfer due to turbulent motions is zero: $\overline{\rho \, v_i'} = 0$.

In the Reynolds-averaged Navier–Stokes equation, we find the appearance of an additional term dependent on the pulsating velocity (with a prime) arising due to the non-linearity of the original equation:

$$\rho \left(\frac{\partial \, \overline{v_i}}{\partial t} + \frac{\partial \, \overline{v_i \, v_k}}{\partial x_k} + \frac{\partial \, (\overline{v_i' v_k'})}{\partial x_k} \right) = \overline{f_i} - \frac{\partial \, (\overline{P} \, \delta_{ik})}{\partial x_k} + \frac{\partial \overline{w_{ik}}}{\partial x_k} .$$

To find out the meaning of the last term, we consider the average flow of momentum:

$$\overline{\Pi_{ik}} = \overline{P} \, \delta_{ik} + \rho \, \overline{v_i \, v_k} - (\overline{w_{ik}} - \rho \, \overline{v_i' v_k'}) . \tag{1.28}$$

The two first terms on the right-hand side are responsible for the reversible (mechanical) transfer of momentum by the average motion.

We see that for turbulent motion, the viscous tensor, dependent on the properties of the medium, is accompanied by the term connected with chaotic flows. Thus, turbulent motions lead to exchange of momentum between different regions of the fluid. In other words, turbulent mixing acts like viscosity. The following way of

writing the Reynolds equations emphasizes this interpretation:

$$\frac{\partial \overline{v_i}}{\partial t} + \overline{v_k} \frac{\partial \overline{v_i}}{\partial x_k} = \overline{f_i} - \frac{1}{\rho} \frac{\partial \left(\overline{P} \, \delta_{ik} \right)}{\partial x_k} + \frac{\partial}{\partial x_k} \left(\eta \frac{\partial \overline{v_i}}{\partial x_k} - \overline{v_i' v_k'} \right) . \tag{1.29}$$

Here, we use the expression for the viscous stress tensor in an incompressible fluid $w_{ik} = \eta \left(\partial v_i / \partial x_k + \partial v_k / \partial x_i \right)$ (see, for example, Chapter 2 in Landau and Lifshitz 1959) and apply the incompressibility condition of the fluid.

The quantity

$$R_{ik} = -\rho \, \overline{v_i' \, v_k'} \tag{1.30}$$

is called the Reynolds tensor for turbulent viscosity. The form of this term is unknown and we should make more or less empirically based assumptions to solve the Reynolds equations. The main problem of the phenomenological theory of turbulence is finding the unknown turbulent flows (flow of momentum for the equations above) expressed in the averaged parameters of the properties of the medium. This problem is referred to as a closure problem.

1.3.1.1 Compressible Fluids

In the case of a compressible fluid, instead of the Reynolds average, the weighted average as suggested by Favre (1969) is used. The weighted average velocity is equal to $\widetilde{v_i} = \overline{\rho \, v_i} / \overline{\rho}$, where bars over the values indicate the Reynolds average (time average). The velocity of the flow is then represented by the sum of the weighted average and the fluctuating velocities: $v_i = \widetilde{v_i} + v_i''$. Now $\overline{v_i''} \neq 0$ (average over the ensemble) for $\widetilde{v_i''} = 0$ (weighted average, average over the ensemble), but, as before, the turbulent motions do not lead to transfer of mass, $\overline{\rho v_i''} = 0$ (see, for example, Marov and Kolesnichenko 2011, their chapter 3).

After such a representation of the hydrodynamic functions and averaging over time of the Navier-Stokes equation for $\rho \neq const$, we arrive at an equation of motion, which also can be written in compact form, analogous to (1.29), but with an additional term, which corresponds to the turbulent viscosity, of a more complicated form:

$$R_{ik}^{*} = -\overline{\rho v_i'' v_k''} + \eta \left(\frac{\partial \overline{v_i''}}{\partial x_k} + \frac{\partial \overline{v_k''}}{\partial x_i} - \frac{2}{3} \delta_{ik} \frac{\partial \overline{v_k''}}{\partial x_k} \right) . \tag{1.31}$$

We ignore here fluctuations in the coefficient of molecular viscosity η. Thus, if density fluctuations are present in the medium, the viscosity tensor cannot be divided into two constituents, one dependent on the properties of the environment only (the viscosity η and the average velocity $\overline{v_i}$ of the laminar flow) and the other dependent

only on the turbulent dynamics of the flow (terms with fluctuating velocity). It is expected, however, that the second term in the last expression, the term that includes the molecular viscosity, is significantly smaller than the first term (Pletcher et al. 1997).

1.3.2 The Closure Problem

The form of the Reynolds tensor cannot be found from the hydrodynamic equations. The second-order moment tensors for the velocity field $\overline{v_i' v_k'}$ can be expressed from the third- or higher-order moments ($\overline{v_i' v_j' v_k'}$, etc.), but the number of unknowns is always greater than the number of equations. The impossibility of finding a closed system of equations for a finite number of moments is a consequence of the non-linearity of the equations of hydrodynamics. In the case of weighted averaging, the problem becomes even more complicated (Marov and Kolesnichenko 2011, their chapter 3).

The need to solve practical problems have led to the performance of a large number of experiments regarding turbulent flows. Based on these studies, semi-empirical theories of turbulence have been worked out, which systematize the obtained results.

Important steps in this direction were taken by Boussinesq (in the end of the nineteenth century) and by Taylor, Prandtl and Karman in the 1920s and 1930s. The semi-empirical models of turbulence are based on the analogy between turbulence and molecular viscosity. An application of the simplest models allows us to close the very first equations for hydrodynamic fields—the ones for lower moments (the Reynolds equations). As a result, the Reynolds equations can be solved if R_{ik} is expressed from certain large-scale characteristics of the flow. These characteristics describe the transfer of heat and momentum through the turbulent medium. Large-scale characteristics of turbulence are to a great deal dependent on the geometry of the boundaries of the flow and the nature of external influences, which are always different in different situations. Therefore, on the one hand, we talk about the ambiguity of semi-empirical closing relations. On the other hand, using more complex closing relations leads to neither more general nor more exact solutions. Thus, in most cases, preference is given to the simpler models, and the limits to their applicability are studied (see Marov and Kolesnichenko 2011, their Sect. 1.1.6).

1.3.3 Coefficient of Turbulent Viscosity

The Reynolds equations can be solved only with the addition of closing relations, which use the averaged characteristics of the turbulent flow (pressure, density, temperature, and average velocity). This is the way semi-empirical models for

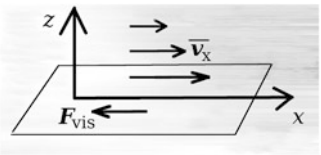

Fig. 1.1 Coordinates in a plane flow

turbulence are constructed. Most of these models are based on Boussinesq's gradient hypothesis (1897) which suggests that there is a linear connection between the turbulent viscous tensor and the shear tensor which in turn is a linear combination of the terms $\partial \bar{v}_j / \partial x_i$ together with certain local proportionality coefficients (coefficients of turbulent transfer). It is, however, necessary to make concrete assumptions regarding these coefficients.

Let us consider a small area inside a turbulent flow (Fig. 1.1). We consider this area to be flat and assume that the average motion is directed along the plane of the area (along the x-axis). Let the area be located in the plane $z = 0$. The frictional force acting on a unit area, directed along the x-axis is equal to:

$$\overline{w_{xz}} - \rho \, \overline{v_x' v_z'} = \rho \, \nu \, \frac{\partial \overline{v_x}}{\partial z} - \rho \, \overline{v_x' v_z'} \, .$$

According to what is called Bussinesq's gradient hypothesis, there is an analogy between the viscous and the turbulent flow of momentum and we may set:

$$- \rho \, \overline{v_x' v_z'} = \rho \, \nu_t \, \frac{\partial \overline{v_x}}{\partial z} \, , \tag{1.32}$$

introducing the proportionality constant ν_t. This approach allows us to solve the Reynolds equations using standard methods if we know the kinematic coefficient of turbulent viscosity ν_t that replaces the usual coefficient of molecular viscosity. The turbulent viscosity coefficient cannot be derived from microscopic considerations.

The gradient model works well for quasi-stationary flows. It is assumed that a local equilibrium is formed in the structure of developed turbulence, in which the characteristics of turbulence at every point of the flow are completely determined by the local characteristics of the field of the averaged flow in the vicinity of this point and by the local averaged parameters of the state of the medium itself.

In general, ν_t is significantly larger than ν. The turbulent viscosity coefficient, as opposed to the molecular viscosity coefficient, does not describe the physical properties of the fluid but the statistical properties of the fluctuations. Its value depends on the method of averaging over the ensemble of analogous flows. A semi-empirical model of turbulence can be constructed if ν_t is estimated in the course of experiments. For example, it is known that in the case of motion of a turbulent flow in a plane channel, ν_t cannot be constant since it has been established empirically that $\nu_t \to 0$ close to the walls. In an infinite turbulent flow, however, it is often quite reasonable to assume that $\nu_t = const$ (see Sect. 5.8 in Monin and Yaglom 1971).

And thus, we moved from the unknown Reynolds tensor to the turbulent viscosity coefficient, which is also unknown. Choosing this parameter is another separate task and, to solve it, other semi-empirical theories have been proposed in turn. These theories, in particular, use the concept of mixing length. This concept plays an important role in the theory of turbulent viscosity in accretion discs.

1.3.4 Mixing Length

The concept of mixing length introduced by Prandtl to the theory of turbulence (1925) allows us not only to express simply the coefficients of turbulent mixing (in particular, the turbulent viscosity coefficient), using the length of the mixing path, but also to obtain defining relations for turbulent flows in some particular cases. The mixing length is the distance which a unit volume of gas travels in a turbulent flow before this volume is mixed completely with the surrounding medium. This distance is in a sense analogue to the mean free path in kinetic gas theory.

Turbulent stresses are the result of transfer of momentum due to fluctuations of turbulent velocity. Prandtl's hypothesis is that vortices, shifting as 'trickles' along the z-axis for the path of the 'mixing length' ξ_z', retain their momentum. This is similar to the picture of turbulent diffusion of impurities. At the height $z + \xi_z'$, a fluctuation v_x' may be represented as the difference between the proper velocity of a trickle $\overline{v}_x(z)$ (the average velocity at the initial level) and the velocity of the surrounding flow $\overline{v}_x(z + \xi_z')$. Linearization of the profile of the average velocity $\overline{v}_x$ yields: $\overline{v_x}(z + \xi_z') = \overline{v_x}(z) + \xi_z' \, \partial\overline{v_x}/\partial z$. We thus write the Prandtl relation for transfer of momentum as:

$$v_x' = -\xi_z' \, \partial\overline{v_x}/\partial z \, . \tag{1.33}$$

In the case of a plane shear flow, we get for the component of the Reynolds tensor (1.30):

$$R_{xz} \equiv -\rho \, \overline{v_x' \, v_z'} = \rho \, \overline{\xi_z' \, v_z'} \, \frac{\partial \overline{v_x}}{\partial z} \, . \tag{1.34}$$

If we define the kinematic coefficient of turbulent viscosity as

$$\nu_\mathrm{t} = \overline{\xi_z' \, v_z'} \, , \tag{1.35}$$

formula (1.34) is terminologically consistent with the gradient hypothesis (See expression (1.32)). Formula (1.35) is similar to the formula for the molecular viscosity coefficient: $\nu = l_\mathrm{m} v_\mathrm{m}$, where l_m is the mean free path of the molecules and v_m is the velocity of their thermal motion. The 'amount of exchange' in a turbulent flow ν_t is also a product of the distance and velocity at which turbulent exchange takes place—the mixing speed. The value of ξ_z' is essentially a random (fluctuating) quantity.

In order for formula (1.34) to be applied in practice, the mixing speed v_z' should also be estimated, which Prandtl does (1925). As a result of mixing, the mixing speed itself should decrease as the conditions (velocities) in the medium are leveled out. From this follows the assumption that the mixing speed should be proportional to the velocity gradient of the average motion $\partial\overline{v_x}/\partial z$. This simultaneously means that the fluctuations of velocity in different directions have similar absolute values, i.e. $v_z' \sim v_x'$ (Monin and Yaglom 1971).

We thus use (1.33), substituting in (1.34), and obtain:

$$R_{xz} = \rho\,\overline{(\xi_z')^2}\left|\frac{\partial\overline{v_x}}{\partial z}\right|\frac{\partial\overline{v_x}}{\partial z},$$

where the modulus is inserted in order that the sign of the turbulent viscosity tensor be the same as for $\partial\overline{v_x}/\partial z$. This corresponds to the fact that momentum is transferred from layers moving faster to those moving more slowly. Then for the kinematic coefficient of the turbulent viscosity we obtain the Prandtl formula (1925):

$$\nu_\mathrm{t} = \alpha^*\,L^2\left|\frac{\partial\overline{v_x}}{\partial z}\right|, \tag{1.36}$$

where α^* is a dimensionless quantity of the order of 1. The local mixing path ξ_z' is a too uncertain quantity and cannot be measured. Here, the distance L, or the mixing length, is already not a random quantity. Its magnitude is of the order of $\sqrt{\overline{(\xi_z')^2}}$ and characterizes the scale of turbulence. Now, what is left is to establish the dependence of L on the coordinates, for example, empirically.

The expression (1.36) may also be retrieved from dimensional considerations. For this we use the principle of local similarity of turbulent transfer (Sect. 3.3 in Marov and Kolesnichenko (2011)),—the coefficients of turbulent transfer in each point depend only on the properties of the medium in this point, the local size of the scale of turbulence L and on certain characteristics of the averaged flow. In other words, ν_t is a function of the quantities ν, L, and $\partial\overline{v_x}/\partial z$. The scale L characterizes the geometry of the turbulent flow or the characteristic size. Far away from the hard surface, ν can be excluded from the list of parameters, and the dimensional considerations yield the Prandtl formula (1.36).

The constant factor α^* is determined for each specific type of motion on the basis of experimental data.

1.3.5 Turbulent Viscosity Parameter α

Let us consider an accretion disc, with orbital motion in circular orbits and orbital velocities in the plane parallel to the disc symmetry plane. Placing an imaginary wall perpendicular to the radius in a given point at a distance $r_\star$ from the centre, we find the frictional force applied per unit area of the wall.

The averaged velocity of matter in the disc is tangential to the radius with great accuracy since the orbital velocity dominates over other components. Let the imaginary wall rotate around the centre with the averaged velocity of the flow. The frictional force is directed tangentially and is equal to the density of the flow of the φ-component of momentum in the radial direction. If we assume, as mentioned in Sect. 1.3.1.1 after formula (1.31), that the first term in the turbulent viscosity tensor, defined only by the dynamics of the flow, dominates over the others, which contain the molecular viscosity coefficient η, then the $r\varphi$-component for the frictional stress on the wall is equal to

$$(\overline{w_{r\varphi}} - \overline{\rho\, v_r'' v_\varphi''})_{r=r_\star} = (\overline{\rho\,\nu}\, r \frac{\mathrm{d}\omega}{\mathrm{d}r} - \overline{\rho\, v_r'' v_\varphi''})_{r=r_\star},$$

where we used the expression for the component of the stress tensor in cylindrical coordinates (see Chapter 2 in the book by Landau and Lifshitz 1959).

According to common practice, we will define $w^{\mathrm{t}}_{r\varphi}$ as the quantity with opposite sign to the component of the viscous stress tensor in the disc $w_{r\varphi}$.[1] Using the gradient hypothesis (see Sect. 1.3.3 and (1.32)) we can write:

$$w^{\mathrm{t}}_{r\varphi} \equiv \overline{\rho\, v_r'' v_\varphi''} = -\overline{\rho}\ \nu_{\mathrm{t}}\, r \frac{\mathrm{d}\omega}{\mathrm{d}r}, \tag{1.37}$$

where ν_{t} is the kinematic coefficient of the turbulent viscosity [cm^2/s]. For a Keplerian disc, we get from (1.37):

$$w^{\mathrm{t}}_{r\varphi} = \frac{3}{2}\,\omega_{\mathrm{K}}\,\nu_{\mathrm{t}}\,\overline{\rho}\,. \tag{1.38}$$

As a consequence of the Prandtl hypothesis (1.35), $\nu_{\mathrm{t}} = \overline{v_t\, l_t}$, where v_t and l_t are the velocity and length of turbulent mixing, respectively, which both take random values in a turbulent flow.[2] Applying the Prandtl relation to describe the radial transport of turbulent velocity

$$v_t = l_t\, r \left|\frac{\mathrm{d}\omega}{\mathrm{d}\, r}\right|$$

(cf. (1.33)), we get, substituting in (1.37), that

$$w^{\mathrm{t}}_{r\varphi} = \overline{\rho}\ \overline{v_t^2} \equiv m_t^2\, \overline{\rho}\, v_{\mathrm{s}}^2,$$

[1] With this definition, $w^{\mathrm{t}}_{r\varphi}$ will be positive in accretion discs. In other literature on the subject, the definition $t_{r\varphi} = -w^{\mathrm{t}}_{r\varphi}$ is often used instead.

[2] They are analogous to the quantities v_x' and ξ_z' discussed in Sect. 1.3.4.

where the averaged turbulent velocity squared (fluctuating component of the velocity of matter in the disc) $\overline{v_t^2}$ is expressed using the sound speed v_s and the Mach number $m_t^2 = \overline{v_t^2}/v_\mathrm{s}^2$.

The last formula can be rewritten as

$$w_{r\varphi}^{\mathrm{t}} = \alpha P \,, \tag{1.39}$$

where the dimensionless quantity α is called the turbulent parameter and P is the total pressure (the sum of gas and radiation pressures).

Disc models, in which turbulence is taken to be the source of viscosity and where the connection (1.39) is used, are called α-discs. In the simplest models, this coefficient is considered fixed within the whole accretion disc. Its value may be found from a comparison with observations of transient phenomena, which are manifestations of viscous evolution of discs in the case of non-stationary accretion onto space objects.

Equating (1.38) to the quantity $\alpha\overline{\rho}\, v_\mathrm{s}^2$, we obtain a relation between the dimensionless turbulence parameter and the kinematic viscosity coefficient in a Keplerian disc:

$$\nu_\mathrm{t} = \frac{2}{3}\,\alpha\, v_\mathrm{s}^2\, \frac{1}{\omega_\mathrm{K}} = \frac{2}{3}\,\alpha\, v_\mathrm{s}\, z_\mathrm{hyd} \,, \tag{1.40}$$

where we introduce the 'hydrostatic half-thickness' of the disc, which can be found from approximate integration of (1.18):

$$z_\mathrm{hyd} \equiv \sqrt{\frac{p}{\rho}\,\frac{1}{\omega_\mathrm{K}^2}} = \frac{v_\mathrm{s}}{\omega_\mathrm{K}} \,.$$

Using (1.35), which is a consequence of the Prandtl hypothesis, we may write:

$$\alpha = \frac{\overline{v_t\, l_t}}{\frac{2}{3}\, v_\mathrm{s}\, z_\mathrm{hyd}} \,.$$

From general considerations it is clear that the α-parameter is a quantity whose value does not exceed unity. Indeed, if the turbulent motions have velocities exceeding the sound speed, these motions are quickly quenched by shock-waves. The inequality $l_t > z_\mathrm{hyd}$ would suggest that the turbulence has an anisotropic character since the transverse thickness of the disc is limited by the quantity $\sim z_\mathrm{hyd}$.

The use of the α-parameter is justified in situations where it may be considered approximately constant. As proved during the last decades, such an approximation describes well a variety of observed phenomena in sources with disc accretion. Numerical modelling of outbursts in dwarf novae and X-ray transients demonstrates that the α-parameter can be considered constant for certain ranges of physical

conditions in these astrophysical discs. Typical values from observations are $10^{-2} - 1$ (Meyer and Meyer-Hofmeister 1984; Cannizzo 1998; Kotko and Lasota 2012).

1.4 Thin Discs

1.4.1 Equations of Radial Structure

Let us write down the equations for disc accretion for geometrically thin α-discs. We will neglect any dependence of the physical parameters in the disc on z, averaging (integrating) along the vertical. We will consider discs without radial advection (transfer of heat with matter moving radially) and without mass loss from the disc surface. In such discs, the angular velocity of the rotating matter at each radius r is approximately equal to the angular rotational velocity of a free particle. In other words, $v_r \ll v_\varphi$.

The parameters determining the structure of a geometrically thin disc are the mass of the gravitating centre M, the inner radius of the accretion disc $r_{\rm in}$ and the accretion rate $\dot{M}$.

1.4.1.1 Mass Conservation Equation

We introduce the surface density

$$\Sigma_0(t, r) = \int_{-z_0}^{+z_0} \rho(t, r, z)\, \mathrm{d}z\,, \tag{1.41}$$

where z_0 is the disc half-thickness at radius r. As agreed earlier, the velocities in thin discs are independent of z. Integrating (1.2) along the disc height, we obtain:

$$\frac{\partial \Sigma_0}{\partial t} = -\frac{1}{r}\frac{\partial}{\partial r}(\Sigma_0\, v_r\, r)\,. \tag{1.42}$$

The product within parentheses on the right-hand side of this equation, multiplied by 2π, is equal to the radial flow of the matter in the disc [g/s] through a cylindrical surface with radius r.

1.4.1.2 The r-Component of the Equation of Motion

For a thin stationary disc, the dominant terms in this equation are

$$\frac{v_\varphi^2}{r} = \frac{\partial \Phi}{\partial r}\,. \tag{1.43}$$

For a Newtonian potential, this equation corresponds to Kepler's law:

$$\omega_{\mathrm{K}} = \frac{\sqrt{G\,M}}{r^{3/2}}\,.$$

Other potentials that take into account the curvature of space around a Schwarzschild black hole are discussed in Sect. 1.4.4.

1.4.1.3 The φ-Component of the Equation of Motion

After multiplying by $\rho\, r^2$, we integrate vertically (1.4) and obtain the law of conservation of the angular momentum

$$\Sigma_0\, v_r\, r\, \frac{\partial\,(\omega\, r^2)}{\partial r} = -\frac{\partial}{\partial r}\,(W_{r\varphi} r^2)\,, \tag{1.44}$$

where

$$W_{r\varphi}(t, r) = \int_{-z_0}^{+z_0} w^{\mathrm{t}}_{r\varphi}(t, r, z)\,\mathrm{d}z \tag{1.45}$$

is the height-integrated component of the viscous stress tensor.

1.4.2 Solution for a Constant Accretion Rate

From the continuity equation (1.42) it follows that in the stationary regime

$$\Sigma_0\, v_r\, r = const\,.$$

We determine the accretion rate as the mass of matter intersecting the surface of a cylinder with radius r per unit time:

$$\dot{M} \equiv -2\pi r\, v_r\, \Sigma_0\,. \tag{1.46}$$

The minus sign is inserted in order to make a quantity $\dot{M}$ positive and to compensate for the fact that as matter moves towards the centre, $v_r < 0$.

For a constant accretion rate, the equation of motion (1.44) can be easily integrated:

$$\dot{M}\,\omega\, r^2 - 2\,\pi\, W_{r\varphi}\, r^2 = const\,. \tag{1.47}$$

This is the law of conservation of angular momentum for a stationary disc. The constant can be determined from the boundary conditions at the inner edge of the disc:

$$\dot{M}\,(h - h_{\rm in}) = F - F_{\rm in},$$

where F is the momentum of viscous forces between adjacent rings of the disc (the viscous torque, a positive quantity in our notation)

$$F = 2\,\pi\,W_{r\varphi}\,r^2\,, \tag{1.48}$$

and $h = \omega\,r^2$ is the specific angular momentum, where the subscript indicates quantities at the inner disc radius.

The equation of conservation of angular momentum can be written in the form:

$$W_{r\varphi} = \frac{\dot{M}\,\omega}{2\,\pi}\,f(r) \quad \text{or} \quad F = \dot{M}\,h\,f(r)\,, \tag{1.49}$$

where the function $f(r) = 1 - h_{\rm in}/h + F_{\rm in}/(\dot{M}\,h)$ contains information about inner boundary conditions for the viscous stress tensor (the form of $f(r)$ at $\dot{M}(r) \neq const$, see Sect. 1.5.3). For example, in the case of black holes, the viscous stress tensor is set to zero since the inner radius of the disc is determined by the radius of the last stable orbit, from which matter falls freely onto the black hole. Then, far away from the inner radius, $f(r) \approx 1$. For accretion onto a magnetized star, the stress tensor at the inner edge of the disc depends on the strength of the magnetic field and its radial distribution changes accordingly. For central objects with a sufficiently strong magnetic field, accretion may seize at the inner radius of the disc. Such discs are called disc reservoirs (Syunyaev and Shakura 1977). In a disc reservoir F is radially constant close to the inner boundary, and at large radii F is affected by the conditions at the outer boundary.

1.4.3 Radial Velocity of Matter in the Disc

Let us estimate the radial component of the velocity of matter in a disc in the stationary regime from the φ-component of the equation of motion. For this, we use (1.49) in the approximation $f(r) \sim 1$, which is valid in the quasi-stationary case, far away from the centre, and definition of accretion rate (1.46):

$$|v_r| = \frac{\dot{M}}{2\,\pi\,r\,\Sigma_0} = \frac{W_{r\varphi}}{\omega\,r\,\Sigma_0}\,.$$

Obviously, this velocity, with which matter approaches the gravitating object, depends on the value of the viscosity. We use the formula (1.38) and obtain:

$$|v_r| = \frac{3}{2}\,\frac{\nu_\mathrm{t}}{r}\,, \tag{1.50}$$

where $W_{r\varphi} \approx 2\,z_0\,w^\mathrm{t}_{r\varphi}$ and $\Sigma_0 \approx 2\,z_0\,\rho$ (cf. (1.41), and (1.45)).

The characteristic time scale for movement of the matter radially towards the centre is

$$\tau_\mathrm{vis} \sim \frac{r}{|v_r|} = \frac{2}{3}\,\frac{r^2}{\nu_\mathrm{t}}\,.$$

Making an assumption regarding the α-viscosity in the disc and using the relation (1.40) between ν_t and α, we re-write the obtained formulas in the form:

$$|v_r| = \alpha\,v_\mathrm{s}\,\frac{z_0}{r} = \alpha\,v_\varphi\,\left(\frac{z_0}{r}\right)^2\,, \tag{1.51}$$

$$\tau_\mathrm{vis} = \frac{1}{\alpha\,\omega_\mathrm{K}}\,\left(\frac{z_0}{r}\right)^{-2}\,. \tag{1.52}$$

In a geometrically thin disc, the viscous time scale is much larger than the characteristic dynamic time scale

$$\tau_\mathrm{dyn} \sim \frac{r}{v_\varphi} \sim \frac{1}{\omega_\mathrm{K}}\,. \tag{1.53}$$

1.4.4 Accretion Onto a Black Hole

In Chap. 3, devoted to relativistic standard discs, a theory will be presented, the basics of which were worked out by Novikov and Thorne (1973). For further acquaintance with the astrophysical aspects of this theory we also recommend the books by Shapiro and Teukolsky (1983), Thorne et al. (1986). Here, we outline only the basics of the behavior of an accretion disc around a black hole.

Close to the black hole the curvature of space-time plays a crucial role for the formation of an accretion disc. The thin-disc approximation, according to which matter rotates in approximately circular orbits, breaks down. The flow of matter onto the black hole speeds up, becomes highly supersonic in the radial direction and, starting from some certain radius, goes in the free-fall regime.

At free fall, the momentum of the in-falling matter is conserved. In this case, there is no outward flux flow of the viscous tensor, implying that it is equal to zero at the disc inner boundary: $F_\mathrm{in} = 2\pi\,W_{r\varphi}r^2_\mathrm{in} = 0$. This condition is confirmed by numerical one-dimensional calculations of the equations of hydrodynamics in a

post-Newtonian potential (Shafee et al. 2008). It turns out that the conditions for the viscous stress tensor to be equal to zero are satisfied close to the innermost stable circular orbit.

For non-rotating black holes, the radius of the innermost stable circular orbit $r_{\rm ISCO} = 3\,R_{\rm g}$, where the Schwarzschild radius $R_{\rm g}$ is the event-horizon radius of a non-rotating black hole:

$$R_{\rm g} = 2\,G\,M/c^2\,.$$

The radius $r_{\rm ISCO}$ for a rotating black hole is determined in the Kerr space-time metric and given by formula (3.22) in Sect. 3.1.3.

At radii less than $3\,R_{\rm g}$, there is no energy release due to viscosity. We note that in this area radiation may be generated as a result of processes which involve plasma and magnetic fields.

Thus, for accretion onto a Schwarzschild black hole, the boundary condition at the inner radius is written as

$$W_{r\varphi}(r = 3\,R_{\rm g}) = 0\,.$$

We use Eq. (1.47) for $\dot{M} = const$ in the form

$$\dot{M}(\omega_{\rm in} - \omega) = 2\,\pi\;\; W_{r\varphi}\,,$$

or, for the viscous torque,

$$F = \dot{M}(h - h_{\rm in})\,, \tag{1.54}$$

where $h_{\rm in}$ is the specific angular momentum of the matter at the innermost orbit around the black hole.

If the viscous stress tensor is equal to zero at the inner boundary of a stationary infinite disc, the function in (1.49) is:

$$f(r) = 1 - h_{\rm in}/h(r) + F_{\rm in}/(\dot{M}\,h) = 1 - h_{\rm in}/h(r). \tag{1.55}$$

In the Newtonian approximation, $f(r) = 1 - \sqrt{r_{\rm in}/r}$ and

$$W_{r\varphi} = \frac{\dot{M}\,\omega}{2\,\pi}\,(1 - \sqrt{r_{\rm in}/r})\,.$$

To approximately take into account the effects of general relativity in the vicinity of non-rotating black holes, the Paczynski–Wiita potential can be used (Paczynsky and Wiita 1980):

$$\Phi_{\rm PW} = -\frac{G\,M}{r - R_{\rm g}}\,. \tag{1.56}$$

For free particles in circular orbits, the velocities can be found from (1.3):

$$\frac{v_\varphi^2}{r} = \frac{\mathrm{d}\Phi}{\mathrm{d}r}\,. \tag{1.57}$$

As a result, we obtain

$$\frac{v_\varphi^{\mathrm{PW}}}{c} = \frac{1}{\sqrt{2}}\,\frac{\sqrt{r\,R_\mathrm{g}}}{(r-R_\mathrm{g})}\,,$$

and the specific angular momentum of a test particle in the Paczynski-Wiita potential is:

$$h^{\mathrm{PW}} = v_\varphi^{\mathrm{PW}}\,r = \sqrt{\frac{G\,M\,r}{(1-\frac{2\,G\,M}{c^2\,r})^2}}\,. \tag{1.58}$$

The modified potential (1.56) is often used (for example when substituting into (1.43)) since it fits quite well the curvature effects of the space-time metric around a Schwarzschild black hole. Other approximate potentials, in particular such applicable to the case of rotating black holes, can be found in the book by Kato et al. (1998).

Let us write down the Schwarzschild stationary metric as the square of the interval between two events separated in time and space

$$\mathrm{d}s^2 = -(1-R_\mathrm{g}/r)\,\mathrm{d}t^2 + (1-R_\mathrm{g}/r)^{-1}\,\mathrm{d}r^2 + r^2(\mathrm{d}\theta + \sin^2\theta\,\mathrm{d}\varphi)\,.$$

Here, t, r, θ, φ are the Schwarzschild coordinates. Due to the curvature of space-time near a black hole, the distance element $\mathrm{d}l$ along the radius, as measured by a local observer, is longer than the corresponding coordinate element $\mathrm{d}r$ (see Fig. 1.2):

$$\mathrm{d}l = \frac{\mathrm{d}r}{\sqrt{1-R_\mathrm{g}/r}}\,.$$

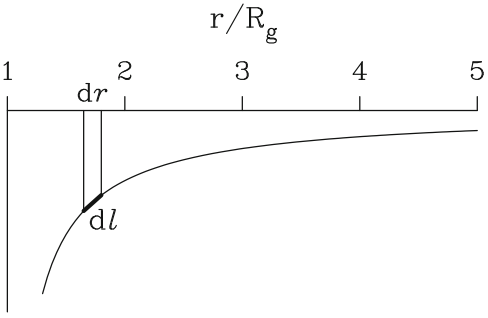

Fig. 1.2 Illustration of the 'shrinking' of a coordinate element $\mathrm{d}r$, corresponding to an element of distance $\mathrm{d}l$, measured by a stationary observer

To describe the relativistic motion in the vicinity of a Schwarzschild black hole, we may use the following 'logarithmic' potential (Landau and Lifshitz 1973; Thorne et al. 1986; Abramowicz 2016):

$$\Phi = \frac{c^2}{2} \ln\left(1 - \frac{R_\mathrm{g}}{r}\right) = c^2 \ln\sqrt{1 - \frac{R_\mathrm{g}}{r}}\,. \tag{1.59}$$

Here $\sqrt{1 - R_\mathrm{g}/r}$ is the lapse function in the Schwarzschild metric. It determines the redshift of the signal emitted from the vicinity of the black hole and the difference between two time intervals, one of which, $\mathrm{d}t$, is measured at infinity and the other, $\mathrm{d}\tau_l$, by an observer in the local stationary reference frame:

$$\mathrm{d}\tau_l/\mathrm{d}t = \sqrt{1 - R_\mathrm{g}/r}\,. \tag{1.60}$$

The time measured in the frame of moving particle is related to the time measured by the local stationary observer as

$$\mathrm{d}\tau_\mathrm{p}/\mathrm{d}\tau_l = \sqrt{1 - v^2/c^2}\,. \tag{1.61}$$

The momentum $\boldsymbol{p}$ and the energy E_local of a relativistic particle with rest mass m_o relative to the local stationary observer are

$$\boldsymbol{p} = \frac{m_o\,\boldsymbol{v}}{\sqrt{1 - v^2/c^2}}\,, \quad \text{and} \quad E_\mathrm{local} = \frac{m_o\,c^2}{\sqrt{1 - v^2/c^2}}\,,$$

respectively, where $v^2 = v_r^2 + v_\varphi^2$ for particles moving in the equatorial plane. We may also introduce the notion of 'energy at infinity' E. This value remains unchanged along the particle trajectory. Let us determine it.

Consider a particle travelling past a stationary observer who is located at a distance r from the centre of a black hole. The equation of particle motion in the reference system of this observer looks as follows:

$$\frac{\mathrm{d}\boldsymbol{p}}{\mathrm{d}\tau_l} = -\frac{m_o}{\sqrt{1 - v^2/c^2}}\,\boldsymbol{\nabla}\Phi\,. \tag{1.62}$$

Note that the potential Φ is spherically symmetric. On multiplying Eq. (1.62) by $\boldsymbol{v}$, we obtain

$$\boldsymbol{v}\,\frac{\mathrm{d}}{\mathrm{d}\tau_l}\left(\frac{m_o\boldsymbol{v}}{\sqrt{1 - v^2/c^2}}\right) = -\frac{m_o\,\boldsymbol{v}}{\sqrt{1 - v^2/c^2}}\,\boldsymbol{\nabla}\Phi = -\frac{m_o\,\boldsymbol{v}\,\boldsymbol{e}_r}{\sqrt{1 - v^2/c^2}}\,\frac{\mathrm{d}\Phi}{\mathrm{d}l}\,, \tag{1.63}$$

where $\boldsymbol{e}_r$ is a unit radial vector in the Cartesian reference system of the local observer. Further, we differentiate the left-hand side of (1.63):

$$\frac{1}{2}\,\frac{m_o}{\sqrt{1-v^2/c^2}}\,\frac{\mathrm{d}v^2}{\mathrm{d}\tau_l}+\frac{1}{2}\,\frac{m_o\,v^2/c^2}{(1-v^2/c^2)^{3/2}}\,\frac{\mathrm{d}v^2}{\mathrm{d}\tau_l}=-\frac{m_o\,\boldsymbol{v}\,\boldsymbol{e}_r}{\sqrt{1-v^2/c^2}}\,\frac{\mathrm{d}\Phi}{\mathrm{d}l}\,.$$

When multiplying this by $(1-v^2/c^2)^{3/2}$, cancelling out the two equal terms with opposite signs in the left-hand part of the equation and using the equality $v_r = \mathrm{d}l/\mathrm{d}\tau_l$ for the radial velocity, we obtain

$$\frac{1}{2}\,\frac{\mathrm{d}}{\mathrm{d}\tau_l}\,(1-v^2/c^2)=(1-v^2/c^2)\,\frac{\mathrm{d}l}{\mathrm{d}\tau_l}\,\frac{\mathrm{d}}{\mathrm{d}l}\ln(1-R_\mathrm{g}/r)^{1/2}\,,$$

which is equivalent to the following equation

$$\frac{\mathrm{d}}{\mathrm{d}\tau_l}\,\ln(1-v^2/c^2)=\frac{\mathrm{d}}{\mathrm{d}\tau_l}\,\ln(1-R_\mathrm{g}/r)\,.$$

Finally, we obtain the following relationship:

$$(1-R_\mathrm{g}/r)\Big/(1-v^2/c^2)=const.$$

Hence, the value

$$E=\frac{m_o\,c^2}{\sqrt{1-v^2/c^2}}\sqrt{1-\frac{R_\mathrm{g}}{r}}=E_\mathrm{local}\sqrt{1-\frac{R_\mathrm{g}}{r}}=const\,, \tag{1.64}$$

does not change for a freely moving particle, while the locally measured energy E_local varies in the gravitational field of the black hole. This value E is termed 'energy-at-infinity' (Thorne et al. 1986). For a photon, the rest mass of which is $m_o = 0$, Eq. (1.64) yields the relation between its frequency in the reference system of the local observer ν_o and its frequency detected at infinity $\nu_\infty = \nu_o\sqrt{1-R_\mathrm{g}/r}$, describing the redshift effect.

In the non-relativistic approximation, the expression for the energy $\mathscr{E}_\mathrm{N}$ of the particle has the well-known form

$$E-m_o\,c^2=\mathscr{E}_\mathrm{N}=m_o\,v^2/2-m_o\,G\,M/r\,.$$

Let us now determine the components of the particle velocity in the equatorial plane. A freely moving particle with mass m_o keeps its angular momentum unchanged

$$h_\mathrm{p}=\frac{m_o\,v_\varphi\,r}{\sqrt{1-v^2/c^2}}\,. \tag{1.65}$$

When taking into consideration that $v^2 = v_r^2 + v_\varphi^2$, Eqs. (1.64) and (1.65) yield

$$\frac{v_r^2}{c^2} = 1 - \frac{m_o^2\, c^4}{E^2}\left(\frac{h_\mathrm{p}^2}{r^2\, m_o^2\, c^2} + 1\right)\left(1 - \frac{R_\mathrm{g}}{r}\right). \tag{1.66}$$

Multiplying this by a factor $E^2/(m_o^2\, c^4)$ and using (1.61) and (1.64) together with the relation

$$\frac{v_r^2}{c^2} = \frac{1}{c^2}\left(\frac{\mathrm{d}r}{\mathrm{d}\tau_\mathrm{p}}\right)^2 \frac{m_o^2\, c^4}{E^2},$$

we may rewrite (1.66). As a result, we obtain the law of motion for a particle with energy E, which is identical to the exact solution in GR, see Shapiro and Teukolsky (1983):

$$\frac{1}{c^2}\left(\frac{\mathrm{d}r}{\mathrm{d}\tau_\mathrm{p}}\right)^2 = \frac{E^2}{m_o^2\, c^4} - \left(\frac{h_\mathrm{p}^2}{r^2\, m_o^2\, c^2} + 1\right)\left(1 - \frac{R_\mathrm{g}}{r}\right).$$

Note that in the approximation of the Newtonian potential, this law of motion looks as follows:

$$v_r^2 = \frac{2}{m_o}\left(\mathscr{E}_\mathrm{N} + m_o\,\frac{G\,M}{r}\right) - \frac{h_\mathrm{N}^2}{r^2\, m_o^2},$$

where $h_\mathrm{N} = m_o\, v_\varphi\, r = const$.

Let us consider particles moving in circular orbits around a Schwarzschild black hole. For such motion, both v_r and $\mathrm{d}r/\mathrm{d}\tau_\mathrm{p}$ become zero. For the sake of convenience, we may introduce an effective potential (Shapiro and Teukolsky 1983):

$$V(r) = \left(\frac{h_\mathrm{p}^2}{r^2\, m_o^2\, c^2} + 1\right)\left(1 - \frac{R_\mathrm{g}}{r}\right).$$

For circular orbits, the first derivative of this potential becomes zero (the potential has an extremum). The system of equations

$$\frac{\mathrm{d}r}{\mathrm{d}\tau_\mathrm{p}} = 0\,, \qquad \frac{\partial V(r)}{\partial r} = 0$$

yields the following angular momentum in a circular orbit:

$$h_\mathrm{p}^2 = \frac{m_o^2\, r\, R_\mathrm{g}\, c^2}{2 - 3R_\mathrm{g}/r}. \tag{1.67}$$

After squaring (1.65), we derive the tangential velocity, as measured by the local observer, from (1.67):

$$\frac{v_\varphi}{c} = \frac{1}{\sqrt{2}}\sqrt{\frac{R_\mathrm{g}}{r - R_\mathrm{g}}}\,. \tag{1.68}$$

For the local observer, the angular velocity of a particle is

$$\omega_l = \frac{v_\varphi}{r} = \frac{c}{\sqrt{2}\,r}\sqrt{\frac{R_\mathrm{g}}{r - R_\mathrm{g}}}\,. \tag{1.69}$$

Using (1.60), we obtain for an observer at infinity:

$$\omega = \frac{c\,\sqrt{R_\mathrm{g}}}{\sqrt{2}\,r^{3/2}} = \frac{\sqrt{G\,M}}{r^{3/2}}\,, \tag{1.70}$$

that is, the classical expression following from Kepler's law.

According to the Rayleigh criterion (Rayleigh 1917), stable orbits cannot exist where $\mathrm{d}h_\mathrm{p}/\mathrm{d}r < 0$. This criterion implies that the last stable circular orbit has a radius $r_\mathrm{ISCO} = 3\,R_\mathrm{g}$.

When substituting the velocity $v_\varphi = c/2$, which corresponds to r_ISCO, into (1.64), we determine the energy of a particle rotating in the innermost possible stable orbit. The energy of this particle, $E = m_o\,c^2\,2\sqrt{2}/3$, is less than its rest energy at infinity, $m_0\,c^2$. This means that when a particle moves from infinity towards the Schwarzschild black hole, that is, in the process of accretion, the released energy is $(m_0\,c^2 - E) \approx 0.0572\,m_0\,c^2$. Thus, the energy conversion efficiency in the accretion process onto a non-rotating black hole is equal to $\sim 6\%$. A calculation using the Kerr metric shows that the binding energy of the particle is largest for an extremely-fast rotating black hole and equals to $1 - \sqrt{1/3} \approx 0.423$ times the rest energy (Kato et al. 2008).

Extracting the square root of (1.67), we find the specific angular momentum of a particle in circular orbit in the Schwarzschild metric:

$$h = \frac{h_\mathrm{p}}{m_o} = \frac{\sqrt{G\,M\,r}}{\sqrt{1 - \frac{3\,G\,M}{c^2\,r}}}\,. \tag{1.71}$$

Figure 1.3 (upper panel) shows the dependence of the specific angular momentum of a test particle on the radius of the orbit in the gravitational field of the black hole. In addition, the respective dependencies are shown in the Newtonian potential (*dashed line*) and in the Paczynski–Wiita potential (*dotted line*). In the gravitational field of the Schwarzschild black hole, the specific angular momentum h becomes minimum at the radius of the innermost stable circular orbit $6\,G\,M/c^2$. In contrast to the case of the Newtonian potential, the first derivative of the specific angular momentum,

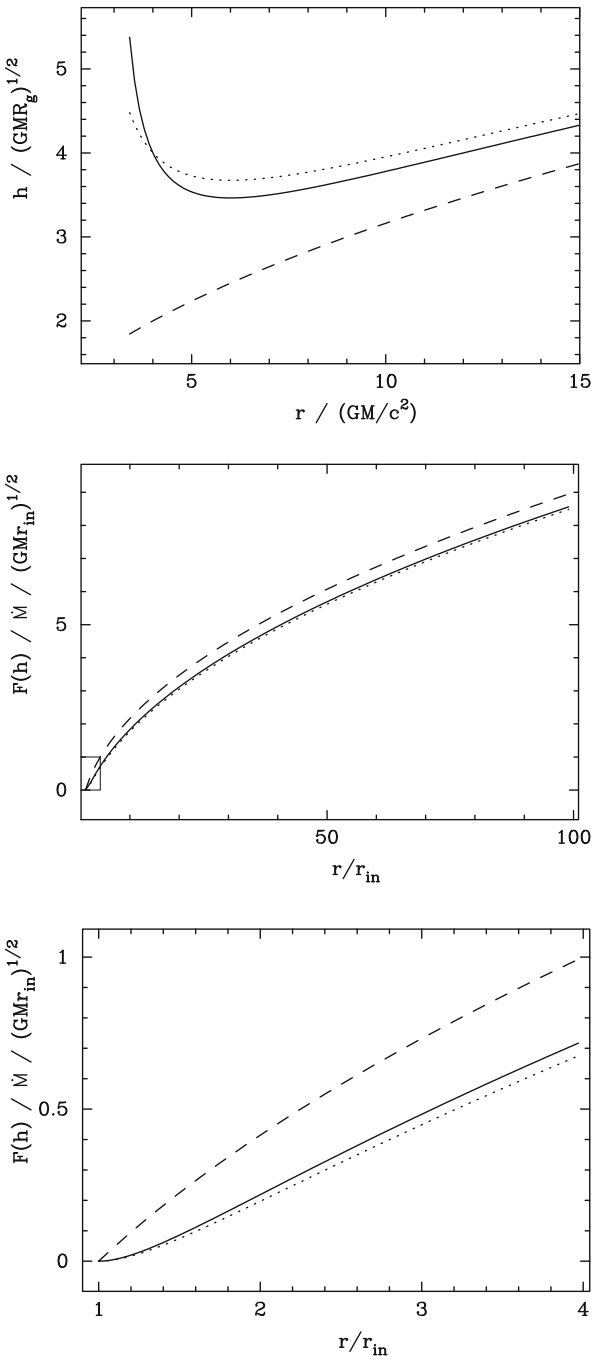

Fig. 1.3 Specific angular momentum h of a test particle in the gravitational field of a black hole (uppermost panel) and the viscous torque $F(h)$ in a stationary disc, normalised values (lower panels). The inner radius of the disc is $r_{\rm in} = 3\,R_{\rm g} = 6\,G\,M/c^2$. *Solid lines* show the dependence in the exact logarithmic potential (1.59), *dotted lines* show the same in the Paczynski–Wiita potential, dashed lines—in the Newtonian approximation. In the middle panel, a rectangular area is drawn, shown enlarged in the lower panel

$\mathrm{d}h/\mathrm{d}r$, vanishes at this radius (see Fig. 1.3, upper panel). The innermost stable orbit is located at $3\,R_\mathrm{g}$ in both the approximate Paczynski–Wiita potential (1.56) and the exact potential (1.59). The binding energy in the Paczynski–Wiita potential, however, differs from the value in the Schwarzschild metric:

	$(m_0\,c^2 - E)/(m_0\,c^2)$
Newtonian potential:	$1/12$
Paczyński–Wiita potential:	$1/16$
Logarithmic potential and Schwarzschild metric:	$1 - 2\sqrt{2}/3$

Circular orbits exist only down to the radius where $v_\varphi = c$. In the logarithmic potential, the innermost circular orbit lies at $3\,R_\mathrm{g}/2$, which coincides with the exact value predicted by general relativity. In the Paczynski–Wiita potential, the innermost circular orbit is located at $2\,R_\mathrm{g}$.

Figure 1.3 also shows the viscous torques in the disc as functions of radius given by formula (1.54). Note that, for both the Paczynski–Wiita and the logarithmic potentials, the torque itself, as well as its first derivative, vanishes at the innermost stable orbit (see Fig. 1.3, lower panel).

1.4.5 Energy Release in Geometrically Thin Discs

Let us return to the study of discs in the Newtonian approximation. A detailed analysis of the energy balance equation is given, for example, in the appendix of the book by Kato et al. (1998). The energy dissipated in the disc per unit volume per unit time is equal to

$$\varepsilon = \rho\,\nu_\mathrm{t}\,r^2\left(\frac{\mathrm{d}\omega}{\mathrm{d}r}\right)^2 . \tag{1.72}$$

In the general case of optically thick discs, the energy release ε can be given in the form of a power-law function of temperature and density (Tayler 1980).

In the simplest approximation for a geometrically thin disc, all the energy released due to friction in a disc ring is radiated away from the top and bottom surfaces of this ring. The energy released per unit time per unit surface area of a geometrically thin disc in a calculation per one side of the disc is

$$Q_\mathrm{vis}(t,r) \equiv \int_0^{+z_0} \varepsilon(t,r,z)\,\mathrm{d}z = -\frac{1}{2}\,W_{r\varphi}\,r\,\frac{\mathrm{d}\omega}{\mathrm{d}r} . \tag{1.73}$$

Note that the last formula works also in the case of disc reservoirs (Syunyaev and Shakura 1977), in which the accretion rate is zero. In view of (1.49), we have for an

accreting disc:

$$Q_{\rm vis} = -\frac{\dot{M}}{4\pi}\,\omega\, r\,\frac{{\rm d}\omega}{{\rm d}r}\,f(r)\,. \tag{1.74}$$

For a Keplerian disc, the above expressions can be re-written in the form (using (1.72)):

$$\varepsilon = \frac{3}{2}\,\omega_{\rm K}\,w^{\rm t}_{r\varphi} = \frac{9}{4}\,\rho\,\nu_{\rm t}\,\omega_{\rm K}^2\,, \qquad Q_{\rm vis} = \frac{3}{4}\,\omega_{\rm K}\,W_{r\varphi} = \frac{3}{8\pi}\,\dot{M}\,\frac{G\,M}{r^3}\,f(r)\,. \tag{1.75}$$

One can see that the viscous time scale (1.52) in a geometrically thin disc is much larger than the characteristic thermal time scale, on which the thermal energy in a unit volume changes:

$$\tau_{\rm th} \sim \frac{\rho\, v_{\rm s}^2}{\varepsilon} \sim \frac{1}{\alpha\,\omega_{\rm K}}\,, \tag{1.76}$$

where we have replaced $\nu_{\rm t}$ using (1.40).

For an accretion disc with a zero viscous torque at the inner boundary and with a Keplerian distribution of angular momentum, we have (see Eq. (1.55)):

$$Q_{\rm vis} = \frac{3}{8\pi}\,\dot{M}\,\frac{G\,M}{r^3}\left(1-\sqrt{\frac{r_{\rm in}}{r}}\right),$$

where $r_{\rm in}$ is the radius of the inner boundary of the disc.

The most general expression for the viscous heat in a Keplerian disc, including one with zero accretion rate, is:

$$Q_{\rm vis} = \frac{3}{8\pi}\,\frac{\omega_{\rm K}\,F}{r^2} \quad \text{or} \quad Q_{\rm vis} = \frac{3}{8\pi}\,F\,\frac{(G\,M)^4}{h_{\rm K}^7}\,, \tag{1.77}$$

where $h_{\rm K}$ is the specific angular momentum and F is the viscous torque (1.48).

The energy balance equation for geometrically thin discs reflects the fact that the thermal energy released due to viscosity at radius r is completely radiated away at the same radius:

$$Q_{\rm vis}(r) = Q_{\rm rad}(r)\,, \tag{1.78}$$

where $Q_{\rm rad}(r)$ is the radiated flux from one of the two surfaces of the accretion disc. The last equation requires a modification if the accretion rate is high, $\gtrsim \dot{M}_{\rm Edd}$. It turns out that the radial transport of heat should also be taken into account.

In the approximation of a disc radiating like a blackbody, it is possible to characterize its flux with an effective temperature:

$$Q_{\rm rad} = \sigma_{\rm SB}\, T_{\rm eff}^4\,, \qquad T_{\rm eff} \propto r^{-3/4}\,. \tag{1.79}$$

The effective temperature at the disc surface has its maximum $T_{\rm max}$ at radius

$$r_{\rm max} = \left(\frac{7}{6}\right)^2 r_{\rm in}\,,$$

and is equal to

$$T_{\rm max} = 2^{3/4}\left(\frac{3}{7}\right)^{7/4}\left(\frac{G\,M\,\dot{M}}{\pi\,\sigma_{\rm SB}\,r_{\rm in}^3}\right)^{1/4} = 2\left(\frac{3}{7}\right)^{7/4}\left(\frac{L_{\rm d}}{\pi\,\sigma_{\rm SB}\,r_{\rm in}^2}\right)^{1/4}.$$

We introduced in the last formula the total bolometric luminosity from both sides of the disc, equal to half the released gravitational energy of the matter falling from infinity to the gravitating centre:

$$L_{\rm d} = 4\,\pi\int_{r_{\rm in}}^{r_{\rm out}} Q_{\rm rad}\, r\,{\rm d}r = \frac{1}{2}\,\dot{M}\,\frac{G\,M}{r_{\rm in}}\,.$$

The specific potential energy of a particle moving from infinity to the inner edge of the disc decreases from zero to $-G\,M/r_{\rm in}$. Half of this energy heats the disc and is radiated and the other half goes into kinetic energy of rotation.

This 'virial theorem' does not apply to individual rings in the disc. We integrate the energy released from the disc at distances $r \gg r_{\rm in}$ from both sides of the disc:

$$2\int \frac{3}{8\pi}\,\dot{M}\,\frac{GM}{r^3}\,2\,\pi\,r\,{\rm d}r = \frac{3}{2}\,\dot{M}\,\frac{GM}{r}\,,$$

and find that it is three times as high as the amount of released gravitational energy. This happens since along with angular momentum, transferred outwards from the centre during the accretion process, a part of the energy is transferred as well.

Indeed, using the definitions of the integrated quantities (1.45), (1.46), and (1.73), let us multiply the energy balance equation (1.26) by $2\pi r$ and integrate it over disc thickness, keeping in mind that we agreed to use the positive value $w^{\rm t}_{r\varphi} = -w_{r\varphi}$ for accretion discs. We obtain

$$\dot{M}\,\frac{\partial}{\partial r}\left(\frac{v_\varphi^2}{2} + \Phi\right) = 2\,\pi\,r \times 2\,Q_{\rm vis} + \frac{\partial}{\partial r}(\omega_{\rm K}\,F)\,, \tag{1.80}$$

where $F = 2\,\pi\,r^2 W_{r\varphi}$ is the total viscous torque between neighboring rings in the disc, introduced in Sect. 1.4.2. And thus, the energy from gravitational interaction,

released as matter moves towards the centre, is dissipated (radiated from both sides of the disc) and is redistributed over the disc as a result of the work of viscous forces transferring angular momentum.

Another important conclusion can be drawn from considering the last equation. The disc releases heat and radiates even if the accretion rate is zero. If the matter cannot pass through the inner boundary, the radial motion of matter towards the disc centre may be interrupted. This happens, for example, if the central object is a neutron star with a strong magnetic field. While $\dot{M} = 0$, the viscous forces do not stop working, the matter is heated up and the heat turns into radiation. The energy in such a disc, along with the angular momentum, comes from the neutron star through the inner boundary of the disc.

1.4.6 Disc Radiation

The radiative flux in a unit solid angle from a flat accretion disc at distance d from the disc is equal to

$$F_\nu = \frac{2\,\pi}{d^2}\,\cos i \int_{r_{\rm in}}^{r_{\rm out}} I_\nu\, r\,{\rm d}r\,, \tag{1.81}$$

where i is the inclination of the disc to the line of sight and $I_\nu(r)$ is the intensity of radiation from the disc surface.

In the disc photosphere, the following radiative processes are frequently considered (see, for example, Kato et al. 2008):

- Free-free and bound-free transitions,
- Scattering off free electrons,
- Compton scattering (scattering off cold electrons),
- Inverse Compton scattering (if the energy of the electrons and/or ions are very high),
- Line broadening caused by the rotation of the disc.

The Planck spectrum describes the spectral density of electromagnetic radiation emitted by an isothermal atmosphere if scattering is not taken into account. At every radius, the disc radiates like a blackbody of temperature $T_{\rm eff}$ with intensity:

$$B_\nu(T_{\rm eff}) = \frac{2\,h\,\nu^3}{c^2}\,\frac{1}{e^{h\nu/kT_{\rm eff}} - 1}\,. \tag{1.82}$$

The spectral flux integrated along the disc radius in shown in Fig. 1.4.

For a disc spectrum as shown in Fig. 1.4, the power-law distribution describes the middle interval. Let is determine the power-law index of this distribution. Almost the whole disc, with the exception of the central parts (which, however, give an overwhelming contribution to the total amount of the radiated energy),

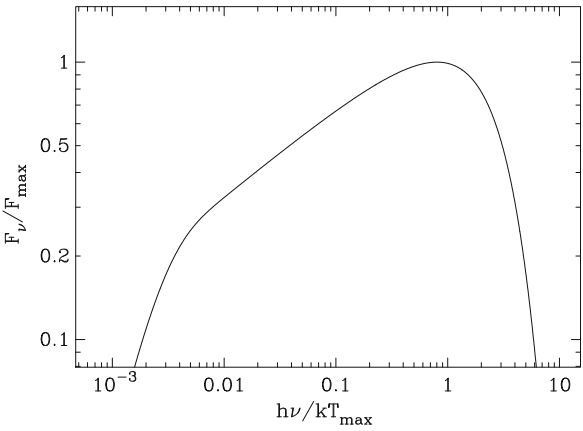

Fig. 1.4 Spectral distribution of radiative flux density from a standard optically thick, geometrically thin disc in the Newtonian metric. The horizontal axis shows the normalised radiation frequency. The vertical axis shows the spectral radiative flux density in units of [erg/Hz/cm^2/s] normalised to the maximum flux density at $h\,\nu/k\,T_{\rm max} \approx 0.8$. The maximum of distribution νF_ν is at $h\,\nu/k\,T_{\rm max} \approx 2.5$

may be characterized by the effective temperature in the form of a simple power-law function of radius (1.79). Substituting $r = r_0(T_0/T_{\rm eff})^{4/3}$ and (1.82) in the integral (1.81), we get

$$F_\nu = \frac{16\,\pi}{3\,d^2}\,\cos i\,\left(\frac{k\,T_0}{h}\right)^{8/3}\,\frac{h\,\nu^{1/3}}{c^2}\,r_0^2\int_{x_{\rm in}}^{x_{\rm out}}\frac{x^{5/3}}{e^x-1}\,{\rm d}x\,,$$

where we have made the substitution $x = h\nu/kT_{\rm eff} = (h\nu/kT_0)\,(r/r_0)^{3/4}$.

The radius r_0 can be chosen rather close to $r_{\rm in}$, implying that $T_0 \approx T_{\rm max}$ with fairly good accuracy. Then $x = (h\nu/kT_{\rm max})(r/r_{\rm in})^{3/4}$. At those frequencies where the conditions $x_{\rm in} \ll 1$ and $x_{\rm out} \gg 1$ are satisfied, the value of the integral in the last expression varies only little for different ν, and is approximately equal to the integral from zero to infinity when expressed with the help of the special gamma function and Riemann zeta function as $(10/9)\,\Gamma(2/3)\,\zeta(8/3) \approx 1.93$. Thus, for a wide frequency range $(r_{\rm in}/r_{\rm out})^{3/4} < h\nu/kT_{\rm max} < 1$, the spectral flux density of disc radiation depends on the frequency according to $F_\nu \propto \nu^{1/3}$.

For a homogeneous atmosphere where scattering is present, the spectrum will differ from that of a blackbody (Felten and Rees 1972):

$$I_\nu \simeq \sqrt{\frac{\varkappa_{\rm a}}{\varkappa_{\rm a}+\varkappa_{\rm sc}}}\,B_\nu(T_{\rm eff})\,,$$

where $\varkappa_{\rm a}$ is the absorption coefficient and $\varkappa_{\rm sc}$ is the coefficient for scattering off free electrons. If electron scattering dominates over absorption and if the disc spectrum is susceptible to Comptonization, the change in shape of the X-ray spectrum from a disc around a stellar mass compact object is approximately described by the spectral hardening factor f_c:

$$F_\nu = \frac{1}{f_c^4}\,\pi\,B_\nu(f_c\,T_{\rm eff})\,,$$

where F_ν is the flux from a unit surface into a half-space. The product $f_c\, T_{\rm eff}$ is called the colour temperature. The power of four is explained by the fact that the total radiated energy from the disc is independent of the spectral shape.

1.5 Stationary α-Discs

As we have seen in Sect. 1.4, the use of the continuity equation and the equation of motion, integrated (or averaged) along the vertical coordinate, enable us to find out the radial structure of thin stationary accretion discs. Is is possible to separately study the vertical and the radial structure of the disc because the characteristic time scales, namely, viscous and hydrostatic ones, are significantly different. The characteristic hydrostatic time scale corresponds to the time scale for changes in the thickness of the disc at a given radius as a result of a change of its central temperature. For dimensional reasons, this quantity is proportional to the disc half-thickness divided by the sound speed, $z_0/v_{\rm s} \sim 1/\omega_{\rm K} \sim \tau_{\rm dyn}$, and corresponds to the dynamical time which is much smaller than the viscous time in a thin disc (see Sect. 1.4.3).

The vertical structure of accretion discs in the general case (stationary as well as non-stationary) is described by a system of four ordinary differential equations, the exact solution to which, for given boundary conditions, can be found using numerical methods. In some sense, a calculation of the vertical structure of a disc is similar to the calculation of the internal structure of stars (Tayler 1980). The system of differential equations for the vertical structure of a disc was solved by a number of authors (see, for example, Meyer and Meyer-Hofmeister (1982), Shaviv and Wehrse (1986), Suleimanov (1992), Cannizzo (1992), Ketsaris and Shakura (1998), Hameury et al. (1998), Dubus et al. (1999)).

The disc can be divided into different zones (A, B, and C) according to the processes predominant in opacity formation and depending on comparative role of gaseous and radiative pressure (Shakura and Sunyaev 1973). A high temperature zone with main contribution from radiation pressure may arise in the central parts of the disc—the so-termed zone A. In this region, the opacity is determined by electron scattering. There are a number of studies devoted to the instabilities in this region (Lightman and Eardley 1974; Shibazaki and Hōshi 1975; Shakura and Sunyaev 1976). It was shown that zone A is thermally and viscously unstable. Its vertical structure can be described using the polytrope approximation. Convection plays an important role in the energy transfer to the disc surface (Bisnovatyi-Kogan and Blinnikov 1976; Shakura et al. 1978). In addition, the standard model should be modified since it is necessary to take into account non-Keplerian motion of gas in the disc due to a significant contribution of the pressure gradient in the equation of motion. It is also important to address the non-local character of the energy balance equation because the heat is effectively transported together with the radially moving matter (Paczynski and Bisnovatyi-Kogan 1981).

For quick estimates, one can use the following expressions. The boundary between zones A and B, where the gas pressure equals the radiative pressure, is located at

$$R_{\rm AB}/(3\,R_{\rm g}) \sim 80\,(m_x\,\alpha)^{2/21}\,(\dot{M}/\dot{M}_{\rm Edd})^{16/21}\,.$$

The boundary between zones B and C, where the cross-sections of absorption and scattering of photons are equal:

$$R_{\rm BC}/(3\,R_{\rm g}) \sim 330\,(\dot{M}/\dot{M}_{\rm Edd})^{2/3}\,.$$

The outer boundary of zone C, beyond which recombination of hydrogen starts:

$$R_{\rm C}/(3\,R_{\rm g}) \sim 10^5\,(\dot{M}/\dot{M}_{\rm Edd}/m_x)^{1/3}\,.$$

We have normalised here the accretion rate to its critical value $\dot{M}_{\rm Edd} = 1.4 \times 10^{18}\,m_x$ g/s (see Sect. 1.1), the radius, to the characteristic value of the inner radius of a disc around a compact object, $3\,R_{\rm g} \approx m_x \times 8.9 \times 10^5$ cm (see Sect. 1.4.4), and the mass of the central body, to the solar mass: $m_x = M/M_\odot$.

In this section, we consider only the stable zones of the disc where the standard model holds. In Sect. 1.5.1 we write down the standard disc equations (Shakura and Sunyaev 1973). In Sects. 1.5.2 and 1.5.3 we consider zones B and C, for which we present stationary solutions.

1.5.1 Equations of Vertical Structure

1.5.1.1 Equation of Hydrostatic Balance

The equation of hydrostatic equilibrium along the z-coordinate in the Newtonian metric in the case of a thin disc has the form:

$$\frac{1}{\rho}\,\frac{{\rm d}P}{{\rm d}z} = -\omega_{\rm K}^2\,z\,, \tag{1.83}$$

where $P(z)$ is the total pressure in the disc, equal to the sum of the radiation pressure $P_{\rm rad}(z) = aT^4/3$, where $a = 7.56 \times 10^{-15}$ erg/cm^3/K^4 is the radiation constant, and the gas pressure $P_{\rm gas}(z)$, which is determined from the equation of an ideal gas:

$$P_{\rm gas} = \frac{\rho}{\mu}\,\frac{kT}{m_{\rm p}}\,,$$

where μ is the mean molecular weight of matter in the disc, $T(z)$ is the temperature and $\rho(z)$ the density of the matter.

1.5.1.2 Energy Generation

The heat dissipated in the disc at a given radius between the plane of symmetry of the disc and a given level at height z is a function of the vertical coordinate z:

$$Q_{\rm vis}(z) = \int_0^z \varepsilon \, {\rm d}\tilde{z} \, .$$

The rate of energy generation ε [erg/cm^3/s] in a Keplerian disc is determined by the viscous stress tensor. From (1.75) we have:

$$\frac{{\rm d}Q_{\rm vis}}{{\rm d}z} = \frac{3}{2} \, \omega_{\rm K} \, w^{\rm t}_{r\varphi} \, . \tag{1.84}$$

The component of the turbulent viscosity tensor in the disc $w^{\rm t}_{r\varphi}(z)$ is locally expressed in terms of the total pressure in this location with the help of the α-parameter

$$w^{\rm t}_{r\varphi} = \alpha \, P \, .$$

These equations represent the simplest hypothesis regarding energy release in the disc. It is possible to model the disc vertical structure under more complicated assumptions. For example, Nakao and Kato (1995) study the case of a disc with turbulent diffusion determining the dependence of viscous heating, and the α-parameter itself, on z.

1.5.1.3 Radiative Transfer in the Disc

If the opacity in the disc does not exceed certain values, energy is transferred vertically towards the disc surfaces by electromagnetic radiation. Let us assume that the condition of local thermodynamic equilibrium (LTE) holds inside the disc, i.e. Kirchhoff's law applies, according to which (Sobolev 1969)

$$j_\nu = 4\pi \varkappa_{\rm a}(\nu) \, B_\nu(T) \, ,$$

where j_ν is the emission coefficient per gram [erg/Hz/s/g/sr], $\varkappa_{\rm a}(\nu)$ is the absorption coefficient per gram [cm^2/g], $B_\nu(T)$ is the Planck distribution [erg/Hz/cm^2/s/sr] and $T(z)$ is the temperature.

We write down the moments of the stationary equation for radiative transfer (Mihalas and Mihalas 1984), assuming that the medium is motionless in the direction of radiation propagation, along the z-axis. The zeroth moment of the transfer equation is given as a result of integrating the basic radiative transfer

equation over all solid angles. After integrating over all frequencies we get

$$\frac{1}{\rho}\frac{\mathrm{d}Q_{\mathrm{rad}}(z)}{\mathrm{d}z} = 4\pi(\varkappa_{\mathrm{P}}\, B(T) - \varkappa_{\mathrm{a}}\, J(z))\,, \tag{1.85}$$

where $\varkappa_{\mathrm{a}}$ is the frequency-averaged absorption coefficient per gram, which is equal to the Planck mean opacity coefficient $\varkappa_{\mathrm{P}}$ (Mihalas and Mihalas 1984) at thermodynamic equilibrium, $Q_{\mathrm{rad}}(z)$ is the radiative energy flux along the z-axis, $B(T) = \sigma_{\mathrm{SB}} T^4/\pi$ the Planck function integrated over frequency and $J(z)$ the mean intensity of radiation entering the layer $\mathrm{d}z$, integrated over frequency. The physical meaning of this equation is clear: the change in the flux of radiative energy is equal to the input of energy as a result of radiation of the matter (this term is written with the help of Kirchhoff's law) minus the energy absorbed by the matter.

The first moment of the equation of radiative transfer is obtained when we multiply it by the cosine of the angle to the unit area, divide by c, and integrate over all solid angles. This equation in principle expresses the conservation of the total momentum of radiation.

$$\frac{1}{\rho}\frac{\mathrm{d}P_{\mathrm{rad}}(\nu, z)}{\mathrm{d}z} = -(\varkappa_{\mathrm{a}}(\nu) + \varkappa_{\mathrm{s}}(\nu))\frac{Q_{\mathrm{rad}}(\nu, z)}{c}\,. \tag{1.86}$$

where $\varkappa_{\mathrm{s}}(\nu, z)$ is the scattering coefficient, which is generally frequency-dependent, $Q_{\mathrm{rad}}(\nu, z)$ is the radiative energy flux along the z-axis, and $P_{\mathrm{rad}}(\nu, z)$ is the radiation pressure at frequency ν. Thus, the radiation pressure force balances the change in momentum of the radiation caused by interaction with the matter.

If we consider the moments of the equation, we get rid of the angular coordinate. The mean intensity of the radiation J_ν is the zeroth moment of the intensity. The spectral flux of radiative energy Q_ν is the first moment, and the radiation pressure P_{rad} is the second moment. As is well known, every moment of the transfer equation contains a quantity a higher order. The solution to such systems of equations requires imposition of certain additional closing relations. The main closing method for an isotropic field is the Eddington approximation.

The mean intensity of radiation $J(z)$ is related by definition to the radiation energy density via the relation:

$$\varepsilon_{\mathrm{rad}} = \frac{4\pi J}{c}. \tag{1.87}$$

For an isotropic radiation field, there exists a simple relation between the radiation energy density and the radiation pressure:

$$P_{\mathrm{rad}} = \frac{\varepsilon_{\mathrm{rad}}}{3}\,. \tag{1.88}$$

This approximation works well in the case of a geometrically thin disc (optically thin as well as optically thick).

An optically thick disc (optical depth $\tau \gg 1$) may be studied in the 'diffusion approximation'. Let us consider the first moment of the radiative transfer equation (1.85). We assume that the change in $Q_{\rm rad}$ is insignificant there, and the left-hand side of (1.85) is zero. Thus, the radiation field spectrum is close to that of a blackbody: $J(z) = B(T)$. It follows from relation (1.87) that $\varepsilon_{\rm rad} = 4\pi B(T)/c \equiv aT^4$, and taking into account the isotropy of the radiation field, integrating the second moment of the radiative transfer equation (1.86) over frequency, we obtain:

$$\frac{c}{3\varkappa_{\rm R}\rho}\frac{{\rm d}(aT^4)}{{\rm d}z} = -Q_{\rm rad}\,, \tag{1.89}$$

where the Rosseland opacity $\varkappa_{\rm R}(z)$ is introduced

$$\frac{1}{\varkappa_{\rm R}} \equiv \frac{\int_0^\infty \frac{1}{\varkappa_{\rm a}(\nu)+\kappa_{\rm s}(\nu)}\frac{\partial B_\nu(T)}{\partial T}\,{\rm d}\nu}{\int_0^\infty \frac{\partial B_\nu(T)}{\partial T}\,{\rm d}\nu}\,. \tag{1.90}$$

If we consider quantities averaged over z, we obtain:

$$Q_{\rm rad} = \frac{1}{3}\frac{c}{\varkappa_{\rm R}\,\rho\,z_0}\,\varepsilon_{\rm rad}\,. \tag{1.91}$$

With allowance for convection, the vertical structure of discs was studied by Meyer and Meyer-Hofmeister (1982) for two variants of viscosity: proportional to the gas pressure and to the total pressure.

1.5.1.4 Dependence of the Surface Density on z

We introduce the quantity $\Sigma(z)$ for the surface density of the disc 'gathered' up to a certain height z, and with the help of this quantity we rewrite (1.41):

$$\frac{{\rm d}\Sigma}{{\rm d}z} = \rho\,. \tag{1.92}$$

1.5.2 Solution for the Vertical Structure

This section describes an approach to the solution of the disc vertical structure equations, proposed and implemented by Ketsaris and Shakura (1998). The method consists in finding similar solutions to the system of equations converted to a dimensionless form. The opacity coefficient and the rate of energy release are expressed as power-law functions of ρ and T. The obtained solution is compared to the numerical results of Suleimanov et al. (2007), and the agreement of the two methods is shown.

For sufficiently high temperatures ($> 10^6$ K), Thomson scattering off free electrons plays the most important part. The corresponding region of the disc, in which gas pressure dominates at the same time, is called zone B. Further out from the centre, where photo-ionization of ions from heavy elements and free-free transitions dominate, we have zone C. The contribution of radiation pressure to the total pressure in these two zones is neglected. In zone B, this assumption significantly limits the accuracy of the solution if $P_{\rm rad} \gtrsim (0.2\text{–}0.3)\, P_{\rm gas}$.

When calculating the disc vertical structure, we will assume that all heat from the work of viscous forces at given r and z is transformed to radiative energy. In particular, local energy balance (1.78) will apply. We replace everywhere $Q_{\rm rad}(z) = Q_{\rm vis}(z) = Q(z)$.

We list together the equations of the vertical structure of the disc (1.83), (1.84), (1.89), and (1.92):

$$\begin{aligned} \frac{1}{\rho}\frac{{\rm d}P}{{\rm d}z} &= -\omega_{\rm K}^2 z\,, \\ \frac{{\rm d}\Sigma}{{\rm d}z} &= \rho\,, \\ \frac{{\rm d}Q}{{\rm d}z} &= \frac{3}{2}\,\omega_{\rm K}\, w^{\rm t}_{r\varphi}\,, \\ \frac{c}{3\varkappa_{\rm R}\rho}\frac{{\rm d}(aT^4)}{{\rm d}z} &= -Q\,. \end{aligned} \tag{1.93}$$

The rate of energy release ε in α-discs is proportional to the pressure. The opacity coefficient is written as follows:

$$\varkappa_{\rm R} = \varkappa_0\,\frac{\rho^{\varsigma}}{T^{\Upsilon}}\,. \tag{1.94}$$

For hydrogen discs:

$$\varsigma = \Upsilon = 0, \quad \varkappa_0 = 0.4\,{\rm cm}^2/{\rm g}\,, \quad \text{if} \quad \varkappa_{\rm T} \gg \varkappa_{\rm ff}\,, \tag{1.95}$$

$$\varsigma = 1,\, \Upsilon = 7/2, \quad \varkappa_0 = 6.45\times 10^{22}\,{\rm cm}^5\,{\rm K}^{7/2}/{\rm g}^2\,, \quad \text{if} \quad \varkappa_{\rm ff} \gg \varkappa_{\rm T}\,, \tag{1.96}$$

and for discs with solar chemical abundances (Frank et al. 2002; Kurucz 1970, 1993):

$$\begin{aligned} \varsigma = \Upsilon = 0, \quad \varkappa_0 &= 0.335\,{\rm cm}^2/{\rm g}\,, \quad \text{if} \quad \varkappa_{\rm T} \gg \varkappa_{\rm ff}\,, \\ \varsigma = 1,\, \Upsilon = 7/2, \quad \varkappa_0 &\approx 5\times 10^{24}\,{\rm cm}^5\,{\rm K}^{7/2}/{\rm g}^2\,, \quad \text{if} \quad \varkappa_{\rm ff} \gg \varkappa_{\rm T}\,, \end{aligned} \tag{1.97}$$

Calculations of absorption in the plasma, including collective and quantum effects, electron degeneracy, etc., performed by the OPAL project at Livermore laboratory

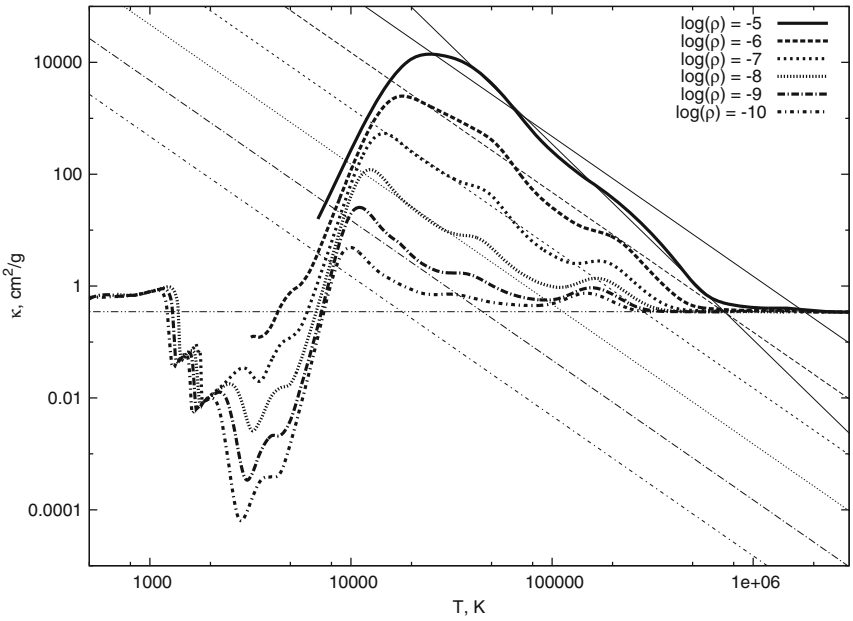

Fig. 1.5 Dependence of the opacity coefficient on density and temperature according to the OPAL project (Iglesias and Rogers 1996) and calculations for the low-temperature region in a medium with solar composition (Ferguson et al. 2005). The *horizontal line* corresponds to the value of the scattering coefficient off free electrons $\varkappa_0 \simeq 0.34\,\mathrm{cm}^2/\mathrm{g}$. Two fits are shown for a density of $\rho = 10^{-5}\,\mathrm{g/cm}^3$, namely, (1.98) and the dependence $\varkappa_\mathrm{R} = 1.2 \times 10^{25}\,\rho\,T^{-7/2}\,\mathrm{cm}^5\,\mathrm{K}^{7/2}/\mathrm{g}^2$ that gives a better fit in the high-temperature region (*solid lines*)

(Iglesias and Rogers 1996) (see Fig. 1.5) better fit another law in the absorption-dominated region:

$$\varsigma \approx 1,\ \Upsilon \approx 5/2, \quad \varkappa_0 \approx 1.5 \times 10^{20}\,\mathrm{cm}^5\,\mathrm{K}^{5/2}/\mathrm{g}^2\,, \quad \text{if} \quad \varkappa_\mathrm{ff} \gg \varkappa_\mathrm{T}\,. \tag{1.98}$$

For convenience, we introduce the dimensionless variable[3]

$$\sigma = \frac{2\,\Sigma(z)}{\Sigma_0}\,,$$

and in addition the dimensionless functions of this variable:

$$p = P(z)/P_\mathrm{c}\,, \quad \theta = T(z)/T_\mathrm{c}\,, \quad z' = z/z_0\,, \quad j = \rho(z)/\rho_\mathrm{c} \quad \text{and}\ q = Q(z)/Q_0\,.$$

[3]In the original paper by Ketsaris and Shakura (1998), the parameter Σ_0 was defined as half the total surface density of the disc. Due to this, there is a difference in the numerical coefficients in some of the formulas given below compared to the formulas in Ketsaris and Shakura (1998).

The symbols P_c, T_c, and ρ_c represent physical quantities in the equatorial plane of the disc and $Q_0 = (ac/4)\, T_{\rm eff}^4$ is the blackbody flux from one surface of the disc. We rewrite the system of Eq. (1.93) in the following form:

$$\begin{aligned}
&\frac{{\rm d}p}{{\rm d}\sigma} = -\Pi_1\, \Pi_2\, z' \,; \quad \Pi_1 = \frac{\omega_{\rm K}^2\, z_0^2\, \mu}{\Re\, T_c} \,; \\
&\frac{{\rm d}z'}{{\rm d}\sigma} = \Pi_2\, \frac{\theta}{p} \,; \qquad \Pi_2 = \frac{\Sigma_0}{2\, z_0\, \rho_c} \,; \\
&\frac{{\rm d}q}{{\rm d}\sigma} = \Pi_3\, \theta \,; \qquad \Pi_3 = \frac{3}{4}\, \frac{\alpha\, \omega_{\rm K}\, \Re\, T_c\, \Sigma_0}{Q_0\, \mu} \equiv \frac{\alpha\, \Re\, T_c\, \Sigma_0}{W_{r\varphi}\, \mu} \,; \\
&\frac{{\rm d}\theta}{{\rm d}\sigma} = -\Pi_4\, \frac{q\, j^\varsigma}{\theta^{\Upsilon+3}} \,; \; \Pi_4 = \frac{3}{32} \left(\frac{T_{\rm ef}}{T_c}\right)^4 \frac{\Sigma_0\, \varkappa_0\, \rho_c^\varsigma}{T_c^\Upsilon} \,.
\end{aligned} \tag{1.99}$$

The heating per gram $\varepsilon/\rho = \partial Q/\partial \Sigma$ determines the dependence of the temperature on z. In principle, the intensive mixing in the disc can lead to a situation where the energy output per unit mass is not dependent on the height z. The quantity ε depends in this case only on the density. The temperature dependence disappears from the equation describing the energy release (the third line in (1.99)), and Π_3 becomes equal to 1. A solution for such a case was also obtained by Ketsaris and Shakura (1998).

To find a solution to (1.99), i.e. to find the four functions $p(\sigma)$, $z'(\sigma)$, $q(\sigma)$, $\theta(\sigma)$ and the four unknown parameters, it is necessary to set eight boundary conditions—four at the surface of the disc and four in its symmetry plane. Ketsaris and Shakura (1998) performed a numerical integration of the equations and tabulated values $\Pi_{1..4}$. These values are given in Tables 1.1 and 1.2. Figure 1.7 shows functions $z'(\sigma)$, $p(\sigma)$, $\theta(\sigma)$, and $q(\sigma)$ in the Kramer opacity regime. Plots for other cases can be found in the work by Ketsaris and Shakura (1998).

In the symmetry plane of the disc for $\sigma = 0$, we have the obvious conditions:

$$p(0) = 1; \quad z'(0) = 0; \quad q(0) = 0; \quad \theta(0) = 1 \,.$$

The first two boundary conditions at the disc surface can also be straightforwardly determined as:

$$z'(1) = 1; \qquad q(1) = 1 \,.$$

The surface of the disc is defined as the level at which thermalization of radiation occurs. We may find boundary conditions for the pressure and temperature from approximate solutions to the equations of radiative transfer and hydrostatic balance close to the disc surface. Note that there is a difference in boundary conditions for different opacity regimes (see Fig. 1.6). In zone B, where absorption dominates, the disc surface is defined as the level in the photosphere where the optical depth,

Table 1.1 Dimensionless parameters of the solution to the equations of vertical structure for Thomson opacity versus the decimal logarithm of the free parameter δ

$\log \delta$	Π_1	Π_2	Π_3	Π_4
6.00	6.99	0.492	1.150	0.460
5.80	6.96	0.493	1.150	0.460
5.60	6.92	0.495	1.150	0.460
5.40	6.87	0.496	1.150	0.460
5.20	6.82	0.498	1.150	0.460
5.00	6.77	0.500	1.150	0.460
4.80	6.70	0.503	1.150	0.460
4.60	6.63	0.505	1.150	0.460
4.40	6.55	0.508	1.150	0.460
4.20	6.47	0.512	1.150	0.460
4.00	6.37	0.516	1.150	0.460
3.80	6.26	0.520	1.149	0.460
3.60	6.13	0.525	1.149	0.460
3.40	5.99	0.531	1.149	0.460
3.20	5.84	0.538	1.149	0.460
3.00	5.67	0.546	1.149	0.459
2.80	5.48	0.555	1.148	0.459
2.60	5.26	0.566	1.147	0.458
2.40	5.02	0.578	1.146	0.458
2.20	4.76	0.593	1.145	0.456
2.00	4.47	0.610	1.142	0.454
1.80	4.15	0.629	1.138	0.450
1.60	3.81	0.652	1.133	0.444
1.40	3.43	0.678	1.126	0.435
1.20	3.03	0.707	1.117	0.420
1.00	2.61	0.740	1.105	0.398
0.80	2.19	0.776	1.091	0.366
0.60	1.77	0.813	1.075	0.324
0.40	1.38	0.849	1.059	0.274
0.20	1.03	0.884	1.044	0.219
0.00	0.74	0.914	1.032	0.166

calculated from the outside inwards, is equal to 2/3. In the zone with predominant Thomson scattering, the disc surface is taken as the level where the effective optical depth, calculated including scattering, is equal to 1.

Let us derive the remaining boundary conditions in two opacity regimes.

1.5.2.1 Kramers Opacity

We will measure the optical depth τ from the surface of the disc in the direction of its symmetry plane, i.e. in the direction of decreasing height z. Deep inside the photosphere, where $\tau \sim 1$, we will use the solution to the equations of radiative

Table 1.2 Dimensionless parameters of the solution to the equations of vertical structure for Kramers opacity versus the decimal logarithm of the free parameter τ_0

$\log \tau_0$	Π_1	Π_2	Π_3	Π_4	$\log \tau$
6.00	7.75	0.465	1.131	0.399	6.046
5.80	7.71	0.466	1.131	0.399	5.847
5.60	7.67	0.468	1.131	0.399	5.646
5.40	7.62	0.469	1.131	0.399	5.445
5.20	7.56	0.471	1.131	0.399	5.245
5.00	7.50	0.473	1.131	0.399	5.045
4.80	7.44	0.475	1.131	0.399	4.845
4.60	7.36	0.477	1.131	0.399	4.644
4.40	7.27	0.480	1.131	0.399	4.444
4.20	7.18	0.483	1.131	0.399	4.244
4.00	7.07	0.487	1.131	0.399	4.043
3.80	6.95	0.491	1.131	0.399	3.843
3.60	6.82	0.496	1.131	0.399	3.643
3.40	6.67	0.501	1.131	0.399	3.443
3.20	6.50	0.508	1.131	0.398	3.243
3.00	6.31	0.515	1.131	0.398	3.043
2.80	6.10	0.524	1.130	0.398	2.842
2.60	5.87	0.534	1.130	0.398	2.642
2.40	5.60	0.546	1.129	0.397	2.442
2.20	5.31	0.560	1.128	0.397	2.241
2.00	4.98	0.576	1.126	0.395	2.040
1.80	4.62	0.596	1.124	0.393	1.839
1.60	4.23	0.619	1.120	0.389	1.638
1.40	3.79	0.647	1.114	0.383	1.434
1.20	3.33	0.679	1.106	0.371	1.232
1.00	2.83	0.716	1.095	0.354	1.025
0.80	2.34	0.756	1.081	0.326	0.819
0.60	1.86	0.798	1.065	0.286	0.613
0.40	1.42	0.838	1.050	0.237	0.406
0.20	1.05	0.876	1.036	0.185	0.202
0.00	0.75	0.908	1.025	0.136	−0.001

The rightmost column shows the decimal logarithm of the disc optical depth (1.114)

transfer and radiation balance for the case of LTE and for a frequency-independent absorption coefficient in the Eddington approximation (Sobolev 1969):

$$\frac{T}{T_{\rm eff}} = \left(\frac{1+\frac{3}{2}\tau}{2}\right)^{1/4} . \tag{1.100}$$

Let the dimensionless variable $\sigma = 1$ at the level where $\tau = 2/3$ and $T = T_{\rm eff}$. Using the definition of the parameter Π_4, we obtain the boundary condition for the

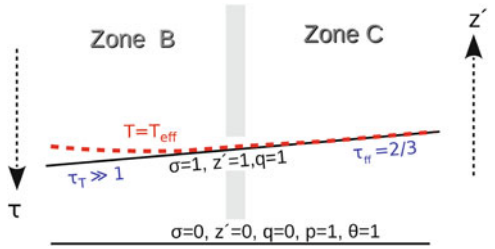

Fig. 1.6 The surfaces at which the boundary conditions are set, the upper surface of the disc and its equatorial plane (*solid lines*). Values of the dimensionless coordinate σ and functions at these surfaces are shown. The *arrows* indicate directions of increasing height $z' = z/z_0$ and optical depth τ, calculated from the exterior towards the equatorial plane. The two disc zones with different opacity regimes are separated nominally by the grey bar. In zone B (on the left), the optical depth at the disc surface $\tau_{\rm T}(\tau^* = 1) \gg 1$. In zone C (on the right), $\tau_{\rm ff} = 2/3$. The *dashed line* is the level where the disc temperature equals the effective temperature of the outgoing radiation

dimensionless temperature θ:

$$\theta\,(\sigma = 1) = \left[\frac{16}{3}\,\frac{\Pi_4}{\tau_0}\right]^{1/4},$$

where we have introduced the dimensionless parameter τ_0, proportional to the total optical depth of the accretion disc (see (1.96)):

$$\tau_0 = \frac{\Sigma_0\,\varkappa_0\,\rho_{\rm c}}{2\,T_{\rm c}^{7/2}}\,.$$

This quantity is a free parameter of the problem and varies widely (from a few to $\sim 10^6$).

To determine the boundary condition for the dimensionless pressure, we use the equation of hydrostatic balance (the first in system (1.93)). We divide both parts of this equation by the opacity coefficient $\varkappa_{\rm R}$ and replace variables using the formula

$$\mathrm{d}\,\tau = -\varkappa_{\rm R}\,\rho \mathrm{d}z$$

and making use of (1.96), arrive at:

$$\frac{1}{2}\,\frac{\mathrm{d}P^2}{\mathrm{d}\tau} = \frac{\omega_{\rm K}^2\,z_0\,\Re\,T^{9/2}}{\varkappa_0\,\mu}\,.$$

Close to the photosphere, the z coordinate practically does not change and is equal to z_0. Integrating the last equation from $\tau = 0$ to $\tau = 2/3$, we get as a result the

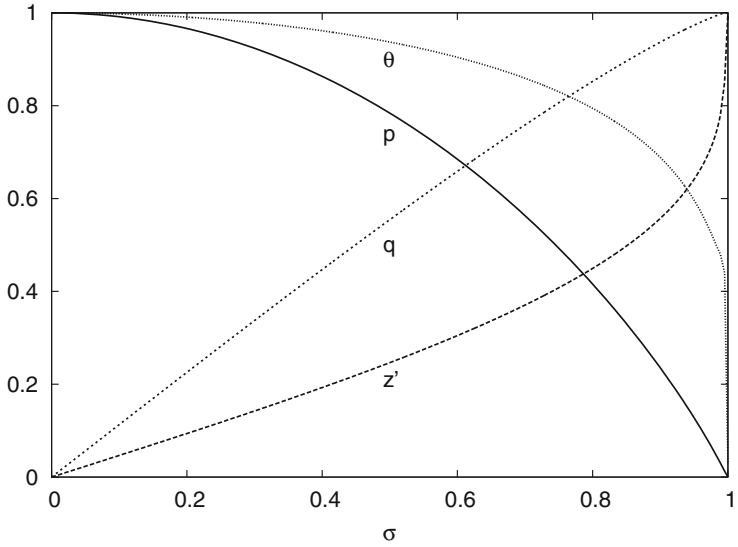

Fig. 1.7 Solution to the system of Eq. (1.99) in the form of dimensionless functions of the dimensionless variable σ, proportional to the column density: temperature $\theta(\sigma)$, pressure $p(\sigma)$, radiative flux $q(\sigma)$, and height from the equatorial plane $z'(\sigma)$. In the equatorial plane $\sigma = 0$, at the disc surface $\sigma = 1$

boundary condition for the dimensionless pressure:

$$p\,(\sigma = 1) = \left[\frac{3}{16 \times 2^{1/8}} \frac{\Pi_1\,\Pi_2}{\Pi_4} \left(\frac{16}{3} \frac{\Pi_4}{\tau_0} \right)^{17/8} f(\tau = 2/3) \right]^{1/2} ,$$

where

$$f(\tau) = \int_0^{\tau} (1 + \frac{3}{2}\tilde{\tau})^{9/8}\,\mathrm{d}\tilde{\tau}\,, \qquad f(\tau = 2/3) \approx 1.05\,.$$

Figure 1.7 shows the solution to the system of equations for the given case.

1.5.2.2 Thomson Scattering

If scattering processes are of high importance in the photosphere, thermalization occurs at the depth where the so-termed effective optical depth is of the order of 1:

$$\tau^* = -\int_{z_0}^{\infty} (\varkappa_{\mathrm{ff}}\,\varkappa_{\mathrm{T}})^{1/2}\,\rho\,\mathrm{d}z \approx 1\,.$$

The effective optical depth is accumulated as $\sqrt{\varkappa_{\rm ff}(\varkappa_{\rm T}+\varkappa_{\rm ff})}\,\rho\,{\rm d}z$ (see for example Zel'dovich and Shakura 1969, Mihalas 1978), which approximately gives the above condition. At this level, the optical depth due to scattering is much larger than 1:

$$\tau_{\rm T}(\tau^*=1) = -\int\limits_{z_0}^{\infty} \varkappa_{\rm T}\,\rho\,{\rm d}z \gg 1$$

and $T \simeq T_{\rm eff}\,(3\,\tau_{\rm T}/4)^{1/4}$ from (1.100). Thus, the boundary condition for the dimensionless temperature has the following form:

$$\theta\,(\sigma=1) \simeq \left[\frac{8\,\Pi_4\,\tau_{\rm T}(\tau^*=1)}{\varkappa_{\rm T}\,\Sigma_0}\right]^{1/4}.$$

For the pressure, we have:

$$p\,(\sigma=1) = 2\,\Pi_1\,\Pi_2\,\frac{\tau_{\rm T}(\tau^*=1)}{\varkappa_{\rm T}\,\Sigma_0}\,.$$

A convenient free parameter turns out to be the quantity

$$\delta = \frac{\varkappa_{\rm T}\,\Sigma_0/2}{\tau_{\rm T}(\tau^*=1)}\,. \tag{1.101}$$

This parameter is the ratio of half the total optical depth due to scattering to the optical depth due to scattering at the thermalization depth.

1.5.3 Radial Dependence of Physical Parameters in Stationary α-Discs

In order to explain observations of sources with accretion discs as extended objects, whose properties vary significantly from the centre to the periphery, we have to calculate radial dependencies of the disc physical parameters. For this it is necessary to solve the equation of angular momentum transfer, which was done for the case of a stationary disc in Sect. 1.4, and also to solve the equations of vertical structure (see the previous section). Analytical approximations for radial dependencies of the disc parameters were given in the work by Suleimanov et al. (2007). We will describe these analytical approximations below.

We consider the following physical parameters: surface density $\Sigma(r)$, disc half-thickness $z_o(r)$, density $\rho_{\rm c}(r)$ and temperature $T_{\rm c}(r)$ at the symmetry plane of the disc for $z = 0$. It is necessary to define what we consider to be the surface of the

disc. When studying observed spectra it turns out to be convenient to assume that the disc surface corresponds to the level where the Rosseland optical depth $\tau_{\rm R} = 2/3$.

The vertical structure of the disc is determined by Eq. (1.99) for known values of the dimensionless parameters $\Pi_{1..4}$. We express the quantities z_0, Σ, $\rho_{\rm c}$, and $T_{\rm c}$ from (1.99). The resulting expressions contain the basic given parameters of the disc (accretion rate, mass of the central object, the turbulent α-parameter) as well as the radial structure defined by $\omega_{\rm K}(r)$ and $W_{r\varphi}(r)$. We take the radial dependence of the vertically integrated component of the viscous stress tensor $W_{r\varphi}(r)$ for the case of a stationary disc (1.74), and the angular velocity of rotation we set equal to the Keplerian angular velocity $\omega_{\rm K} = \sqrt{GM/R^3}$. The radial distribution of the radiative flux from the disc surface is determined by viscous stresses $W_{r\varphi}(r)$. We recall that the function $f(R)$, which describes the influence of the boundary conditions on the surface tension $W_{r\varphi}(r)$, is written as (cf. (1.49)):

$$f(r) = \frac{2\,\pi\, W_{r\varphi}(r)}{\dot{M}\,\omega} = \frac{F}{\dot{M}\,h}$$

in a disc with constant accretion rate. For a thin disc with a stress-free inner radius, we have

$$f(r) = \frac{8\,\pi}{3}\,\frac{Q_{\rm vis}}{\dot{M}\,\omega^2} = 1 - \frac{h_{\rm in}}{h}\,.$$

For the case $\dot{M} = \dot{M}(r,t) \neq const$, it is necessary to use the function $f(r)$ in its general form

$$f(r) = \frac{F(h,t)}{\dot{M}_{\rm in}(t)\,h} = \frac{F(h,t)/h}{\partial F(h,t)/\partial h\big|_{h=h_{\rm in}}}\,. \tag{1.102}$$

We normalise the accretion rate at the inner boundary of the disc and other parameters to their characteristic values in binary systems with stellar mass components:

$$\begin{aligned} &M = m_x\,M_\odot, && \dot{M} = \dot{M}_{17}\times 10^{17}{\rm g/s},\\ &r = R_7\times 10^7{\rm cm\ (zone\ B)} && \text{or } r = R_{10}\times 10^{10}{\rm cm\ (zone\ C)}. \end{aligned} \tag{1.103}$$

As a characteristic value for the coefficient $\varkappa_0$ from expression (1.94) we use the quantity $\varkappa_{\rm T}^* = 0.335\,{\rm cm^2/g}$ in zone B, taken from an approximation to the tabulated values (Kurucz 1970, 1993), for a medium with mass fraction of hydrogen $X = 0.69$ and helium $Y = 0.27$ and $\varkappa_0^* = 5\times 10^{24}\,{\rm cm^5\,K^{7/2}/g^2}$ in zone C (see Frank et al. 2002, their chapter 5). The corresponding molecular weight μ=0.62. In a medium with such chemical composition, absorption of the radiation is mainly due to photoionization of ions of heavy elements. If we assume that all parameters $\Pi_{1..4}$ are equal to 1, $\varkappa_{\rm T} = 0.4\,{\rm cm^2/g}$, $\varkappa_0 = 6.4\times 10^{22}\,{\rm cm^5\,K^{7/2}/g^2}$, and $\mu = 0.5$, then the expressions for the radial dependencies of the physical parameters become identical to the expressions by Kato et al. (1998, their chapter 3) derived for hydrogen discs.

1.5.3.1 Zone B

In this zone, the main contribution to the optical depth comes from scattering off free electrons, and gas pressure dominates over radiation pressure. If we use expression (1.74) for the heat dissipated in the disc due to viscosity, normalising the parameters according to (1.103), we can solve the system of algebraic equations for $\Pi_{1..4}$ (the right part of the system (1.99)) and obtain:

$$
\begin{aligned}
z_0/r &= 0.0092\, m_x^{-7/20}\, \dot{M}_{17}^{1/5}\, \alpha^{-1/10}\, R_7^{1/20}\, f(r)^{1/5} \left(\frac{\mu}{0.6}\right)^{-2/5} \left(\frac{\varkappa_\mathrm{T}}{\varkappa_\mathrm{T}^*}\right)^{1/10} \Pi_z\,, \\
\Sigma_0 &= 5.1\times 10^3\, m_x^{1/5}\, \dot{M}_{17}^{3/5}\, \alpha^{-4/5} R_7^{-3/5}\, f(r)^{3/5} \left(\frac{\mu}{0.6}\right)^{4/5} \left(\frac{\varkappa_\mathrm{T}}{\varkappa_\mathrm{T}^*}\right)^{-1/5} \Pi_\Sigma\ [\mathrm{g/cm^2}], \\
\rho_\mathrm{c} &= 2.8\times 10^{-2}\, m_x^{11/20}\, \dot{M}_{17}^{2/5}\, \alpha^{-7/10}\, R_7^{-33/20}\, f(r)^{2/5} \left(\frac{\mu}{0.6}\right)^{6/5} \times \\
&\qquad \times \left(\frac{\varkappa_\mathrm{T}}{\varkappa_\mathrm{T}^*}\right)^{-3/10} \Pi_\rho\ [\mathrm{g/cm^3}], \\
T_\mathrm{c} &= 8.2\times 10^6\, m_x^{3/10}\, \dot{M}_{17}^{2/5}\, \alpha^{-1/5}\, R_7^{-9/10}\, f(r)^{2/5} \left(\frac{\mu}{0.6}\right)^{1/5} \left(\frac{\varkappa_\mathrm{T}}{\varkappa_\mathrm{T}^*}\right)^{1/5} \Pi_\mathrm{T}\ [\mathrm{K}].
\end{aligned}
\tag{1.104}
$$

The combinations of the dimensionless parameters Π_z, Π_Σ, Π_ρ, and Π_T are related in the following way to the parameters $\Pi_{1..4}$:

$$
\begin{aligned}
\Pi_z &= \Pi_1^{1/2}\, \Pi_3^{1/10}\, \Pi_4^{-1/10} \approx 2.6\,, \\
\Pi_\Sigma &= \Pi_3^{4/5}\, \Pi_4^{1/5} \approx 0.96\,, \\
\Pi_\rho &= \Pi_1^{-1/2}\, \Pi_2^{-1}\, \Pi_3^{7/10}\, \Pi_4^{3/10} \approx 0.67\,, \\
\Pi_\mathrm{T} &= \Pi_3^{1/5}\, \Pi_4^{-1/5} \approx 1.2\,.
\end{aligned}
\tag{1.105}
$$

Their values versus the free parameter δ are shown in Fig. 1.8, left panel. The free parameter δ is derived from the expression (1.101) and may be estimated from the total optical depth of the disc τ and other disc parameters in the following way:

$$
\delta = \sqrt{\frac{\kappa_0 \rho_\mathrm{c} T_\mathrm{c}^{-7/2}}{\varkappa_\mathrm{T}}}\, \tau\, X(\delta)\,, \tag{1.106}
$$

where $\tau = \varkappa_\mathrm{T}\, \Sigma_0/2$. The numerical factor

$$
X(\delta) = \delta \int_{1-1/\delta}^{1} (P/P_\mathrm{c})^{1/2}\, (T/T_\mathrm{c})^{-9/4} \mathrm{d}\sigma \sim 2\,, \tag{1.107}
$$

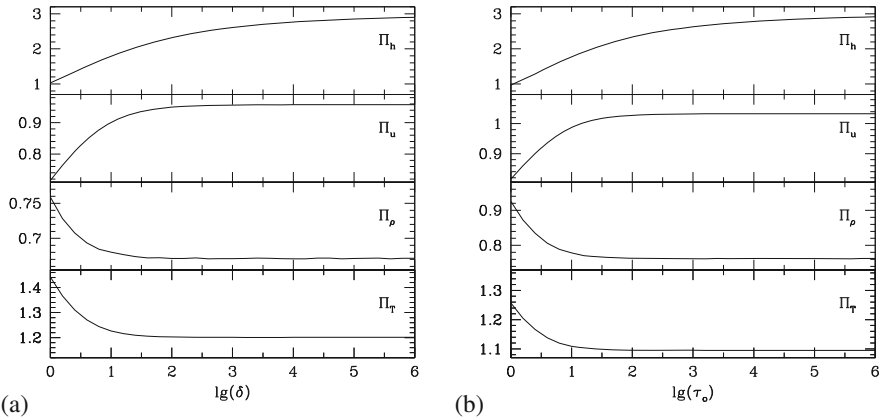

Fig. 1.8 (**a**) Left: The dependence of the dimensionless factors Π_z, Π_Σ, Π_ρ and Π_T for zone B (formulas (1.105)). (**b**) Right: The same factors for zone C (formulas (1.111)). The logarithms of the dimensionless parameters, characterizing the optical depth in each zone, are displayed along the horizontal axes. The dependencies are borrowed from Suleimanov et al. (2007) and constructed for values from Table 1.1 (graph to the left) and Table 1.2 (graph to the right)

which is independent of the absolute values of the disc parameters, is determined through integration of the equations of vertical structure. The value of δ may be found recursively with any desired precision, but this approach will be redundant in the sense of astronomical application of the obtained radial dependencies. It is sufficient to use the following estimate:

$$\delta = 440\, m_x^{-1/20}\, \dot{M}_{17}^{1/10}\, \alpha^{-4/5}\, R_7^{3/20}\, f(R)^{1/10} \left(\frac{\mu}{0.6}\right)^{21/20} \left(\frac{\varkappa_\mathrm{T}}{\varkappa_\mathrm{T}^*}\right)^{-1/5} \left(\frac{\varkappa_0}{\varkappa_0^*}\right)^{1/2}. \tag{1.108}$$

At high accretion rates, there is a zone in the disc where radiation pressure dominates (zone A). The radius at which the radiation pressure $a\,T_\mathrm{c}^4/3$ is comparable to the gas pressure $\rho_\mathrm{c}\Re T_\mathrm{c}/\mu$ in the symmetry plane of the disc (the boundary between zones A and B, see Shakura and Sunyaev (1973)) may be approximately estimated as

$$R_\mathrm{AB} \sim 10^7\, m_x^{1/3}\, \dot{M}_{17}^{16/21}\, \alpha^{2/21} \left(\frac{\mu}{0.6}\right)^{8/21} \left(\frac{\varkappa_\mathrm{T}}{\varkappa_\mathrm{T}^*}\right)^{6/7} \mathrm{cm}. \tag{1.109}$$

Here, we used characteristic values (1.105) for the dimensionless parameters $\Pi_{1..4}$ and $f(r) = 1$.

When the accretion rate decreases, zone B shifts radially towards the centre of the disc, giving way to zone C.

1.5.3.2 Zone C

The main contribution to the opacity in zone C comes from absorption processes in the form of free-free and bound-free transitions, and the gas pressure is much higher than the radiation pressure. As before, from the right-hand part of the system of Eq. (1.99) and from the expressions (1.74) and (1.103), we may find the radial dependencies of the parameters of the disc:

$$
\begin{aligned}
z_0/r &= 0.020\, m_x^{-3/8}\, \dot{M}_{17}^{3/20}\, \alpha^{-1/10}\, R_{10}^{1/8}\, f(r)^{3/20} \left(\frac{\mu}{0.6}\right)^{-3/8} \left(\frac{\varkappa_0}{\varkappa_0^*}\right)^{1/20} \Pi_z\,, \\
\Sigma_0 &= 33\, m_x^{1/4}\, \dot{M}_{17}^{7/10}\, \alpha^{-4/5}\, R_{10}^{-3/4}\, f(r)^{7/10} \left(\frac{\mu}{0.6}\right)^{3/4} \left(\frac{\varkappa_0}{\varkappa_0^*}\right)^{-1/10} \Pi_\Sigma \ [\mathrm{g/cm^2}], \\
\rho_\mathrm{c} &= 8.0\times 10^{-8}\, m_x^{5/8}\, \dot{M}_{17}^{11/20}\, \alpha^{-7/10}\, R_{10}^{-15/8}\, f(r)^{11/20} \left(\frac{\mu}{0.6}\right)^{9/8} \times \\
&\qquad \times \left(\frac{\varkappa_0}{\varkappa_0^*}\right)^{-3/20} \Pi_\rho \ [\mathrm{g/cm^3}], \\
T_\mathrm{c} &= 4.0\times 10^{4}\, m_x^{1/4}\, \dot{M}_{17}^{3/10}\, \alpha^{-1/5}\, R_{10}^{-3/4}\, f(r)^{3/10} \left(\frac{\mu}{0.6}\right)^{1/4} \left(\frac{\varkappa_0}{\varkappa_0^*}\right)^{1/10} \Pi_\mathrm{T} \ [\mathrm{K}],
\end{aligned}
\tag{1.110}
$$

We recall that $\dot{M}_{17}$ is the normalised accretion rate at the inner disc boundary. Note that if $\dot{M}(r,t) \neq const$, we need to substitute the value of the accretion rate at the inner boundary when using (1.104) and (1.110). This is convenient since in most cases this value determines the energetics of observed accreting systems.

The combinations of dimensionless parameters are related to the parameters $\Pi_{1..4}$ in the following way:

$$
\begin{aligned}
\Pi_z &= \Pi_1^{19/40}\, \Pi_2^{-1/20}\, \Pi_3^{1/10}\, \Pi_4^{-1/20} \approx 2.6\,, \\
\Pi_\Sigma &= \Pi_1^{1/20}\, \Pi_2^{1/10}\, \Pi_3^{4/5}\, \Pi_4^{1/10} \approx 1.03\,, \\
\Pi_\rho &= \Pi_1^{-17/40}\, \Pi_2^{-17/20}\, \Pi_3^{7/10}\, \Pi_4^{3/20} \approx 0.76\,, \\
\Pi_\mathrm{T} &= \Pi_1^{-1/20}\, \Pi_2^{-1/10}\, \Pi_3^{1/5}\, \Pi_4^{-1/10} \approx 1.09\,,
\end{aligned}
\tag{1.111}
$$

and are shown in Fig. 1.8b as a function of the free parameter τ_0,

$$
\tau_0 = \frac{\varkappa_0 \rho_\mathrm{c}}{T_\mathrm{c}^{7/2}}\, \frac{\Sigma_0}{2} = 500\, \frac{\dot{M}_{17}^{1/5}\, f(r)^{1/5}}{\alpha^{4/5}} \left(\frac{\mu}{0.6}\right) \left(\frac{\varkappa_0}{\varkappa_0^*}\right)^{2/5} \frac{\Pi_3^{4/5}\, \Pi_4^{3/5}}{\Pi_1^{1/5}\, \Pi_2^{2/5}}\,, \tag{1.112}
$$

approximately equal to

$$
\tau_0 \sim 300\, \dot{M}_{17}^{1/5}\, \alpha^{-4/5} \left(\frac{\varkappa_0}{\varkappa_0^*}\right)^{2/5}\,. \tag{1.113}
$$

The full optical depth of the disc

$$\tau = \int_0^h \varkappa_0 \, \rho^2 \, T^{-7/2} \mathrm{d}z \tag{1.114}$$

is determined in the process of numerical solution of the vertical structure and is uniquely dependent on τ_0 (see Table 1.2). We also give the following formula, approximating the tabulated values to an error of less than 1% for $\tau_0 > 6$:

$$\tau \approx 1.042 \, \tau_0^{1.006} \, . \tag{1.115}$$

The dependencies of the parameters in zones B and C are depicted in Figs. 1.9 and 1.10. The boundary between zones B and C is approximately determined from

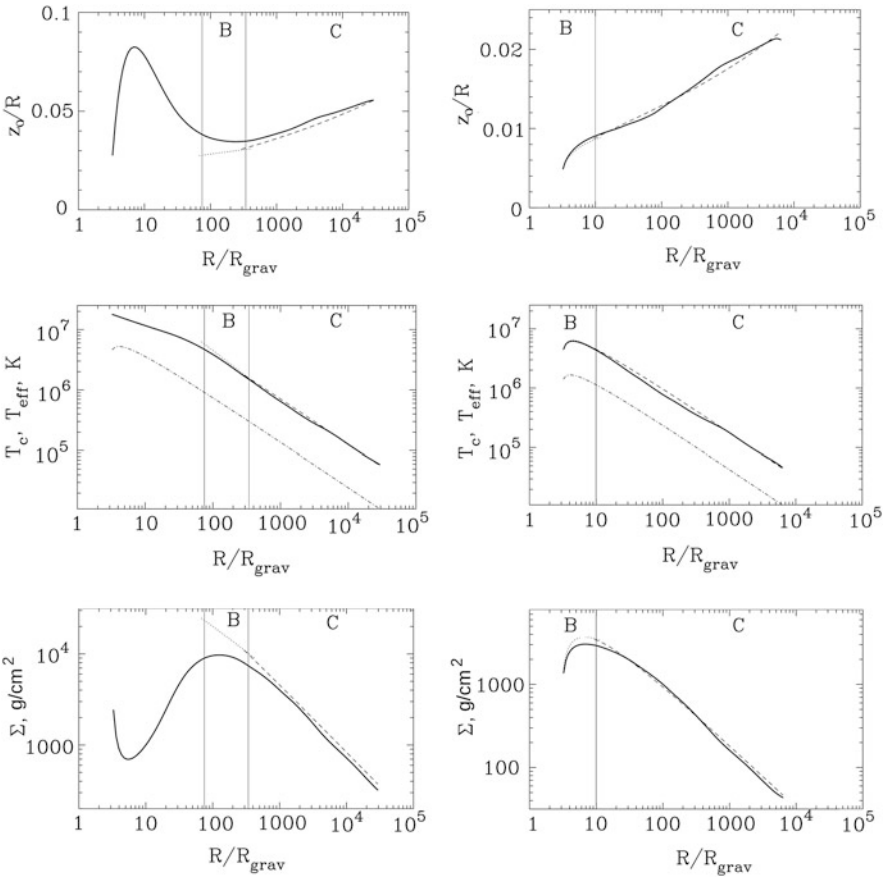

Fig. 1.9 From the top down: relative disc half-thickness z_0/r, central T_c and effective temperature $T_{\rm eff}$ (dot-dashes) and surface density Σ_0. The disc parameters are $m_x = 10$, $\mu = 0.62$, $\alpha = 0.3$, left: $\dot{M}_{17} = 33.6$ or $L_{\rm bol} = 0.2\, L_{\rm Edd}$, right: $\dot{M}_{17} = 0.336$ or $L_{\rm bol} = 0.002\, L_{\rm Edd}$. The *solid line* shows the result from the numerical calculation in Suleimanov et al. (2007). The *dotted line* shows the formulas (1.104) in zone B and the *dashed line* the formulas (1.110) in zone C. Figures from Suleimanov et al. (2007)

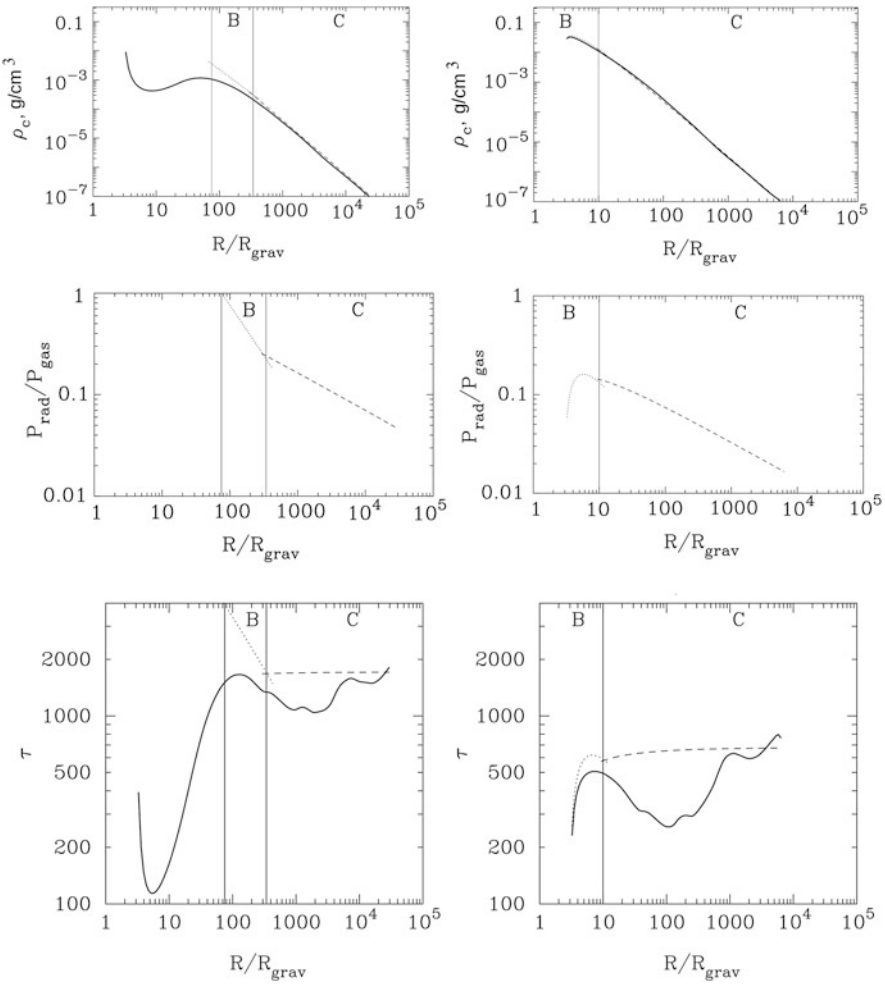

Fig. 1.10 From the top down: density in the disc symmetry plane ρ_c, ratio between radiation and gas pressure, and optical depth τ. Disc parameters: $m_x = 10$, $\mu = 0.62$, $\alpha = 0.3$, left: $\dot{M}_{17} = 33.6$ or $L_{bol} = 0.2\,L_{Edd}$, right: $\dot{M}_{17} = 0.336$ or $L_{bol} = 0.002\,L_{Edd}$. Notations as in Fig. 1.9. Figures from Suleimanov et al. (2007)

equating $\varkappa_T$ and $\varkappa_0 \rho T^{-7/2}$ in the equatorial plane of the disc

$$R_{BC} \sim 5 \times 10^7\, m_x^{1/3}\, \dot{M}_{17}^{2/3} \left(\frac{\mu}{0.6}\right)^{-1/3} \left(\frac{\varkappa_0}{\varkappa_0^*}\right)^{-2/3} \left(\frac{\varkappa_T}{\varkappa_T^*}\right)^{4/3} \text{cm}$$

for characteristic values of the dimensionless parameters $\Pi_{1..4}$ and $f(r) = 1$.

As outer boundary of zone C we take the radius where recombination of hydrogen atoms sets in (at $T_{eff} \sim 10^4$ K). When this happens, thermal instabilities in

the disc start developing, and due to a significant increase in the opacity coefficient of the matter, convection starts playing a role in the transfer of energy to the surface (Meyer and Meyer-Hofmeister 1981, 1982). In such regions, it is no longer correct to approximate the opacity coefficient $\varkappa_{\rm R}$ using Kramers law. Equating the right-hand side of (1.74) and $\sigma_{\rm SB}\, T_{\rm eff}^4$, we get:

$$R_{\rm C} \approx 3.5 \times 10^{10}\, m_x^{1/3}\, \dot{M}_{17}^{1/3} \left(\frac{T_{\rm eff}}{5000\ {\rm K}}\right)^{-4/3} {\rm cm}. \tag{1.116}$$

Due to irradiation of the outer parts of the disc by the central source, the boundary $R_{\rm C}$ can be further from the centre. This happens if the radiative X-ray flux, falling on the surface of the disc, thermalizes in its outer layers and heats them up so that the effective temperature of the disc surface does not drop below $\sim 10^4$ K (Dubus et al. 1999).

1.5.3.3 Thickness of the Disc

For the discs in binary systems with stellar-mass components during outbursts, the quantities $\lg(\delta)$ and $\lg(\tau_0)$ lie in the range of 2–4. For these values, the considered combinations of the quantities $\Pi_{1,2,3,4}$ practically do not change with radius, and inside each zone we may use the following characteristic values:

$$\text{(zone B)} \quad \Pi_z \approx 2.6, \quad \Pi_\Sigma = 0.96, \quad \Pi_\rho = 0.67, \quad \Pi_{\rm T} = 1.2, \tag{1.117}$$

$$\text{(zone C)} \quad \Pi_z \approx 2.6, \quad \Pi_\Sigma = 1.03, \quad \Pi_\rho = 0.76, \quad \Pi_{\rm T} = 1.09. \tag{1.118}$$

Let us consider a disc with matter consisting solely of hydrogen plasma ($\mu = 0.5$), choosing for the opacity a value $\varkappa_{\rm R} = 6.4 \times 10^{22}\, \rho\, T^{-7/2}$ cm^2/g (Kato et al. (1998); in the work by Shakura and Sunyaev (1973) a similar value was used), which is determined only by free-free electron transitions in the plasma. This value is two orders of magnitude less than the value of the opacity due to bound-free transitions $\varkappa_0^*$. However, the physical parameters depend only weakly on the opacity coefficient (1.110). For example, the half-thickness of the disc changes due to a direct decrease of $\varkappa_0$, μ, and also Π_z, since τ_0 decreases almost by a factor of 10 (see (1.112) and Fig. 1.8b). Thus, the disc half-thickness z_0 is $\sim 25\%$ less for $\mu = 0.5$ than for $\mu = 0.62$.

The numerical solution to the equations of vertical structure as described in this section gives a larger disc thickness compared to that of a vertically homogeneous disc, namely, the 'characteristic hydrostatic scale'. The latter is estimated as $v_{\rm s}/\omega$, where $v_{\rm s}$ is the sound speed in the disc symmetry plane. The presence of the factor two was indicated by Shakura and Sunyaev (1973). It is explained by the inhomogeneity of the distribution of density and temperature over the thickness of the disc. More exactly, this factor $\Pi_z \sim \sqrt{\Pi_1} \sim 2.5$, as can be seen from the first

line in the system of Eq. (1.99):

$$z_0 = \sqrt{\Pi_1}\sqrt{\frac{\Re\, T_\mathrm{c}}{\mu}}\,\frac{1}{\omega_\mathrm{K}}\,. \tag{1.119}$$

1.5.3.4 'Dead' Discs

The formulas (1.104) and (1.110), describing radial dependencies in a disc, may be applied also for 'dead' discs or disc reservoirs (Syunyaev and Shakura 1977), i.e. discs in which transfer of matter through the inner boundary is not possible and thus $\dot{M}_\mathrm{in} = 0$. Since the inner accretion rate and $f(r)$ always show up as multiplicative factors in (1.104) and (1.110), the formulas could be converted using $\dot{M}_\mathrm{in}(t)\, f(r) = F(h,t)/h$ (cf. (1.102)).

1.6 Non-stationary Disc Accretion

Outbursts in accreting sources, for example in binary systems and active galactic nuclei, are of special interest. Bright events can be observed by instruments operating in different ranges of the electromagnetic spectrum, supplying a wealth of data about the physics of distant stars. Recently, due to the boom in studies of exoplanets, the subject of disc evolution in protoplanetary systems has become topical in astrophysics.

Transient phenomena in discs may be caused by different kinds of instabilities, which in general develop on different time scales. In this section, we will address the set up of and solution to the problem of non-stationary accretion in a viscous disc. The problem corresponds to the disc evolution that takes place on viscous time scales due to redistribution of angular momentum of matter in the disc.

1.6.1 Basic Equation of Non-stationary Accretion

In Sect. 1.4.1 we introduced the following quantities, integrated along the disc thickness: the surface density Σ_0 (1.41) and the integrated component of the turbulent viscosity tensor $W_{r\varphi}$ (1.45). We write down again the obtained equations for conservation of mass and angular momentum (1.42) and (1.44):

$$\frac{\partial \Sigma_0}{\partial t} = -\frac{1}{r}\,\frac{\partial}{\partial r}(\Sigma_0\, v_r\, r)\,,$$

$$\Sigma_0\, v_r\, r\,\frac{\partial\,(\omega\, r^2)}{\partial r} = -\,\frac{\partial}{\partial r}\,(W_{r\varphi} r^2)\,.$$

Substituting the combination $\Sigma_0\, v_r\, r$ from the second line into the first, we obtain the basic equation for non-stationary accretion:

$$\frac{\partial \Sigma_0}{\partial t} = \frac{1}{r}\,\frac{\partial}{\partial r}\left[\frac{1}{\partial(\omega\, r^2)/\partial r}\,\frac{\partial}{\partial r}(W_{r\varphi}\, r^2)\right]. \tag{1.120}$$

This is an equation of diffusion type, a parabolic equation of the second order in partial derivatives.

The tensor component, integrated over the full thickness of the disc, is written in the framework of the gradient hypothesis of transfer of angular momentum by turbulent motions (1.38) in the following way:

$$W_{r\varphi}(r,t) = 2\int\limits_0^{Z_0} w^{\mathrm{t}}_{r\varphi}\,\mathrm{d}Z \;= 3\,\omega_{\mathrm{K}}\int\limits_0^{Z_0} \nu_{\mathrm{t}}\,\rho\,\mathrm{d}Z\,. \tag{1.121}$$

If the kinematic coefficient of the turbulent viscosity ν_{t} is independent of z, we get:

$$W_{r\varphi}(r,t) = \frac{3}{2}\,\omega_{\mathrm{K}}\,\nu_{\mathrm{t}}\,\Sigma_0\,. \tag{1.122}$$

We introduce as a new independent parameter the specific angular momentum $h(r) = v_\varphi(r)\, r = \omega\, r^2$. We further define the specific angular momentum of a free particle, rotating in a Newtonian potential, as the quantity $h_{\mathrm{K}} \equiv \sqrt{G\,M\,r}$. Herewith, $\mathrm{d}r = 2\,h_{\mathrm{K}}\,\mathrm{d}h_{\mathrm{K}}/(G\,M)$.

In the case of Keplerian orbits, Eq. (1.120) taken together with (1.122) is written in the following form:

$$\frac{\partial \Sigma_0}{\partial t} \;=\; \frac{3}{4}\,\frac{(G\,M)^2}{h^3}\,\frac{\partial^2(\Sigma_0\,\nu_{\mathrm{t}}\,h)}{\partial h^2}\,, \qquad h \equiv h_{\mathrm{K}}\,. \tag{1.123}$$

We also consider an alternative version of this equation, convenient from the point of view of establishing boundary conditions in an evolving disc. It is, in addition, more appropriate for α-discs in models where the viscosity is parametrized using the turbulent α-parameter considered as a constant value, rather than using the kinematic viscosity coefficient ν_{t}.

We introduce the quantity $F = 2\,\pi\, W_{r\varphi} r^2$, which is equal to the total viscous torque, acting between neighbouring rings in the disc. At constant accretion rate in the disc, and using for $W_{r\varphi}$ a notation of the form (1.49), for a stress free inner boundary $W_{r\varphi}(r = r_{\mathrm{in}}) = 0$, we may write the quantity of the total viscous torque in the following way:

$$F = \dot{M}\sqrt{G\,M\,r}\,\left(1 - \sqrt{\frac{r_{\mathrm{in}}}{r}}\right), \qquad \dot{M} = const\,. \tag{1.124}$$

As we can see, F is linearly proportional to the specific angular momentum $h = \sqrt{G\,M\,r}$ at large distances.

In the new variables, the equation of transfer of angular momentum (1.44) takes the form (note that v_r has a negative value):

$$-2\,\pi\,\Sigma_0\,v_r\,r\;=\dot{M}(r,t)=\left[\frac{\partial h}{\partial h_{\rm K}}\right]^{-1}\frac{\partial F}{\partial h_{\rm K}}\,, \tag{1.125}$$

and Eq. (1.120):

$$\frac{\partial\,\Sigma_0}{\partial t}=\frac{1}{4\,\pi}\,\frac{(GM)^2}{h_{\rm K}^3}\,\frac{\partial}{\partial h_{\rm K}}\left(\left[\frac{\partial h}{\partial h_{\rm K}}\right]^{-1}\frac{\partial F}{\partial h_{\rm K}}\right)\,. \tag{1.126}$$

For a Keplerian disc, by definition, $\partial h/\partial h_{\rm K}\equiv 1$.

Which method to use for solving the equation of non-stationary accretion (1.123), depends on the form of the turbulent viscosity coefficient $\nu_{\rm t}=\nu_{\rm t}(r,\,\Sigma_0)$. In the framework of the model for α-turbulence, when the turbulent viscosity tensor is proportional to the pressure in the disc, the form of $\nu_{\rm t}(r,\,\Sigma_0)$, or in other words, the relationship between F and Σ_0, necessary for solving (1.126), may be derived from the equations of vertical structure.

1.6.2 Solutions to the Linear Equation of Viscous Evolution in the Disc

If F is linearly dependent on the surface density Σ_0, in other words, if $\nu_{\rm t}$ is a function only of radius and does not depend on the surface density, then (1.123) becomes a linear differential equation of diffusion type. In 1952, Lüst found particular solutions to the equation of viscous accretion, proposed by his teacher Weizsäcker (1948), and described the principles of constructing a general solution to both infinite and finite problems.

For a disc of infinite extension, Lynden-Bell and Pringle (1974) used a method of superposition of particular solutions to the equation of viscous evolution and, in particular, found Green's functions for two types of boundary conditions at the inner boundary. With the help of Green's functions it is possible to find F or Σ at any moment in time and at any point for arbitrary initial conditions. The inner radius of the disc in their solution is equal to zero. On long time scales, the dependencies in the disc are self-similar and the accretion rate through the inner boundary declines as a power law $\dot{M}\propto t^{-(1+l)}$, where the parameter $l<1$. Pringle (1991) examined, with the help of Green's functions, an infinite disc with central inflow of angular momentum. This problem describes the evolution of a disc surrounding a binary system. A similar problem was solved by Tanaka (2011), with the difference that the inner boundary of the disc was considered to be located at a finite, non-zero

inner radius. King and Ritter (1998) studied the evolution of a disc with finite radius and constant $\nu_{\rm t}$, and found that the accretion rate declines exponentially with time. The problem of a finite disc was also studied numerically in Zdziarski et al. (2009). The special case of Green's function for a finite disc was constructed in Wood et al. (2001) for a zero inner boundary. The full Green's function, which can be used together with an arbitrary initial distribution for two types of boundary conditions, was found by Lipunova (2015). This work also described the procedure of constructing a solution with non-zero and variable accretion rate at the outer boundary.

Note that in all these cases, the characteristic viscous time scale $\tau_{\rm vis} \sim r^2/\nu_{\rm t}$ is constant in time.

1.6.3 Evolution of an Infinite Viscous Disc

Let us recall the solution obtained by Lynden-Bell and Pringle (1974). We write the kinematic viscosity coefficient in the form

$$\nu_{\rm t} = \nu_0\, r^b\ .$$

Then the relation $F = 3\,\pi\, h\, \nu_{\rm t} \Sigma_0$ (cf. (1.122)) may be written in the following way:

$$F = 3\,\pi\, h\, \nu_0\, \Sigma_0\, r^b\ . \tag{1.127}$$

For a Keplerian disc ($h \equiv h_*$), the equation of viscous torque (1.123) takes the following form:

$$\frac{\partial F}{\partial t} = \frac{3}{4}\,\nu_0\, h^{2b-2}\,(G\,M)^{2-b}\,\frac{\partial^2 F}{\partial h^2}\ , \tag{1.128}$$

or in a way similar to the notation in Lynden-Bell and Pringle,

$$\frac{\partial^2 F}{\partial h^2} = \frac{1}{4}\left(\frac{\kappa}{l}\right)^2 h^{1/l-2}\,\frac{\partial F}{\partial t}\ , \tag{1.129}$$

where the constant parameters are related in the following way:

$$\frac{1}{2\,l} = 2 - b\ , \qquad \kappa^2 = \frac{16\,l^2}{3\nu_0\,(G\,M)^{1/2l}}\ . \tag{1.130}$$

The general solution to the linear equation (1.129) may be found by expansion in eigenfunctions and superposition of particular solutions. The method of superposition allows for a general solution, satisfying the given initial or boundary conditions.

In the case of a linear equation, the method of separation of variables may also be used.

We will search for a particular solution of the form $F(h,t) = f(h_c\,\xi) \times \exp(-s\,t)$, where s is some constant of the same dimension as that of the inverse time, $\xi = h/h_c$, and h_c is some characteristic value of the specific angular momentum of the matter in the disc. Substituting such a function $F(h,t)$ into (1.129), we obtain a Lommel's transformation of the Bessel equation (see Sect. 4.31 in Watson 1944):

$$\frac{\mathrm{d}^2 f}{\mathrm{d}h^2} + \frac{s}{4}\left(\frac{\kappa}{l}\right)^2 h^{1/l-2} f = 0\,,$$

with the particular solution

$$f(x) = (k\,x)^l\,[A(k)\,J_l(k\,x) + B(k)\,J_{-l}(k\,x)]\,,$$

where J_l and J_{-l} are Bessel functions of non-integer order, $k^2 = s\,\kappa^2\,h_c^{1/l}$ and l are constants and $x = \xi^{1/2l} = (h/h_c)^{1/2l}$, where ξ is the normalised specific angular momentum. The general solution is equal to the superposition of particular solutions with all values of the parameters k, $A(k)$, $B(k)$ such that the specific boundary and initial conditions are satisfied:

$$F(h,t) = \int_0^\infty \exp\left(-\frac{k^2\,t}{\kappa^2\,h_c^{1/l}}\right)(kx)^l[A(k)\,J_l(k\,x) + B(k)\,J_{-l}(k\,x)]\,\mathrm{d}k\,. \qquad (1.131)$$

For example, the condition $F(h) = 0$ for $h = 0$ leads to the vanishing of all coefficients for Bessel functions with negative index: $B(k) \equiv 0$.

The following method was used to determine the coefficients $A(k)$ and $B(k)$. Let us choose a solution at $t = 0$, with the condition that all viscous stresses at the centre are equal to zero $F(h = 0) = 0$, and write it using (1.131) in the form

$$F(h, t = 0) = \int_0^\infty (kx)^l\,A(k)\,J_l(k\,x)\,\mathrm{d}k\,.$$

We now use the Hankel inversion theorem (chapter II, theorem 19 in Sneddon (1951), see also Watson (1944) and MacRobert (1932)) for continuous functions $f(k)$ in the form

$$f(k') = \int_0^\infty x\,J_l(k'x)\left[\int_0^\infty k\,f(k)\,J_l(k\,x)\mathrm{d}k\right]\mathrm{d}x \quad \text{for } l \geq -1\,.$$

Substituting $f(k) = k^{l-1} A(k)$, we see that the integral within square brackets is equal to $F(h, t = 0)/x^l$. It follows that

$$(k')^{l-1} A(k') = \int_0^\infty F(h)\, J_l(k' x)\, x^{1-l}\, \mathrm{d}x \,, \tag{1.132}$$

where $F_0(h) \equiv F(h, t = 0)$. From here we can determine the coefficients $A(k')$.

If the initial distribution $F_0(h)$ is given, then the solution to the linear differential equation (1.129) has the form

$$F(h, t) = \int_0^\infty G(h, h_1, t)\, F_0(h_1)\, \mathrm{d}h_1 \,,$$

where G is the Green's function that is the solution to (1.129) at all points for $h \neq h_1$ and $t \neq 0$, and for which it is true that $G = 0$ for $t < 0$ in physical systems. It is possible to consider Eq. (1.129) as a linear system with input signal $F_0(h_1)$ and output signal $F(h, t)$, in which the Green's function has the role of a 'weighting function'. As is well known, the Green's function itself is a 'response' of the system to a delta impulse input signal, that is, it is a solution to (1.129), if the initial condition is a Dirac δ-function:

$$F_0 = \delta(x - x_1); \qquad F(h, t) = G(x, x_1, t) \,.$$

Substituting this initial distribution into (1.132), we find an expression for $A(k)$:

$$A(k) = (k\, x_1)^{1-l}\, J_l(k x_1) \,.$$

To obtain the Green's function we substitute $A(k)$ in expression (1.131):

$$G(x, x_1, t) = x^l\, x_1^{1-l} \int_0^\infty \exp\left(-\frac{k^2\, t}{\kappa^2\, h_c^{1/l}}\right) k\, J_l(k x_1)\, J_l(k x)\, \mathrm{d}k \,.$$

The integral is found using Hankel's tables for integral transforms:

$$G(x, x_1, t) = \frac{\kappa^2\, h_c^{1/l}\, x^l\, x_1^{1-l}}{2\, t} \exp\left(-\frac{x_1^2 + x^2}{4t}\, \kappa^2\, h_c^{1/l}\right) I_l\left(\frac{x\, x_1}{2t}\, \kappa^2\, h_c^{1/l}\right) \,, \tag{1.133}$$

where I_l is a modified Bessel function of the first kind (an Infeld function). Figure 1.11 shows the Green's function at four moments in time.

Let us choose the initial distribution F_0 in the form of a Dirac delta function with a physically motivated normalisation. We assume that the initial configuration is a

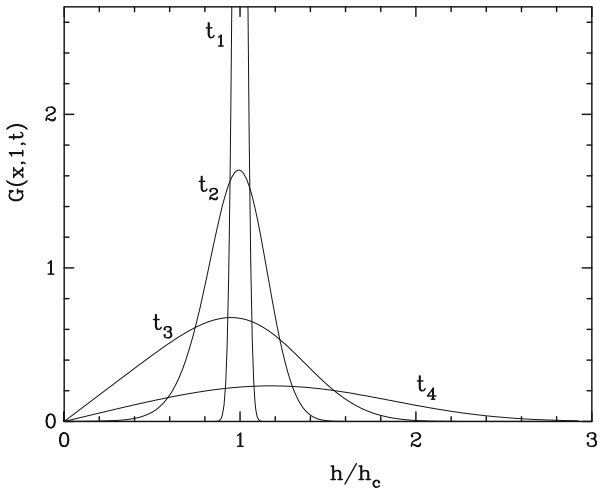

Fig. 1.11 The Green's function (1.133), found by Lynden-Bell and Pringle (1974), at four moments in time: $t_1 = 0.001$, $t_2 = 0.03$, $t_3 = t_{\max} = 0.1875$ and $t_4 = 1$. The parameters of the solution are $\kappa = 1$, $h_c = 1$, $l = 1/3$, $x_1 = 1$

narrow ring at radius r_s with total mass M_0. The specific angular momentum at this radius is equal to $h_s = x_s^{2l} h_c$. We write down the surface density for $t = 0$ as $\Sigma_0(h, t = 0) = M_0 \delta(r - r_s)/2\pi r_s$. Using (1.127) and (1.130) we obtain for the earlier introduced variable $x = (h/h_c)^{1/2l}$:

$$F_0(x) = 2\, l\, M_0\, h_c^{1-1/l}\, \kappa^{-2}\, x_s^{2l-1}\, \delta(x - x_s)\ .$$

Here we used the equality $\delta(x - x_s)\,\mathrm{d}x = \delta(r - r_s)\,\mathrm{d}s$. The evolution of this narrow ring is determined with the help of the obtained Green's function:

$$F(x, t) = \int_0^\infty F_0(x_1)\, G(x, x_1, t)\,\mathrm{d}x_1$$

and has the explicit form:

$$F(x, t) = \frac{M_0\, h_c\, l\, (x\, x_s)^l}{t}\, \exp\left(-\frac{x_s^2 + x^2}{4t}\, \kappa^2\, h_c^{1/l}\right) I_l\left(\frac{x\, x_s}{2t}\, \kappa^2\, h_c^{1/l}\right)\ . \tag{1.134}$$

We now consider the accretion rate at the inner boundary $\dot{M}_{\rm in} = (\partial F/\partial h)|_{h\to 0}$:

$$\dot{M}_{\rm in}(t) = \frac{x^{1-2l}}{2\, l\, h_c}\, \frac{\partial F(x, t)}{\partial x}\Big|_{x\to 0} = \frac{M_0\, \tau_e^l}{\Gamma(l)}\, \frac{e^{-\tau_e/t}}{t^{1+l}}\ .$$

It is possible to rewrite the accretion rate using its peak value

$$\dot{M}_{\rm in}(t) = \dot{M}_{{\rm in},max} \left(\frac{\tau_{\rm pl}}{t}\right)^{1+l} e^{-\tau_e/t} ,$$

where we have introduced the characteristic time scale for exponential growth τ_e and power-law decline $\tau_{\rm pl}$:

$$\tau_e = \frac{\kappa^2 h_{\rm s}^{1/l}}{4} = \frac{1+l}{e} \tau_{\rm pl} .$$

The accretion rate reaches its peak value

$$\dot{M}_{{\rm in},max} = \frac{M_{\rm disc}}{t_{\rm max}} \frac{(1+l)^l}{e^{1+l}\,\Gamma(l)} \tag{1.135}$$

at time

$$t_{\rm max} = \frac{\kappa^2 h_{\rm s}^{1/l}}{4(1+l)} = \frac{\tau_{\rm pl}}{e} . \tag{1.136}$$

1.6.4 Solution for a Disc with a Fixed Outer Radius

The boundary conditions are of high importance for the type of solution to Eq. (1.128). Above, we considered a solution in which the disc increases in size without limitation. A part of the matter in the disc will with time acquire very high values of the specific angular momentum. In a number of astrophysical situations, it is clear that it is necessary to set conditions at a finite radius from the centre. This concerns generally discs in binary systems. The torque of tidal forces, appearing due to gravitational influence of the companion star and acting predominantly in the narrow area inside the Roche lobe, leads to the disc being truncated at a certain radius (Papaloizou and Pringle 1977; Paczynski 1977; Ichikawa and Osaki 1994; Hameury and Lasota 2005). Near the truncation radius, angular momentum is transferred from the disc to orbital motion of the binary system.

Thus, the problem now needs to be solved for a finite interval. The method of superposition of partial solutions is modified, and the general solution is found not as an integral (1.131), but as a sum of all the partial solutions that fulfill the specific boundary conditions (Lüst 1952):

$$F(x,t) = \sum_{i=1}^{\infty} e^{-t\,k_i^2\,\kappa^{-2}\,h_{\rm out}^{-1/l}} (k_i\,x)^l \left[A_i\,J_l(k_i\,x) + B_i\,J_{-l}(k_i\,x)\right] , \tag{1.137}$$

Here we have also changed the characteristic value of the specific angular momentum to the value at the outer boundary $h_{\rm out}$, where the dimensionless parameter $x = 1$.

Let us set the boundary conditions at the outer radius of the disc:

$$\frac{\partial F}{\partial h} = \dot{M}_{\rm out}(t) \ \text{ at } \ h = h_{\rm out} \, . \tag{1.138}$$

In the simplest case, if $\dot{M}_{\rm out}(t) = 0$, this will be a homogeneous Dirichlet boundary condition. At the inner radius, we consider the same condition as earlier: $F(h) = 0$ for $h = 0$. The use of these two conditions gives an equation that every particular solution has to satisfy, that is, for any k

$$l \, J_l(k_i) + k_i \, J_l'(k_i) = 0 \, . \tag{1.139}$$

Since there in the series, representing the general solution, remain only terms with Bessel functions of positive order, the general solution at the starting point $t = 0$ is:

$$F(x, 0) = \sum_{i=1}^{\infty} (k_i \, x)^l \, A_i \, J_l(k_i \, x) \, . \tag{1.140}$$

Series of the form $\sum\limits_{i=1}^{\infty} k_i^l \, A_i \, J_l(k_i \, x)$ with the condition (1.139) are called Dini series (see Watson 1944, Sect. 18.11). The function $f(x) = F(x, 0) \, x^{-l}$ can be expanded in Dini series if it satisfies the Dirichlet conditions at the given interval, and the coefficients of the expansion can be found as $k_i^l \, A_i = 2 \, \bar{f}_J(k_i) \, J_l^{-2}(k_i)$ (Watson 1944; Sneddon 1951), where we have used the finite Hankel transform

$$\bar{f}_J(k_i) = \int\limits_0^1 x \, f(x) \, J_l(k_i \, x) \, {\rm d}x \, .$$

To find the Green's function, we search for a solution to an initial condition of the form of a δ-function: $F(x, 0) = \delta(x - x_1)$. Using its properties, substituting $f(x)$ into the last expression, we get:

$$k_i^l \, A_i = 2 \, x_1^{1-l} \frac{J_l(k_i \, x_1)}{J_l^2(k_i)} \, . \tag{1.141}$$

In this way we obtain the Green's function for a finite disc (Lipunova 2015):

$$G(x, x_1, t) = 2 \, x^l \, x_1^{1-l} \sum_i e^{-t \, k_i^2 \, \kappa^{-2} \, h_{\rm out}^{-1/l}} \, \frac{J_l(k_i \, x_1) \, J_l(k_i \, x)}{J_l^2(k_i)} \, , \tag{1.142}$$

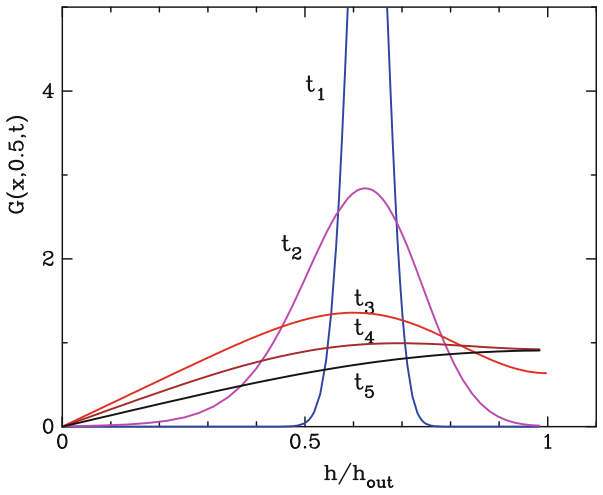

Fig. 1.12 Green's function of a finite disc with a zero torque at the centre at times $t_1 = 0.001$, $t_2 = 0.01$, $t_3 = t_{max}^{\infty} = 3/64$, $t_4 = 0.1$, $t_5 = 0.3$. The ring of matter was located at $x_s = (h/h_{\rm out})^{1/2l} = 0.5$ at time $t = 0$. The parameters are $\kappa = 1$ and $l = 1/3$

where k_i are the positive roots of the transcendental equation (1.139) and $x = (h/h_{\rm out})^{1/2l}$. The Green's function is depicted in Fig. 1.12 for a few moments in time. The curve at $t_3 = t_{\rm max}$ (see (1.136)) corresponds to the maximum accretion rate through the inner boundary of the disc.

For a specific initial distribution $F(x, 0)$, the distribution at any point in time $t > 0$ can be found as

$$F(x,t) = \int_0^1 F(x_1,0)\, G(x,x_1,t)\, {\rm d}x_1\,. \tag{1.143}$$

The accretion rate at any point in time $t > 0$ is

$$\dot{M}(x,t) = \int_0^1 F(x_1,0)\, G_{\dot{M}}(x,x_1,t)\, {\rm d}x_1 \Big/ h_{\rm out}\,, \tag{1.144}$$

where the Green function for the accretion rate is

$$\begin{aligned} G_{\dot{M}}(x,x_1,t) &\equiv \frac{\partial G(x,x_1,t)}{\partial x^{2l}} = \\ &= \frac{(x\,x_1)^{1-l}}{l} \sum_i e^{-t\,k_i^2\,\kappa^{-2}\,h_{\rm out}^{-1/l}}\, k_i\, \frac{J_l(k_i\,x_1)\,J_{l-1}(k_i\,x)}{J_l^2(k_i)}\,. \end{aligned} \tag{1.145}$$

The functions G and $G_{\dot{M}}$ in the particular case of $x_1 = 1$ are found in the form of analytical asymptotics by Wood et al. (2001).

The initial distribution F can be expressed through the distribution of surface density, using (1.127) and (1.130):

$$F(x,0) = \frac{16\,\pi\,l^2}{\kappa^2\,h^{1/l}}\,r^2\,\Sigma(r)\,h\,, \tag{1.146}$$

where $r = h^2/GM$ and $h = h_{\rm out}\,x^{2l}$.

For large times t, the first term in the sum (1.145) dominates and the time dependence can be expressed as a simple exponential:

$$G_{\dot{M}}(0,x_1,t)\Big|_{t>t_{\rm vis}} = \frac{k_1^l\,x_1^{1-l}}{2\,l\,\Gamma(l)}\,\frac{J_l(k_1\,x_1)}{J_l^2(k_1)}\,\exp\left(-\frac{t\,k_1^2}{2\,l\,t_{\rm vis}}\right)\,.$$

The characteristic time scale for exponential decrease of the accretion rate is equal to:

$$t_{\rm exp} = h_{\rm out}^{1/l}\,\frac{\kappa^2}{k_1^2} = \frac{16\,l^2}{3\,k_1^2}\,\frac{r_{\rm out}^2}{\nu_{\rm out}}\,, \tag{1.147}$$

where we have taken into account that $\nu_{\rm out} = \nu_0\,r_{\rm out}^b$. In Table 1.3, the first zero k_1 of the equation is shown for typical values of l. The table also provides the coefficients for calculating characteristic time scales for the growth (1.136) and the exponential decay (1.147) of the solution.

The disc becomes quasi stationary (i.e. the accretion rate practically does not change with radius) in regions where $r/r_{\rm out} < (t/t_{\rm exp})^{2\,l}$. The establishment of quasi stationarity in the central regions of the disc on viscous time scales is a common property for discs with any type of viscosity.

Table 1.3 Parameters of the Green function for a non-stationary disc

b	l	k_1	$t_{\rm max}(r_{\rm s}^2/\nu_{\rm s})^{-1}$	$t_{\rm exp}(r_{\rm out}^2/\nu_{\rm out})^{-1}$	a_0	Comments
0	1/4	1.0585	1/15	0.298	1.267	$\nu = const$
1/2	1/3	1.2430	1/9	0.383	1.363	α-disc with $h/r = const$
3/5	5/14	1.2927	0.125	0.407	1.392	α-disc, $\tau_{\rm T} \gg \tau_{\rm ff}$
3/4	2/5	1.3793	0.152	0.449	1.444	α-disc, $\tau_{\rm ff} \gg \tau_{\rm T}$
1	1/2	1.5708	2/9	0.540	1.571	$F(h) \propto \sin((\pi/2)\,h/h_{\rm out})$
2	∞	–	–	–	–	$t_{\rm vis}$ independent of r

The columns are: Exponent in the power law $\nu \propto r^b$; l from expression (1.130); the first zero of Eq. (1.139); the numerical factor from (1.136) the numerical factor from (1.147); the parameter describing the radial profile, $a_0 = \dot{M}_{\rm in}\,h_{\rm out}/F_{\rm out}$. The solution to the linear equation may apply to α-discs on timescales of the order of or shorter than the viscous timescale. For α-discs the type of opacity is shown

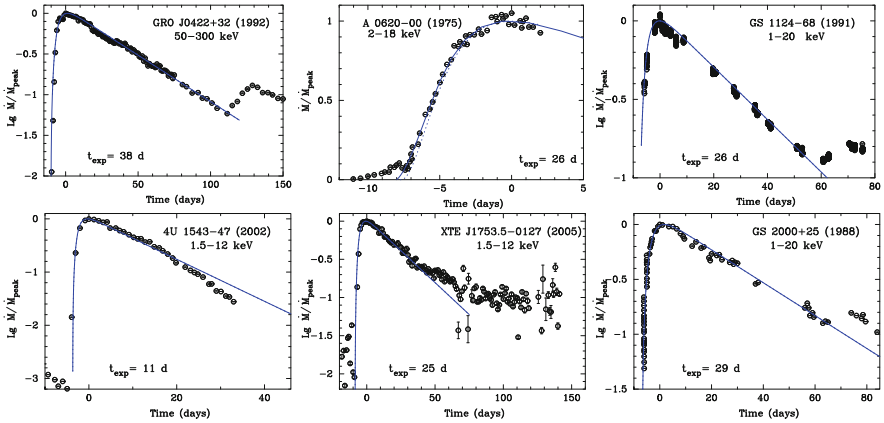

Fig. 1.13 Normalised lightcurves of the X-ray novae GRO J0422+32 (1992), A 0620-00 (1975), GS 1124-68 (1991), GS 2000+25 (1998) from Chen et al. (1997), 4U 1543-47 (2002) and XTE J1753.5-0127 (2005) (results from ASM/*RXTE*). The X-ray energy range for each flare is indicated in the plots. The solid curves show the peak-normalised accretion rates through the inner boundary calculated according to (1.144) for $l = 2/5$ and $t_{\rm exp}$ as indicated for each flare. The initial distribution of surface density in the disc is $\Sigma \propto r$ and the initial inner radius of the hot zone is $0.01 \times r_{\rm out}$. For A 0620-00, two model lightcurves are shown, for inner radii, at $t = 0, 0.001 \times r_{\rm out}$ (*solid line*) and $0.3 \times r_{\rm out}$ (*dotted line*), respectively. Figure from Lipunova (2015)

Bright X-ray flares, known as outbursts of X-ray novae, are observed in binary systems consisting of a compact object and a low-mass normal star. It is well known that in the 'simplest' cases, outbursts in X-ray novae show lightcurves with a fast rise and an exponential decay, which are called FRED profiles (Chen et al. 1997). Such lightcurves are nicely produced within the framework of the model for viscous discs with a viscosity coefficient constant on time scales of the order of $t_{\rm vis}$ (Fig. 1.13). This is explained by the fact that on time scales of the order of one to two $t_{\rm vis}$, a non-stationary α-disc and a disc such as considered in this section show similar evolution.

In order to fit the constant-viscosity solution to the evolution of a viscous α-disc, it is necessary to estimate the most appropriate value of parameter b in (1.128). This can be done using the relation (1.40) between the kinematic viscosity and the turbulence parameter:

$$\nu_{\rm t} = \nu_0\, r^b \simeq \frac{2}{3}\,\alpha\,\omega_{\rm K}\,r^2\,\left(\frac{z_0}{r}\right)^2\,\frac{1}{\Pi_1}, \tag{1.148}$$

where the parameter Π_1 shows up from a consideration of the vertical structure, see (1.99). The solution for a stationary disc with dominant gas pressure and Kramers opacity gives $z_0/r \propto r^{1/8}$ (see (1.110)), thus $b \simeq 3/4$ or, equally, $l \simeq 2/5$, if we neglect the dependence of the disc thickness on the accretion rate.

One can estimate α for an X-ray nova using (1.147) and (1.148) (Lipunova and Malanchev 2017):

$$\alpha \sim 0.15 \left(\frac{r_{\rm out}}{2\,R_\odot}\right)^{3/2} \left(\frac{z_0/r_{\rm out}}{0.05}\right)^{-2} \left(\frac{M}{10\,M_\odot}\right)^{-1/2} \left(\frac{t_{\rm exp}}{30^{\rm d}}\right)^{-1} \times \Pi_1\,. \qquad (1.149)$$

Here, one should substitute z_0 corresponding to the peak of an X-ray nova outburst. The main uncertainty in the above formula is the radius of the disk. In addition, the evolution of the thickness of the α-disk leads to a variation of the numerical factor in (1.149). However, a numerical modelling of the disk evolution can provide a self-consistent value of α (see Sect. 1.7.3).

1.6.5 Solution to the Non-linear Equation for the Evolution of a Viscous α-Disc

Earlier we considered the case when the coefficient of kinematic viscosity depends solely on the radial coordinate in the disc. In the more general case, we may represent $\nu_{\rm t}$ as a power-law function of Σ and r. Such a dependence arises in particular if we consider discs with α-viscosity. In this case, (1.123) becomes a non-linear differential equation in partial derivatives. To search for a solution to such an equation, similarity methods can be used in many cases. A self-similar solution to a non-linear differential equation accurately describes the evolution if enough time has passed since the initial moment.

As we have seen in the previous section, self-similar solutions to a linear differential equation are characterized by the possibility to completely separate the time and coordinate parts of the solution. A particular solution is thus a product of functions of different variables. In the case of a nonlinear differential equation, such a simple separation is in general not possible. To approach the problem, we may use the method of introducing new dimensionless variables (parameters), which contain combinations of the dimensional parameters (for example time and coordinates) raised to various powers.

Self-similar solutions to non-linear differential equations can be divided into two kinds (Barenblatt 1996, 2003). The self-similar solution is of the first kind if the self-similar function, as well as the new dimensionless parameter, can be derived from dimensional analysis. This case is also called a complete self-similarity. The second kind, or incomplete self-similarity, is the more general case. Here the self-similar function is a particular solution to the problem itself (a non-linear eigenvalue problem, see Zeldovich and Raizer (1967)). A dimensional analysis does not allow us to determine the self-similar function, and in particular, find to which powers the dimensional parameters should be raised to produce a self-similarity dimensionless variable. For incomplete self-similarity, the type of solution depends on the value of the self-similar variable.

If the constant coefficients in a self-similar function can be found from conservation laws, then the self-similar solution will be of the first kind (for example energy conservation in J. I. Taylor's blast wave (Barenblatt 2003)) and conservation of the total angular momentum in an accretion disc (see further Sect. 1.6.6.3)). Self-similar solutions of the first kind were found for accretion discs with a nonlinear viscous diffusion equation in the stage of evolution when the accretion rate is decaying (Pringle 1974, 1991). Solutions of the second kind have also been constructed (Lyubarskij and Shakura 1987). These solutions apply to an earlier evolutionary stage, that is, the spreading of an original ring of matter into a disc around the gravitating centre.

The form of the turbulence parameter ν_t is determined by the physical structure of the disc, which is dependent on the astrophysical conditions. For an α-disc with two variants of opacity (Kramers' law and Thomson scattering), within the framework of self-similar solutions of the first kind, it was found that the accretion rate declines as $\propto t^{-19/16}$ and $\propto t^{-5/4}$, respectively (Pringle 1974; Filipov 1984; Lyubarskij and Shakura 1987; Cannizzo et al. 1990; Pringle 1991). Lin and Pringle (1987) considered a molecular disc with a gravitational instability generating an effective viscosity $\nu_t \propto \Sigma^2 r^{9/2}$, and found that $\dot{M} \propto t^{-6/5}$. Lin and Bodenheimer (1982) studied the evolution of a protoplanetary disc under the influence of convective turbulent viscosity ($\nu_t \propto \Sigma^2$), for which $\dot{M} \propto t^{-15/14}$. Ogilvie (1999) investigated an advective accretion flow, the structure of which considerably differs from that of a thin viscous disc, and, using similarity methods, found a solution in the case of conserved total angular momentum.

The type of solution also depends on the boundary conditions. Pringle (1991) in addition considered the general case of an infinite cold protostellar disc with $\nu_t \propto \Sigma^3$ and a central source of angular momentum. Such a formulation of the problem corresponds to the evolution of a disc around a young binary system (see also Ivanov et al. 1999). In Rafikov (2013), a detailed consideration of the evolution of discs around binary black holes was presented, and self-similar solutions were found with different conditions at the inner boundary, suggesting a certain mass transfer through the inner boundary. Rafikov (2016) built self-similar solutions for a 'decretion' disc (disc with mass ejection from the centre).

For a disc with a zero (or very small) viscous stress at the inner boundary and with a limited outer radius, a solution was found by Lipunova and Shakura (2000). According to them, $\dot{M} \propto t^{-10/3}$ for Kramers opacity and $\dot{M} \propto t^{-5/2}$ for Thomson scattering (see Sect. 1.6.7 below).

If $\nu_t = \nu_0 \Sigma^a r^b$, the kinematic viscosity coefficient is not constant in time since the surface density varies. The relation $F = 3\pi h \nu_t \Sigma_0$ (cf. (1.122)) can be presented in the following way:

$$F = 3\pi h \nu_0 \Sigma_0^{a+1} r^b . \tag{1.150}$$

Then, for a Keplerian disc ($h \equiv h_*$), Eq. (1.123) takes the following form:

$$\frac{\partial F}{\partial t} = D\,\frac{F^m}{h^n}\,\frac{\partial^2 F}{\partial h^2}\,, \tag{1.151}$$

where D is a dimensional constant,

$$D = \frac{a+1}{2}\,(G\,M)^2\left(\frac{3}{2}\,\frac{\nu_0}{(2\,\pi)^a\,(G\,M)^b}\right)^{1/(a+1)}\,, \tag{1.152}$$

and m and n are dimensionless constants,

$$m = \frac{a}{a+1}\,, \qquad n = \frac{3a+2-2b}{a+1}\,.$$

The values of the parameters D, m and n may be determined from the equations of vertical structure. The parameter D in (1.151) can be seen as a sort of 'diffusion coefficient'. It may be found from the relation between Σ_0, F and h (Filipov 1984; Lyubarskij and Shakura 1987):

$$\Sigma_0 = \frac{(GM)^2\,F^{1-m}}{4\,\pi\,(1-m)\,D\,h^{3-n}}\,. \tag{1.153}$$

Comparing the equation of disc evolution in the linear and non-linear cases, (1.129) and (1.151), we find that $D = 4\,(l/\kappa)^2$ for $m = 0$.

The non-linear problem of non-stationary accretion has the following distinctive features. Firstly, the self-similar solutions of the second kind exist only for $m \neq 0$. Secondly, self-similar solutions of the first kind in the third stage, while they exist for $m = 0$, have an exponential profile for $r \to \infty$, characteristic for linear problems (see for example Lynden-Bell and Pringle 1974). For $m \neq 0$, the boundary of the disc is fully determined.[4]

1.6.5.1 The α-Discs

Lyubarskij and Shakura (1987) give the equations of vertical structure in a form similar to (1.99). The opacity is given as:

$$\varkappa = \varkappa_0 \frac{\rho^\varsigma}{T^\curlyvee}\,.$$

[4]This property is similar to the one that arises in problems of thermal conductivity, when, due to the non-linearity, the heatwave boundary sharply separates the heated zone from the rest of the region (Zeldovich and Raizer 1967).

Table 1.4 Dimensionless parameters in the equations of non-stationary accretion for different forms of ν_t

	m	n	a	b	ς	Υ	$\alpha_{\rm pl}$
$\varkappa_{\rm T} \gg \varkappa_{\rm ff}$ and (1.94)	2/5	6/5	2/3	1	0	0	−19/16
$\varkappa_{\rm ff} \gg \varkappa_{\rm T}$ and (1.94)	3/10	4/5	3/7	15/14	1	7/2	−5/4
OPAL (Iglesias and Rogers 1996), full ionization of H and He	1/3	1	1/2	1	1	5/2	−11/9
Convective turbulence (Lin and Bodenheimer 1982)	2/3	8/3	2	0	–	–	−15/14
Molecular disc with gravitational instability (Lin and Pringle 1987)	2/3	−1/3	2	9/2	–	–	−6/5

The parameter $\alpha_{\rm pl}$ is the power-law index of the time-dependence during the stage of declining accretion in an infinite disc: $\dot{M} \propto t^{\alpha_{\rm pl}}$

After a few algebraic manipulations of the equations in the right column of (1.99), we may find the relation between Σ_0, $W_{r\varphi}\, r^2$ and $\omega\, r^2$, which together with (1.153) gives[5]:

$$D = \frac{1}{4(1-m)(2\,\pi)^m} \left\{ \frac{2^{6+\varsigma+2\Upsilon}\, \alpha^{8+\varsigma+2\Upsilon}}{\Pi_1^{\varsigma}\, \Pi_2^{2\varsigma}\, \Pi_3^{8+\varsigma+2\Upsilon}\, \Pi_4^2} \left(\frac{\Re}{\mu}\right)^{8+2\Upsilon} \right.$$
$$\left. \times \left(\frac{9\varkappa_0}{8\,a\,c}\right)^2 (GM)^{12+8\varsigma} \right\}^{\frac{1}{10+3\varsigma+2\Upsilon}}, \tag{1.154}$$

where

$$\varsigma = -\frac{11m-2n-2}{7m-n-1}, \qquad \Upsilon = -\frac{1}{2}\,\frac{37m-4n-10}{7m-n-1} \tag{1.155}$$

or

$$m = \frac{4+2\varsigma}{10+3\varsigma+2\Upsilon}, \qquad n = \frac{12+11\varsigma-2\Upsilon}{10+3\varsigma+2\Upsilon} \tag{1.156}$$

(see Table 1.4).

It is important to note that the 'diffusion coefficient' D is only weakly dependent on the opacity coefficient: as a power function of $\varkappa_0$ with an index of 1/5 or 1/10. This reduces the impact of the uncertainty due to the dependence of the real opacity on the disc parameters. The combination of parameters $\Pi_{1,2,3,4}$ in (1.154) depends only weakly on the optical depth τ, i.e. on the radius in the disc (see Tables 1.1

[5]Note that here F is a factor of 2π larger than in the paper by Lyubarskij and Shakura (1987), and our quantity D is smaller by a factor of $(2\,\pi)^m$.

and 1.2). Thus, D may be considered a constant in the basic equation of non-stationary accretion (1.151).

1.6.6 Evolution of α-Disc from a Ring of Matter

It turns out that the global evolution of the disc can in general be divided into three stages: (1) the stage of formation of the disc from an initial ring made up of matter at some radius, (2) the establishment of a quasi-stationary distribution of parameters in the disc, and as a special case, increasing accretion rate onto the central body, and (3) 'spreading' of the disc away from the centre, accompanied by a decrease of the accretion rate.

The ring of matter around a star may be formed as a result of a mass-transfer from the neighbouring component in a binary system. In the presence of effective mechanisms of viscosity, the differentially rotating ring starts to smear out into a disc.

At the first stage, material from the inner edge of the ring, losing angular momentum to the outer layers, starts to move towards the centre. In the region $r \ll R_{\rm out}$, the flow evolves into some self-similar regime whose characteristics are independent of the initial mass distribution profile. The inner edge of the disc, which has the form of a stretched-out 'tounge', reaches the accreting centre in a finite time (Fig. 1.14a). The self-similar solution breaks down close to the radius of the innermost stable orbit around the black hole, or close to the magnetosphere of the neutron star. Nevertheless, after some transition period, accretion again evolves into another self-similar solution, the regime of quasi-stationary accretion (the second stage).

At the second stage, a practically radially constant distribution is rapidly established in the inner regions of the disc, by virtue of the small viscous time scales at small radii. The region of the quasi-stationary solution gradually expands outwards (Fig. 1.14b), while the accretion rate gradually increases in time. Meanwhile, in the outer region, conditions remain close to the original.

Further, the disc gradually evolves into the third final stage (the decay stage, Fig. 1.14c) at which the details of the initial distribution are 'forgotten', and only some integral quantities conserved during the accretion are important in finding the self-similar solution. This final stage is described by a self-similar solution of type I, whereas the two preceding cases are described by self-similar solutions of type II, i.e. solutions in which the self-similarity index is found not from dimensionality arguments but in the process of integrating the ordinary differential equation for the representative function (Lyubarskij and Shakura 1987).

Thus, each stage is characterized by the motions whose distinctive property is a similarity that is conserved in the motion itself. This means that the distribution of any quantity, for example, the viscous torque, may be represented in the form:

$$F(h,t) = h^{A_1}\, t^{A_2}\, f(\xi)\,, \tag{1.157}$$

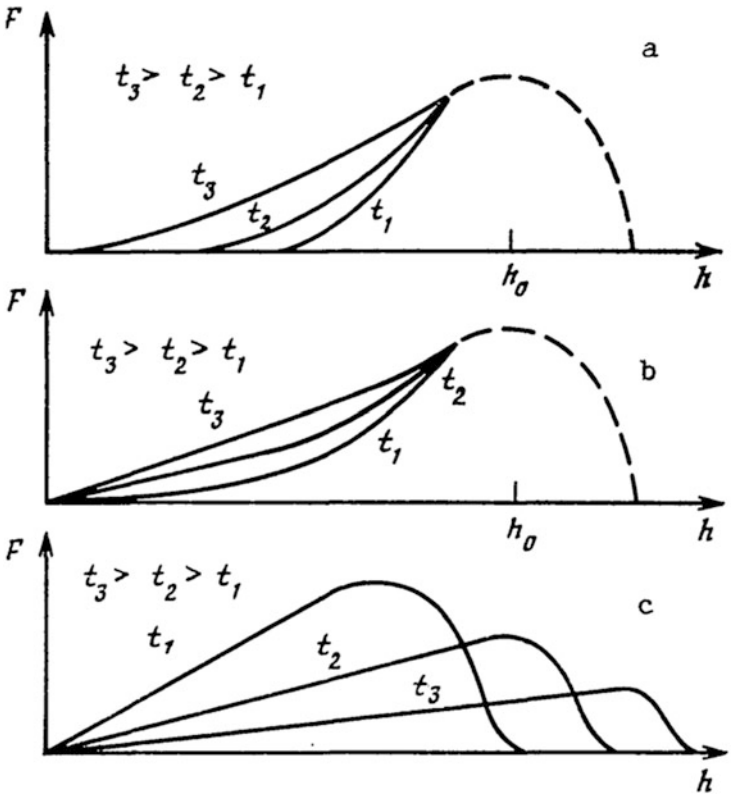

Fig. 1.14 Illustration by Lyubarskij and Shakura (1987) of the process of evolution of non-stationary disc accretion in the form of the dependence of viscous torques acting between adjacent rings of the disc, as a function of the specific angular momentum: (**a**) stage of formation and inward motion of self-similar 'tounge', (**b**) stage of formation of quasi-stationary regime, (**c**) stage of accretion decay. Dashes denote the regions into which the material was ejected and in which the solution is non self-similar. Each figure shows the distribution for three consecutive moments in time t_1, t_2, t_3. The calculated dependencies are shown in Figs. 1.16 and 1.17

where f is a function of a single self-similar variable $\xi = C\, h^{A_3}\, t^{A_4}$. For completely self-similar solutions, the parameters C and $A_{1..4}$ may be determined from dimensional arguments or from conservation laws. To determine the parameters for non completely self-similar solutions, a non-linear problem should be solved; in addition, the obtained parameters will depend on h and t.

1.6.6.1 'Tounge'-Formation Stage

Let us assume that the radius of the inner edge of the disc $r_{\rm in}$ or the equivalent value $h_{\rm in}$ decreases as a power law $h_{\rm in} \propto (-t)^{\gamma}$ ($t = 0$ when the centre is reached, thus the minus sign). As seen from Eq. (1.151), the combination $D\, F^m\, t / h^{n+2}$ is

dimensionless, which permits the solution to be represented as

$$F(h,t) = \frac{h^{(n+2)/m}}{(-D\,t)^{1/m}}\, y(\xi)\,; \qquad 1 \le \xi = \frac{h}{A\,(-t)^{\gamma}} \le \infty\,, \tag{1.158}$$

where $y(\xi)$ is the representative function of the single self-similar variable ξ. It is not possible for the dimensionless variable ξ to be a combination of h, t and D, so we have to introduce the additional constant A of dimensionality $[\mathrm{cm}^2\mathrm{s}^{-(1+\gamma)}]$, where the previously unknown exponent γ must be determined in the course of solving the problem. We thereby arrive at a self-similar problem of the second kind, similar to the problem of a converging shock wave (Zeldovich and Raizer 1967; Barenblatt 1996).

Substituting (1.158) into (1.151), we obtain an ordinary differential second-order equation for the representative

$$y^m\left[\xi^2 y'' + \frac{2(n+2)}{m}\xi y' + \frac{(n+2)(n+2-m)}{m^2}y\right] - \gamma\xi y' - \frac{y}{m} = 0$$

which can be characterised as an equation for a non-linear oscillator with dissipation (if γ is positive).

The boundary conditions are determined in the following manner. It is evident that the accretion rate through the inner edge of the ring can be considered to equal zero. Thus, at the inner boundary h_{in} (corresponding to $\xi = 1$), both the function $F(h_{\mathrm{in}}, t)$ and its derivative $\partial F(h_{\mathrm{in}}, t)/\partial h$ must vanish (cf. (1.125)). Otherwise, a δ-source (sink) appears with the substitution into Eq. (1.151). Consequently, we have two conditions:

$$y(1) = y'(1) = 0\,.$$

Another condition follows from the requirement that all physical quantities remain finite at time $t = 0$ (when the 'tounge' reaches the accreting centre), at any finite radius. It follows from (1.158) that $F(h,t)$ does not diverge as $t \to 0$ and $h \neq 0$ only if

$$y(\xi = \infty) = 0\,.$$

Thus, the solution of the second-order equation must satisfy three conditions, which is possible only for a specific value of γ.

Let us investigate qualitatively the equation for the representative function. For this we turn to the variable $x = \ln\xi + C$ (substituting C will not affect the resulting system of Eq. (1.159), but is important for adjustment of the solutions). The derivative with respect to x will be denoted by a dot. We write the resulting system of two equations of the first order:

$$\begin{aligned} \dot{y} &= p\,, \\ \dot{p} &= \frac{y^{1-m}}{m} + \gamma y^{-m} p - \frac{(n+2)(n+2-m)}{m^2}y - \frac{2n+4-m}{m}p\,. \end{aligned} \tag{1.159}$$

We are interested in the solution which leaves the origin of the plane (p, y) at $\xi = 1$ and returns there at $\xi = \infty$. For $y \ll 1$ and $p \ll 1$, the system (1.159) has asymptotic solutions of the form

$$p = \frac{\gamma}{1-m} y^{1-m}; \qquad y = \left(\frac{\gamma\, m}{1-m} \ln \xi\right)^{1/m}, \tag{1.160}$$

$$p = -\frac{y}{\gamma\, m}; \qquad y = \xi^{-\frac{1}{\gamma\, m}}. \tag{1.161}$$

The functions (1.160) give asymptotics when $\xi \to 1$ and (1.161) when $\xi \to \infty$, respectively. The phase trajectories of the solutions to the equations are shown in Fig. 1.15 for four values of γ.

Each point for which $\dot{y} = 0$ and $\dot{p} = 0$ is a singular point. There is a stable focus in the phase plane with coordinates

$$p = 0, \qquad y_0 = \left[\frac{m}{(n+2)(n+2-m)}\right]^{1/m}.$$

For a certain $\gamma_{\rm cr}$, there exists a closed solution (Fig. 1.15b). Numerical investigation shows that for $m = 2/5$, $n = 6/5$ (the case $\varkappa_{\rm T} \gg \varkappa_{\rm ff}$), the sought after value is $\gamma_{\rm cr} \approx 0.595$, and for $m = 3/10$, $n = 4/5$ ($\varkappa_{\rm ff} \gg \varkappa_{\rm T}$), it is $\gamma_{\rm cr} \approx 0.696$. The phase trajectories are rearranged for some γ_+ and the stability of the focus changes (Fig. 1.15d).

Thus, the inner boundary of the disc moves towards the centre according to the law: $h_{\rm in} = A(-t)^{\gamma_{\rm cr}}$ (see Figs. 1.16 and 1.17). As follows from (1.161), the asymptotic solution of the initial equation (1.151) for $\xi \to \infty$ (i.e. for $t \to 0$, when the 'tongue' reaches the accreting centre), has the form

$$F = \frac{h^{\frac{n+2}{m}}}{(-Dt)^{\frac{1}{m}}}\left[\frac{A(-t)^{\gamma}}{h}\right]^{\frac{1}{\gamma\, m}} = \frac{A^{\frac{1}{\gamma_{\rm cr} m}}\, h^{\frac{n+2}{m}-\frac{1}{\gamma_{\rm cr} m}}}{D^{1/m}}. \tag{1.162}$$

We note that for large h, the profile $F(h, t)$ does not change with time during the 'tongue' formation stage. By 'sewing' the obtained self-similar solution and the initial profile $F_0(h)$ near the radius where the material was ejected at time $(-t_0)$, we may also determine the constant A. Within a dimensionless factor, we have from (1.162)

$$A = F_0^{\gamma_{\rm cr} m} D^{\gamma_{\rm cr}} / h_0^{\gamma_{\rm cr}(n+2)-1},$$

where $h_0 = \sqrt{G\, M\, r_0}$ is determined by the initial radius of the ring r_0.

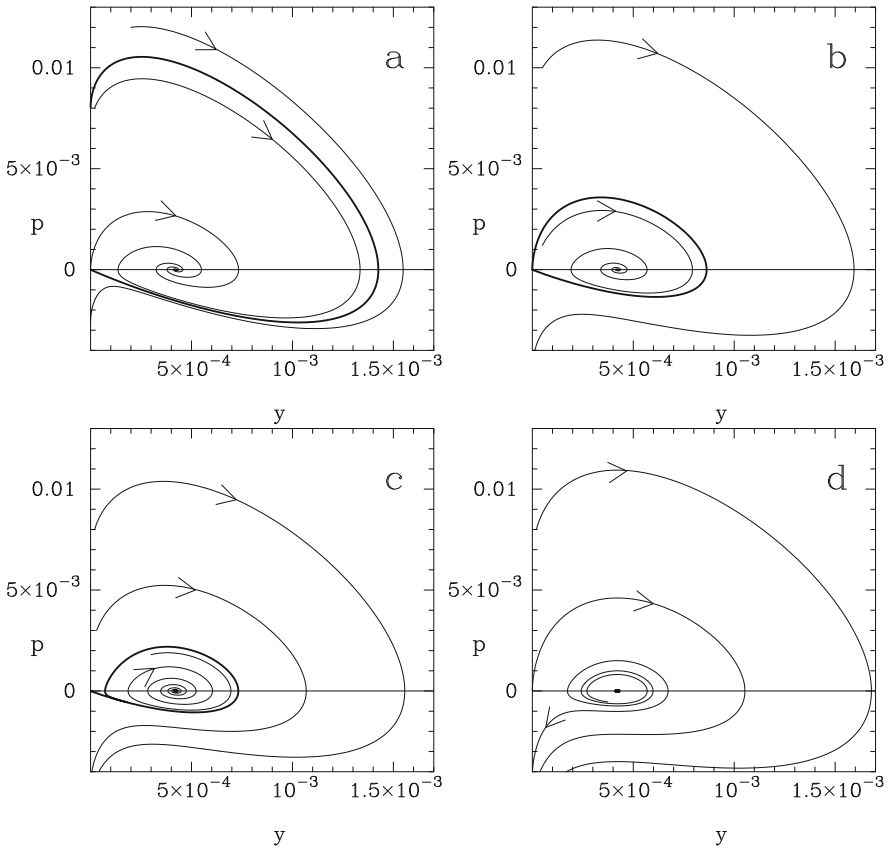

Fig. 1.15 Phase portrait of the system of Eq. (1.165) for different values γ. The *arrows* indicate the direction of change in ξ from 1 to ∞ (x from C to ∞). (**a**) For $\gamma < \gamma_{\rm cr}$ the solution inside the separatrix, shown by the *bold curve*, reaches the stationary point (focus) on the horizontal axis $(0, y_0)$. (**b**) A closed solution is found for $\gamma = \gamma_{\rm cr}$ and coincides with the separatrix. The separatrix at the same time forms a limit cycle of solutions in the region bounded by it, for $x \to -\infty$. (**c**) For $\gamma_{\rm cr} < \gamma < \gamma_+$, the separatrix (*bold curve*) is gradually compressed. (**d**) For $\gamma = \gamma_+$ it is moving towards the point $(0, y_0)$

1.6.6.2 Quasi-Stationary Stage with Increasing Accretion

We seek a solution to (1.151) in the form:

$$F = \frac{h^{\frac{n+2}{m}}}{(D\,t)^{1/m}}\, y(\xi)\,, \qquad 0 \le \xi = \frac{h}{A\,t^{\beta}} \le \infty. \tag{1.163}$$

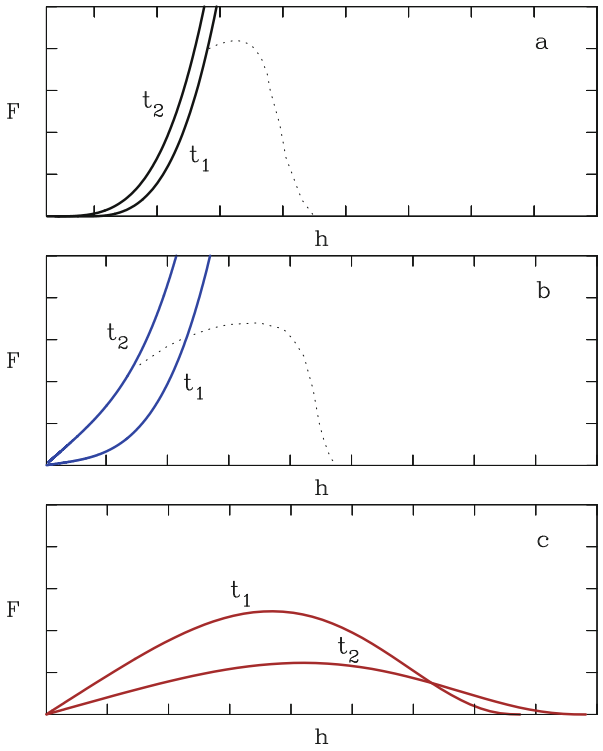

Fig. 1.16 Calculated profile $F(h)$ in the Lyubarski–Shakura solution at three stages of self-similar evolution: (**a**) formation of the 'tongue', $t_2/t_1 = 1/4$ (t is negative and approaches zero); (**b**) quasi-stationary accretion, $t_2/t_1 = 3$ (t is now positive); (**c**) accretion decay, $t_2/t_1 = 2$. The quantities F and h are normalised to arbitrary values. The *dotted lines* in the two upper panels give the symbolic dependence of $F(h)$ for regions where the (unknown) solution is non self-similar. The calculation is performed for opacity parameters $m = 2/5$, $n = 6/5$

The time t is now positive. Substituting (1.163) into (1.151), we obtain the equation for the representative function:

$$y^m \left[\xi^2 y'' + \frac{2(n+2)}{m}\xi y' + \frac{(n+2)(n+2-m)}{m^2} y\right] + \beta\xi y' + \frac{y}{m} = 0 \qquad (1.164)$$

or a system of two equations

$$\dot{y} = p\,;$$
$$\dot{p} = -\frac{y^{1-m}}{m} - \beta\, y^{-m}\, p - \frac{(n+2)\,(n+2-m)}{m^2}\, y - \frac{2n+4-m}{m}\, p \qquad (1.165)$$

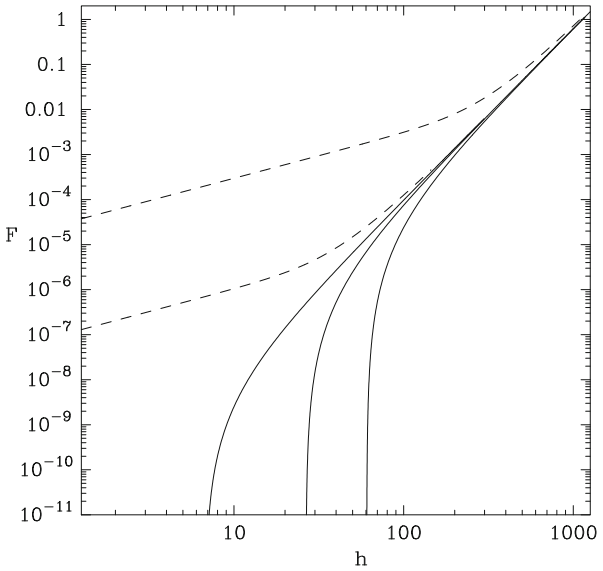

Fig. 1.17 Calculated profiles $F(h)$ in the Lyubarski–Shakura solution at the stages of 'tongue' formation (*solid line*) and quasi-stationary accretion (*dashed line*). At the first stage, we see the movement of the inner edge of the 'tongue' towards the centre. In the second stage, we can see how the zone of quasi-stationary accretion expands with time ($F \propto h$). The accretion rate increases with time from the lowest curve to the top. The quantities F and h are normalised to characteristic values

As $\xi \to \infty$, the asymptotic solution of this system has the form

$$p = -\frac{y}{\beta\, m}\,; \qquad y = \xi^{-\frac{1}{\beta m}}\,; \tag{1.166}$$

we notice that the main contribution comes from the two last terms of (1.164). Hence it follows that only if $\beta = \gamma_{\rm cr}$, the distribution $F(h, t)$ is the same as that at the preceding stage (1.162). Thus, the self-similarity index remains as before. For $\xi \to 0$ (at very large times t or at the accreting centre), there are two asymptotic solutions. (Now the main contribution comes from the terms in square brackets in (1.164)).

$$p = -\frac{n+2}{m}\, y\,; \qquad y = \xi^{-\frac{n+2}{m}}\,, \tag{1.167}$$

$$p = -\frac{n+2-m}{m}\, y\,; \qquad y = \xi^{-\frac{n+2-m}{m}}\,. \tag{1.168}$$

The first corresponds to $(\partial F/\partial h)_{h\to 0} = 0$, i.e. the solution without a material sink ($\dot{M}_{h\to 0} \to 0$), while the second corresponds to an accretion rate, radially constant at small h. Near the gravitating centre, the accretion rate depends on time

according to

$$|\dot{M}| = \left|\frac{\partial F}{\partial h}\right|_{h\to 0} \approx \frac{(At^{\beta})^{\frac{n+2-m}{m}}}{(Dt)^{1/m}} = \frac{A^{\frac{n+2-m}{m}}\, t^{\frac{\gamma_{\rm cr}(n+2-m)-1}{m}}}{D^{1/m}}\,. \tag{1.169}$$

It is this solution with a material sink that describes the second accretion stage in our case (see Fig. 1.16b). We have $|\dot{M}| \propto t^{1.67}$ for $\varkappa_{\rm T} \gg \varkappa_{\rm ff}$ while the accretion rate increases as $|\dot{M}| \propto t^{2.47}$ for $\varkappa_{\rm ff} \gg \varkappa_{\rm T}$.

If we introduce the notation

$$\dot{M}_0 = \frac{F_0}{h_0}, \quad \tau = \frac{h_0^{n+2}}{F_0^m\, D} \quad \text{or} \quad \tau = \frac{h_0^{n+2-m}}{\dot{M}_0^m\, D}\,,$$

the accretion rate $\dot{M}(t)$ onto the gravitating centre during the quasi-stationary stage can be expressed in terms of the accretion rate $\dot{M}_0$, determined by the initial value of the viscous torque F_0 acting on the ring of matter with specific angular momentum h_0:

$$\dot{M} = \dot{M}_0 \left(\frac{t}{\tau}\right)^{\frac{\gamma_{\rm cr}(n+2-m)-1}{m}} \qquad \text{at} \quad t > \tau\,.$$

1.6.6.3 Accretion Decay Stage: Spreading of the Disc

We again seek a solution to (1.151) in the form (1.163), but now the variable ξ varies within the limits $0 \le \xi \le 1$ ($\xi = 1$ corresponds to the outer radius of the disc $r_{\rm out}$ or the specific angular momentum $h_{\rm out} = \sqrt{G\,M r_{\rm out}(t)}$). Thus, the solution for this stage is described, as before, by (1.164) or the equivalent system (1.165) with the boundary conditions $y(0) = y(1) = y'(1) = 0$. The value of the self-similar index β is now found from the law of conservation of the total angular momentum of the material in the disc. Indeed, if the ring was initially located at a radius r_0, much greater than the radius of the innermost stable orbit, then the quantity

$$K = 2\,\pi \int\limits_0^{r_{\rm out}} \Sigma\, h\, r\, {\rm d}r = const\,. \tag{1.170}$$

is conserved during the accretion process. Substituting (1.163) into (1.170), with the use of the relationship (1.153) between Σ_0 and F, we obtain

$$K = \frac{1}{(1-m)\,D} \int\limits_0^{h_{\rm out}} F^{1-m}\, h^{n+1} {\rm d}h = \frac{A^{\frac{n+2}{m}}\, t^{\frac{\beta(n+2)}{m}}}{(1-m)\, D^{1/m}\, t^{\frac{1-m}{m}}} \int\limits_0^1 y^{1-m}(\xi)\, \xi^{\frac{n+2-m}{m}}\, {\rm d}\xi\,. \tag{1.171}$$

From the condition $\partial K/\partial t = 0$, we obtain $\beta = (1-m)/(n+2)$. Moreover, the expression (1.171) gives the exact relation for the constant A. For this β, the required solution to the equation for the representative function (1.164) can be found in explicit form. The method for solution of the non-linear ordinary second order differential equation (1.164), or the equivalent system of first order (1.165), is analogous to the solution of similar equations arising in heat propagation problems with temperature dependent thermal conductivity (Zeldovich and Kompaneets 1950). Since Eqs. (1.165) contain the variable x only as a differential, the order is lowered by introducing $p(y) = \mathrm{d}y/\mathrm{d}x$ as a new unknown function of the variable y

$$y^m \left[p \frac{\mathrm{d}p}{\mathrm{d}y} + \frac{2n+4-m}{m} p + \frac{(n+2)(n+2-m)}{m^2} y \right] + \beta p + \frac{y}{m} = 0 .$$

It is then convenient to introduce function $Z(y) = p(y) + y\,(n+2-m)/m$:

$$y^m \left[\left(Z - \frac{n+2-m}{m} y \right) \frac{\mathrm{d}Z}{\mathrm{d}y} + \frac{n+2}{m} Z \right] + \beta \left(Z - \frac{n+2-m}{m} y \right) + \frac{y}{m} = 0 .$$

We seek a solution of the form $Z(y) = B\, y^{1-m}$. Collecting the coefficients of powers of y^{1-m} in the last equation, we obtain $B = -\beta/(1-m)$. After substitution of $Z(y) = -\dfrac{\beta}{1-m} y^{1-m}$, the equation becomes a linear algebraic equation with respect to y. The left part of the equation vanishes for $\beta = (1-m)/(n+2)$. On the other hand, the equality of β to this value is a necessary condition for the existence of a self-similar solution at the stage of accretion decay (which follows from the condition $\partial K/\partial t = 0$). Thus,

$$p = -\frac{y^{1-m}}{n+2} - \frac{n+2-m}{m} y$$

is a particular solution satisfying the boundary condition $p(y=0) = \left.\dfrac{\mathrm{d}y}{\mathrm{d}x}\right|_{x=0} = 0$. Integrating this expression is elementary, and with the boundary condition $y(\xi = 1) = 0$, the solution can be written as

$$y(\xi) = \left[\frac{m}{(n+2)\,(n+2-m)} \right]^{1/m} \left(\frac{1}{\xi^{n+2-m}} - 1 \right)^{1/m} . \tag{1.172}$$

This solution implies that the integral on the right-hand side of (1.171), which is an Euler integral of the first kind, is reduced to the beta-function $B\left(\dfrac{n+3-m}{n+2-m}, \dfrac{1}{m}\right)$ with some coefficient, and the solution of the key equation (1.151) at the decay stage

finally takes the form:

$$F = \frac{A^{\frac{n+2}{m}}}{D^{1/m}} \left[\frac{m}{(n+2)(n+2-m)}\right]^{1/m} \frac{\xi\,(1-\xi^{n+2-m})^{1/m}}{t} =$$

$$= \frac{K\,m\,(1-m)}{(n+2)\,B\left(\frac{n+3-m}{n+2-m},\,\frac{1}{m}\right)} \frac{\xi\,(1-\xi^{n+2-m})^{1/m}}{t}\,.$$

The accretion rate decays according to:

$$\dot{M} = \left|\frac{\partial F}{\partial h}\right|_{h\to 0} = \frac{A^{\frac{n+2-m}{m}}}{D^{1/m}} \left[\frac{m}{(n+2)(n+2-m)}\right]^{1/m} t^{-\frac{n+3-m}{n+2}}\,.$$

The exponent in the time dependence of $\dot{M}(t)$ can also be expressed through the exponents a and b, appearing in the expression $\nu_{\rm t} \propto \Sigma^a r^b$; it equals then $1 + 1/(5\,a - 2\,b + 4)$. For $\varkappa_{\rm T} \gg \varkappa_{\rm ff}$ we have $\dot{M} \propto t^{-19/16}$ and $\dot{M} \propto t^{-5/4}$ for $\varkappa_{\rm ff} \gg \varkappa_{\rm T}$.

At both the quasi-stationary stage and the decay stage, the total energy release in the disc is determined primarily by the release of gravitational energy in the inner regions of the disc. The disc luminosity is equal to $\eta_{\rm accr}\,\dot{M}_{\rm in}\,c^2$, where $\eta_{\rm accr}$ is the efficiency of energy release. During the 'tongue' stage, the energy release depends largely on the initial distribution $F(h)$ since the heat flux from a unit area of the disc surface $\propto F/h^7$ (cf. (1.75)).

The presented solutions describe processes in real accretion discs to some approximation. The assumption of constant opacity (or constant coefficients m and n) does not hold for the entire disc throughout its full evolution. To completely take into account changes in opacity, numerical calculations are required using tabulated values of the opacity coefficients as functions of temperature and density. On the other hand, the opacity coefficient has little effect on the presented solution, as it appears in D as a factor raised to a very small power. It should be noted that the opacity changes particularly strongly in regions with a variable degree of ionization.

1.6.7 Solution for α-Disc in a Binary System

As we have seen, the viscous evolution of a ring of matter eventually enters a stage of unconstrained spreading, when parts of the matter in the disc acquire a high angular momentum and reaches further and further from the centre. In binary systems, such spreading of the disc cannot continue indefinitely due to the gravitational effects of the companion star. Tidal forces from the companion star force the disc to be limited to within a certain radius from the centre inside the Roche lobe.

Lipunova and Shakura (2000) found a solution describing the evolution of an α-disc in a binary system. The obtained solution was used to model the optical and X-ray lightcurves of the X-ray novae A 0620-00 and GU Mus 1124-68 during the

decline after the peak of their outbursts. As a result, new constrains on the turbulence parameter α were found (Lipunova and Shakura 2002; Suleimanov et al. 2008).

The angular momentum in the region of the outer radius is transferred from the matter in the disc into orbital motion of the binary system. Papaloizou and Pringle (1977) showed that the tidal truncation radius is on average ~ 0.9 times that of the Roche lobe. This radius is close to that of the last non-intersecting periodic orbit calculated for a three-body problem (Paczynski 1977). Numerical calculations have shown that the tidal stress tensor is important only in a rather narrow ring close to the outer radius. Significant perturbations in this region lead to the formation of strong spiral shock waves (Pringle 1991; Ichikawa and Osaki 1994; Hameury and Lasota 2005).

Since the outflow of angular momentum takes place in a narrow region close to the tidal truncation radius, we may choose not to examine this region in detail, considering it simply a δ-type channel. The function F grows as $r^{1/2}$ at radii much smaller than the tidal truncation radius. There, the stationary disc behaves according to the standard model, not 'noticing' the outer boundary conditions, and the dependence of the viscous torque on the radius is described by expression (1.124).

We also assume in the framework of the mathematical problem that the outer radius of the disc does not change, and that the rate of inflow of matter to the outer disc is negligible. The assumption that the outer radius remains unchanged is valid for transient activity phenomena during outbursts in some types of close binary systems. Numerical calculations, in which long-term evolution of non-stationary discs in binary systems (X-ray and dwarf novae) is modelled (DIM, Disc Instability Models), take into account the variability of the outer radius of the disc (Lasota 2001). During powerful flares in X-ray novae, when the brightness of the source may increase with up to a million times, the accretion rate inside the disc may be considered to be much higher than the rate of inflow of matter from the companion star. This corresponds to the vanishing of the derivative $F(h, t)$ with respect to h at the outer radius.

A solution to the basic equation of non-stationary accretion (1.151) for a disc with a constant outer radius can be found using the method of separation of variables:

$$F(h, t) = F(t) \times f_F(h/h_0)\,. \tag{1.173}$$

The quantity $h_0 = (G\,M\,r_{\rm out})^{1/2}$ equals the specific angular momentum at the outer edge of the disc. The above mentioned properties of the viscous torque lead to the following conditions at the outer radius:

$$f_F(1) = 1, \quad f_F'(1) = 0\,, \tag{1.174}$$

the first of which is normalising, and the other expresses the fact that the viscous torque has a maximum at the immediate vicinity of the disc outer radius (Fig. 1.18). This is equivalent to the condition of zero accretion rate at $r_{\rm out}$. It can also be said that the radial component of the velocity in the disc is zero at $r_{\rm out}$. A similar

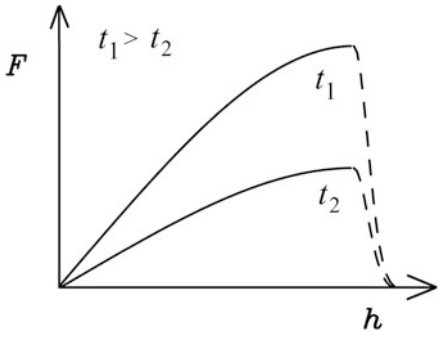

Fig. 1.18 Moment of viscous forces F as a function of the specific angular momentum h in an accretion disc in a binary system at two moments in time. Time t_2 is later than t_1. The accretion rate declines with time

approach was used, for example, by Pringle (1991) in a study of a disc surrounding a binary system. At the inner edge of such a disc, the angular momentum is transferred from the binary system into the disc, and the stars gradually move closer to each other.

Thus, tidal interactions determine the specific boundary conditions at the outer edge of the disc, thereby not changing the form of the equation that we solve (1.123) or (1.151).

Naturally, in reality the inner edge of the disc $r_{\rm in} \neq 0$. In many situations, however, $r_{\rm in}/r_{\rm out} \ll 1$.

Using $h \equiv h_{\rm K}$, we obtain from (1.125):

$$\dot{M}(h,t) = f'_F(h/h_0)F(t)/h_0\,. \tag{1.175}$$

Substituting the product of the functions into the equation for non-stationary accretion (1.151), we obtain the time-dependent part of the solution, which gives the following asymptotic for the disc evolution after the peak of the outburst:

$$F(t) = \left(\frac{h_0^{n+2}}{\lambda\, m\, D\,(t+t_0)}\right)^{1/m}. \tag{1.176}$$

Here, D is a dimensional constant (1.154) that may be obtained by solving the equations of vertical structure, λ is a separation constant, which may be found from the boundary conditions imposed on $f_F(h/h_o)$, and t_0 is the integration constant in units of time.

The law of accretion rate change is written as:

$$\dot{M}(t) = \dot{M}(0)\,(1+t/t_0)^{-1/m}\,, \tag{1.177}$$

where $\dot{M}(0)$ is the accretion rate at a certain moment in time $t = 0$, which can be chosen as any time at the stage of declining accretion. Then, parameter t_0 of the solution is

$$t_0 = \frac{h_0^{n+2}}{\lambda\, m\, D\, F^m(0)}\,,$$

where $F(0)$ is the value of $F(h, t = 0)$ at the outer radius $r_{\rm out}$. Substituting expression (1.152) for D and taking into account that $F_{\rm out} = 3\pi\, h_0\, \nu_{\rm out}\, \Sigma_0$, we get:

$$t_0 = \frac{4}{3\lambda\, a}\, \frac{r_{\rm out}^2}{\nu_{\rm out}(t=0)}\,, \tag{1.178}$$

where a is the power of Σ in the relation $\nu_{\rm t} \propto \Sigma^a\, r^b$.

After a separation of variables in the basic equation, we obtain a non-linear equation for $f_F(\xi)$. It constitutes a particular case of the general Emden-Fowler equation (Zaitsev and Polyanin 2012)

$$\frac{d^2 f_F}{d\xi^2} = -\lambda \xi^n\, f_F^{1-m}\,, \tag{1.179}$$

the solution to which we seek as a polynomial

$$f_F(\xi) = a_0\xi + a_1\xi^k + a_2\xi^l + \dots\,. \tag{1.180}$$

Substituting $f_F(\xi)$ with the polynome into (1.179), we obtain for the second and the third term:

$$\begin{aligned} k &= 3 + n - m, \quad a_1 = \frac{-\lambda a_0^{1-m}}{k(k-1)}\,, \\ l &= 2k - 1, \quad a_2 = \frac{-\lambda a_0^{-m} a_1}{l(l-1)}(1-m)\,. \end{aligned} \tag{1.181}$$

Table 1.5 gives the values for the constants a_0 and λ, derived from the boundary conditions (1.174) on $f_F(\xi)$ in the opacity regimes of pure scattering and pure absorption as well as for an approximation based on the OPAL numerical calculations of opacity (Iglesias and Rogers 1996). The corresponding functions f_F are shown in Fig. 1.19. The OPAL case turns out to be effectively somewhere in the middle.

Table 1.5 Parameters of the analytical solution, presented by (1.176), (1.177), and (1.180), for the truncated α-disc decay

	m	n	λ	a_0	a_1	a_2	k	l
$\varkappa_{\rm T} \gg \varkappa_{\rm ff}$	2/5	6/5	3.482	1.376	−0.396	0.019	3.8	6.6
$\varkappa_{\rm ff} \gg \varkappa_{\rm T}$	3/10	4/5	3.137	1.430	−0.460	0.030	3.5	6.0
OPAL	1/3	1	3.319	1.400	−0.425	0.025	11/3	19/3

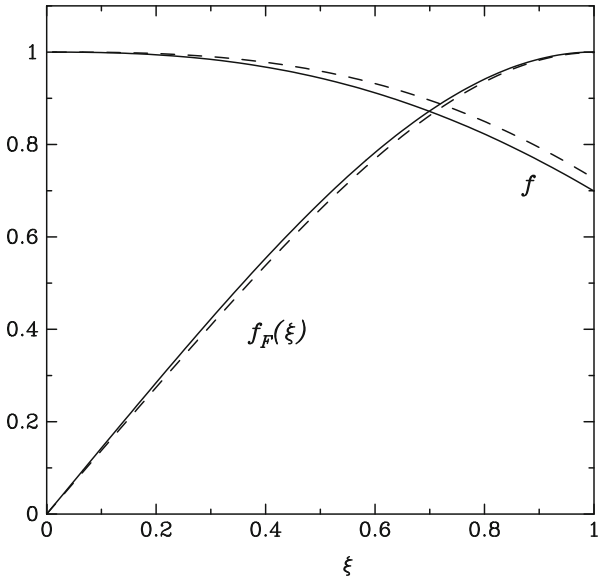

Fig. 1.19 The solution $f_F(\xi)$ for two cases: $\varkappa_{\rm ff} \gg \varkappa_{\rm T}$ (*solid line*) and $\varkappa_{\rm T} \gg \varkappa_{\rm ff}$ (dashes). The plot also shows the function $f(r)$, calculated using (1.102), that is included in the expression for calculating radial dependencies of physical parameters (Sect. 1.5.3). The accretion rate practically does not change with radius in the region, where $f \approx 1$. The variable $\xi = h/h_o$, where h_o is the specific angular momentum at the outer radius

The value a_0, included in the expression for the accretion rate

$$\dot{M}_{\rm in} = \frac{F_{\rm max}}{h_{\rm max}} a_0 \ ,$$

can also be calculated for the self-similar solution by Lyubarski & Shakura during the concluding stage of disc decay (Sect. 1.6.6.3). Omitting the details, we only mention that in an unconstrained disc, $h_{\rm max}$ likewise corresponds to the maximum torque $F_{\rm max}$. It is remarkable that the values of a_0 differ only by 2% between a constrained and an unconstrained disc. This means that the profile $F(h)$,in the region of the disc where $F(h)$ increases, is practically independent of the conditions outside this region.

1.6.7.1 Radial Dependencies for a Non-stationary Disc in a Binary System

Let us find the expressions for the evolution of physical parameters in the disc, using Eqs. (1.99), (1.153), (1.154), and (1.176).

Note that the relations (1.104) and (1.110) contain another function, $f(r)$ without an index. Function $f(r)$ is determined by relation (1.102). In the case of a stationary

disc, we have $f_F = \xi\ f$. In the case of a disc with a radially variable accretion rate, for example a non-stationary disc, $f_F = a_0\,\xi\ f(r)$ (see Fig. 1.19).

Below, we derive expressions for the diffusion parameter D, surface density Σ_o, temperature in the central disc plane T_c, relative half-thickness z_0/r, and optical depth τ. We use for the mass of the compact object $m_\mathrm{x} = M/M_\odot$. The values $\Pi_{1..4}$ should be chosen according to the appropriate opacity regime. The parameter t_0 depends on the accretion rate at $t = 0$:

$$t_0 = \frac{h_0^{n+2-m}\ a_0^m}{\lambda\, m\, D\, \dot{M}_\mathrm{in}^m(t=0)}\,. \tag{1.182}$$

It is important to remember that t_0 depends on the type of opacity.

Scattering-Dominated Opacity Regime ($\varkappa_\mathrm{T} \gg \varkappa_\mathrm{ff}$)

Substituting the numerical values of the constants into (1.154), we obtain:

$$D\ [\mathrm{cm}^{28/5}/\mathrm{g}^{2/5}/\mathrm{s}^{17/5}] \ = 1.40\times10^{38}\ \alpha^{4/5}\, m_\mathrm{x}^{6/5} \left(\frac{\mu}{0.5}\right)^{-4/5} \Pi_\Sigma^{-1}\, \varkappa_\mathrm{T}^{1/5}\,, \tag{1.183}$$

with the help of which we re-write (1.182):

$$t_0\ [\mathrm{days}] = 24.12\,\alpha^{-4/5} \left(\frac{r_\mathrm{out}}{R_\odot}\right)^{7/5} \left(\frac{\dot{M}_\mathrm{in}(t=0)}{10^{18}\mathrm{g/s}}\right)^{-2/5} m_\mathrm{x}^{1/5} \left(\frac{\mu}{0.5}\right)^{4/5} \Pi_\Sigma\, \varkappa_\mathrm{T}^{-1/5}\,, \tag{1.184}$$

where (1.95) determines $\varkappa_\mathrm{T}$. Substituting the combination $M_\mathrm{in}\, t_0^{1/m}$ from (1.184) into the expression for the declining accretion rate $\dot{M}(t) = \dot{M}(0)\,(1 + t/t_0)^{-1/m}$, and further the accretion rate and the function $f(r) = f_F/(a_0\sqrt{r/r_\mathrm{out}})$ into the radial dependencies (1.104) in zone B, we obtain the radial dependencies of the physical parameters in a non-stationary α-disc:

$$\Sigma_0\ [\mathrm{g/cm}^2] = 2.2\times10^2\ \alpha^{-2}\, m_\mathrm{x}^{1/2} \left(\frac{t+t_0}{10^\mathrm{d}}\right)^{-3/2} \left(\frac{r_\mathrm{out}}{R_\odot}\right)^{3/2} \left(\frac{r}{r_\mathrm{out}}\right)^{-9/10} f_F^{3/5} \times \tag{1.185}$$

$$\times \left(\frac{\mu}{0.5}\right)^2 \varkappa_\mathrm{T}^{-1/2} {\Pi_\Sigma}^{5/2}\,,$$

$$T_\mathrm{c}\ [\mathrm{K}] = 1.8\times10^4\,\alpha^{-1}\, m_\mathrm{x}^{1/2} \left(\frac{t+t_0}{10^\mathrm{d}}\right)^{-1} \left(\frac{r_\mathrm{out}}{R_\odot}\right)^{1/2} \left(\frac{r}{r_\mathrm{out}}\right)^{-11/10} f_F^{2/5}\, \frac{\mu}{0.5}\, \Pi_3\,, \tag{1.186}$$

$$\frac{z_0}{r} = 0.04\,\alpha^{-1/2}\, m_\mathrm{x}^{-1/4} \left(\frac{t+t_0}{10^\mathrm{d}}\right)^{-1/2} \left(\frac{r_\mathrm{out}}{R_\odot}\right)^{3/4} \left(\frac{r}{r_\mathrm{out}}\right)^{-1/20} f_F^{1/5}\, (\Pi_1\,\Pi_3)^{1/2}\,, \tag{1.187}$$

The dimensionless constants Π_Σ, $\Pi_{1..4}$ were introduced in Sect. 1.5.2 where we considered the vertical structure of the α-disc. Their interrelations are determined by expression (1.105), in particular $\Pi_3 = \Pi_T\,\Pi_\Sigma$ and $(\Pi_1\,\Pi_3)^{1/2} = \Pi_z\,\Pi_\Sigma^{1/2}$, and their values can be found in Table 1.1 and in Fig. 1.8. The effective optical depth of the disc can be estimated with the help of τ^*:

$$\tau^* = \left(\frac{\varkappa_{0,\mathrm{T}}\,\varkappa_{0,\mathrm{ff}}\,\rho_\mathrm{c}}{T_\mathrm{c}^{7/2}}\right)^{1/2} \Sigma_0 = 1.5\times10^2\,\alpha^{-1}\left(\frac{t+t_0}{10^\mathrm{d}}\right)^{-1/4}\left(\frac{r_\mathrm{out}}{R_\odot}\right)^{1/2}\times$$

$$\times\left(\frac{r}{r_\mathrm{out}}\right)^{1/10} f_F^{1/10}\left(\frac{\mu}{0.5}\right)^{5/4}\varkappa_\mathrm{T}^{-1/4}\left(\frac{\varkappa_{0,\mathrm{ff}}}{10^{22}}\right)^{1/2}\left(\frac{\Pi_3^4\,\Pi_4^3}{\Pi_1\,\Pi_2^2}\right)^{1/4},$$

where the units of $\varkappa_{0,\mathrm{ff}}$ are $[\mathrm{cm}^2\mathrm{K}^{7/2}/\mathrm{g}^2]$.

Absorption-Dominated Opacity Regime ($\varkappa_\mathrm{ff} \gg \varkappa_\mathrm{T}$)

This regime is established at lower temperatures and densities. In a similar fashion, we obtain:

$$D\ [\mathrm{cm}^5/\mathrm{g}^{3/10}/\mathrm{s}^{16/5}] = 2.41\times10^{34}\alpha^{4/5}\,m_\mathrm{x}\left(\frac{\mu}{0.5}\right)^{-3/4}\Pi_\Sigma^{-1}\left(\frac{\varkappa_{0,\mathrm{ff}}}{10^{22}}\right)^{1/10}, \tag{1.188}$$

$$t_0\ [\mathrm{days}] = 36.41\,\alpha^{-4/5}\left(\frac{r_\mathrm{out}}{R_\odot}\right)^{5/4}\left(\frac{\dot{M}_\mathrm{in}(t=0)}{10^{18}\mathrm{g/s}}\right)^{-3/10} m_\mathrm{x}^{1/4}\times \tag{1.189}$$

$$\times\left(\frac{\mu}{0.5}\right)^{3/4}\Pi_\Sigma\left(\frac{\varkappa_{0,\mathrm{ff}}}{10^{22}}\right)^{-1/10}.$$

The value $\varkappa_{0,\mathrm{ff}}$ $[\mathrm{cm}^2\,\mathrm{K}^{7/2}/\mathrm{g}^2]$ can be taken from (1.97) or (1.96).

$$\Sigma_0\ [\mathrm{g/cm}^2] = 9.9\times10^2\,\alpha^{-8/3}\,m_\mathrm{x}^{5/6}\left(\frac{t+t_0}{10^\mathrm{d}}\right)^{-7/3}\left(\frac{r_\mathrm{out}}{R_\odot}\right)^{13/6}\left(\frac{r}{r_\mathrm{out}}\right)^{-11/10}\times \tag{1.190}$$

$$\times f_F^{7/10}\left(\frac{\mu}{0.5}\right)^{5/2}\left(\frac{\varkappa_{0,\mathrm{ff}}}{10^{22}}\right)^{-1/3}\Pi_\Sigma^{10/3},$$

$$T_\mathrm{c}\ [\mathrm{K}] = 3.1\times10^4\alpha^{-1}m_\mathrm{x}^{1/2}\left(\frac{t+t_0}{10^\mathrm{d}}\right)^{-1}\left(\frac{r_\mathrm{out}}{R_\odot}\right)^{1/2}\left(\frac{r}{r_\mathrm{out}}\right)^{-9/10} f_F^{3/10}\left(\frac{\mu}{0.5}\right)\Pi_3, \tag{1.191}$$

$$\frac{z_0}{r} = 0.05\,\alpha^{-1/2}\,m_\mathrm{x}^{-1/4}\left(\frac{t+t_0}{10^\mathrm{d}}\right)^{-1/2}\left(\frac{r_\mathrm{out}}{R_\odot}\right)^{3/4}\left(\frac{r}{r_\mathrm{out}}\right)^{1/20} f_F^{3/20}\,(\Pi_1\,\Pi_3)^{1/2}. \tag{1.192}$$

The dimensionless coefficients Π_Σ, $\Pi_{1..4}$ were introduced in Sect. 1.5.2, when we considered the vertical structure of the α-disc. Their values can be found in Table 1.2 and Fig. 1.8. We recall that the surface density Σ_o is calculated between the bottom and the top surface of the disc. The full optical depth (for which (1.112) applies in the stationary case) is equal to:

$$\tau = \varkappa_{0,\mathrm{ff}}\,\rho_\mathrm{c}\,T_\mathrm{c}^{-7/2}\,\Sigma_0 = 2.4\times10^2\,\alpha^{-4/3}\,m_\mathrm{x}^{1/6}\left(\frac{t+t_0}{10^\mathrm{d}}\right)^{-2/3}\left(\frac{r_\mathrm{out}}{R_\odot}\right)^{5/6}\times \\ \times\left(\frac{r}{r_\mathrm{out}}\right)^{-1/10} f_F^{1/5}\left(\frac{\mu}{0.5}\right)^{3/2}\left(\frac{\varkappa_{0,\mathrm{ff}}}{10^{22}}\right)^{1/3}\left(\frac{\Pi_3^4\,\Pi_4^2}{\Pi_1^{1/2}\,\Pi_2}\right)^{1/3}. \tag{1.193}$$

Luminosity Dependence in an α-Disc with a Constant Outer Radius

In order to calculate the bolometric luminosity of the disc, we assume a quasi-stationary accretion rate $\dot{M}(t) = \dot{M}(0,t)$ (1.175), since the main part of the energy is released at distances from the centre $r \ll r_\mathrm{out}$. The quasi-stationarity is provided by the fact that the characteristic time scale for evolution (viscous time scale) at small radii is much smaller than that at large radii. Figure 1.19 illustrates this behaviour by the fact that the function $f(r)$ becomes approximately constant close to the disc centre.

Substituting t_0 into (1.177), we obtain for the luminosity $L = \eta_\mathrm{accr}\,\dot{M}(t)\,c^2$, where η_accr is the efficiency of accretion:

$$L_\mathrm{T}(t)\ [\mathrm{erg/s}] = 8.1\times10^{38}\,\alpha^{-2}\,m_\mathrm{x}^{1/2}\left(\frac{t+t_0}{10^\mathrm{d}}\right)^{-5/2}\left(\frac{r_\mathrm{out}}{R_\odot}\right)^{7/2}\left(\frac{\eta}{0.1}\right)\times \\ \times\left(\frac{\mu}{0.5}\right)^2\varkappa_\mathrm{T}^{-1/2}\,\Pi_\Sigma^{5/2}, \tag{1.194}$$

if Thomson scattering dominates in the outer parts of the disc, and

$$L_\mathrm{ff}(t)\ [\mathrm{erg/s}] = 6.7\times10^{39}\,\alpha^{-8/3}\,m_\mathrm{x}^{5/6}\left(\frac{t+t_0}{10^\mathrm{d}}\right)^{-10/3}\left(\frac{r_\mathrm{out}}{R_\odot}\right)^{25/6}\left(\frac{\eta}{0.1}\right)\times \\ \times\left(\frac{\mu}{0.5}\right)^{5/2}\left(\frac{\varkappa_{0,\mathrm{ff}}}{10^{22}}\right)^{-1/3}\Pi_\Sigma^{10/3}, \tag{1.195}$$

if Kramer's opacity dominates. The quantities t_0 differ between expressions (1.194) and (1.195) and are determined using formulae (1.184) and (1.189), respectively.

Note that the quantities t_0(T) and t_0(ff) in the two regimes are not independent of each other. In a physically consistent model with a transition between the opacity regimes, it is necessary to find an intersection between the two solutions. This may be done by equating the torques F and the surface densities Σ_0 in the two regimes

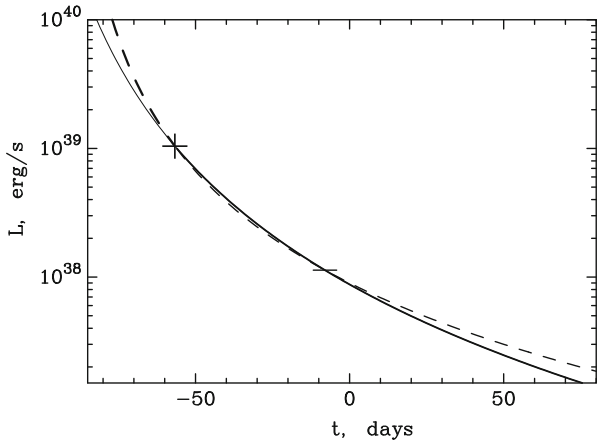

Fig. 1.20 Bolometric disc luminosity $L_{\rm T}$ and $L_{\rm ff}$ for the parameters $m_{\rm x} = 3$, $\alpha = 0.3$, $\mu = 0.5$, $r_{\rm out} = R_\odot$. The *dashed line* shows the scattering dominated opacity regime and the *solid line* shows the absorption dominated regime. The transition from the solution in the scattering regime to the solution in the absorption regime is marked with a *cross*. The second intersection of the curves is marked with a *bar*

at radius $r = 0.5\, r_{\rm out}$. These two conditions specify the intersection time itself and the difference between times t_0 in the two regimes. The value of t_0 in one of the regimes is a free parameter, and can be chosen so that $t = 0$ corresponds to a certain accretion rate.

Figure 1.20 shows the bolometric lightcurves for the parameters $\alpha = 0.3$, $m_{\rm x} = 3$ and $\varkappa_{0,\rm ff} = 6.45 \times 10^{22}\ {\rm cm^5\,K^{7/2}/g^2}$ and $\varkappa_{\rm T} = 0.4\,{\rm cm^2/g}$ in the two opacity regimes. Typical values for $\Pi_{1,2,3,4}$ are used. The normalised time in the absorption regime (1.189) $t_0({\rm ff}) \approx 107$ days is obtained from the condition that the accretion rate is $\dot{M} = 10^{18}\,{\rm g/s}$ at $t = 0$. Equality between F and Σ in the two different regimes occurs at radius $r/r_{\rm out} = 0.5$ when

$$t + t_0({\rm ff}) = t_{\rm tr} \approx 48^{\rm d} (m_{\rm x}/3)^{2/5}\, (\alpha/0.3)^{-4/5}\, (\mu/0.5)^{3/5}\, (r_{\rm out}/R_\odot)^{4/5}\ .$$

The normalised time in the scattering regime can be uniquely determined: $t_0({\rm T}) \approx 90$ days. The intersection of the lightcurves at time $t = t_{\rm tr} - t_0({\rm ff}) \approx -59^{\rm d}$ is marked with a cross in Fig. 1.20. We can see that there is a smooth transition between the solutions in the two regimes at this time. There is another intersection of the lightcurves at $t \approx -3^{\rm d}$, which represent a second point where the two functions $F_{\rm T}(\xi, t + t_0({\rm T})) = F_{\rm ff}(\xi, t + t_0({\rm ff}))$ take on equal values. This intersection exists only in a mathematical sense. The physical conditions in the disc at this moment are such that absorption dominates the opacity, and the values of the physical parameters in the disc, calculated according to (1.183)–(1.193), differ.

Let us not forget that we are working within the framework of the model for a geometrically thin disc with sub-critical accretion. Therefore, the solution

considered is applicable only for luminosity below the Eddington value $L_{\rm Edd} \approx 1.4 \times 10^{38}\, m_{\rm x}$ erg/s. Figure 1.20 shows that the evolution of the disc with $L < L_{\rm Edd}$ proceeds almost entirely in the absorption-dominated opacity regime.

When the temperature in the equatorial disc plane $T_{\rm c}$ drops at large radii down to a value of $\sim 3 \times 10^4$ K, the opacity increases strongly due to the onset of recombination in the plasma. The coefficient D significantly changes, and the given solution is no longer applicable. As the mechanism of heat transfer to the surface changes, the vertical structure of the disc readjusts on the characteristic thermal time scale, and conditions arise for the onset of convection. This happens at $t \approx 80^{\rm d}$ for the disc parameters $m_{\rm x} = 3$ and $\alpha = 0.3$ (Fig. 1.20).

Figure 1.21 shows the bolometric lightcurve together with the lightcurves in two X-ray bands from a disc perpendicular to the line of sight at a distance of 1 kpc. The vertical line shows the moment in time after which the bolometric luminosity of the disc becomes lower than $L_{\rm Edd}$. The shape of the lightcurves describes well the exponential decay of the luminosity observed in outbursts of X-ray novae.

Suleimanov et al. (2008) modelled two outbursts of X-ray novae and compared them with observed lightcurves in the X-ray and optical bands (Fig. 1.22). The model included the illumination of the outer parts of the disc by the X-ray flux and its conversion to optical emission. The model also included the effect of distortion of the photon trajectories in the Kerr metric around the black hole (see Fig. 1.23) as well as the presence of an extended disc atmosphere, capable of scattering the X-ray emission at altitudes higher than the hydrodynamic thickness of the disc. As a result, limits on the parameters of discs and binary systems were found. If we know dynamical parameters of binaries from observations (their periods and companion

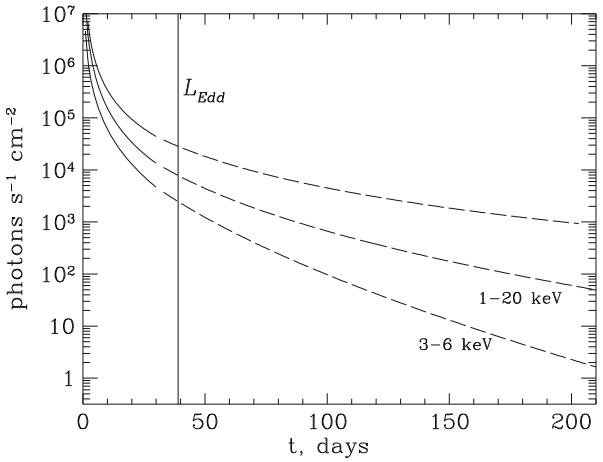

Fig. 1.21 Luminosity of the disc observed from a distance of 1 kpc, for parameters $m_{\rm x} = 3$, $\alpha = 0.3$, $\mu = 0.5$, and $r_{\rm out} = R_\odot$. The bolometric lightcurve (top) is shown together with the lightcurves in two X-ray bands, 1–20 keV and 3–6 keV

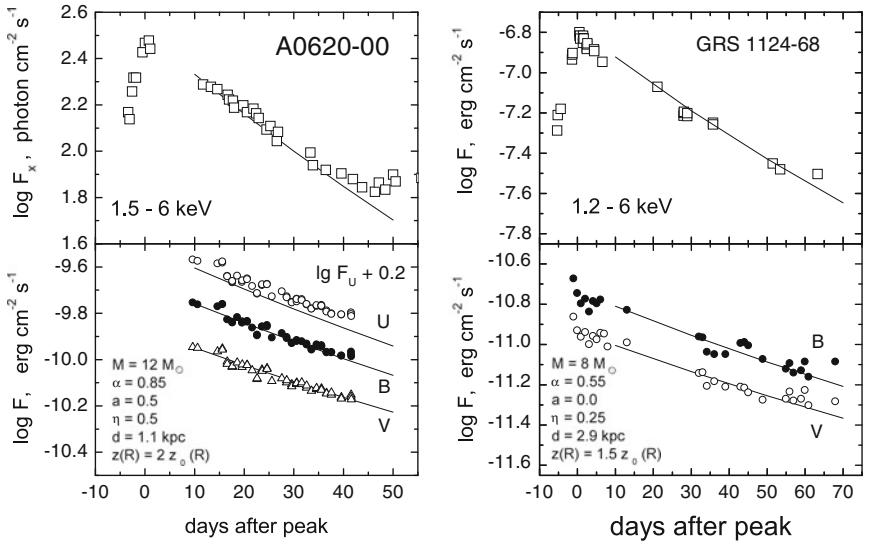

Fig. 1.22 Modelling of outbursts in X-ray novae A 06020-00 (1975) and GU Mus 1124-68 (1991) from Suleimanov et al. (2008). The parameters of the models are shown in the figure. In addition to the notations introduced in the text, we have the following parameters: the dimensionless Kerr parameter a of the black hole, the factor η of conversion of X-rays into optical emission, and the height of the scattering atmosphere $z(r)$

masses), we may find an interval of possible values for the turbulence parameter α. Figure 1.22 shows an example of the modelled lightcurves together with the corresponding parameters of the model.

1.7 Numerical Modelling of Non-stationary Disc Accretion

A numerical scheme, which is described in this section, is implemented in the `FREDDI`[6] code. `FREDDI` is intended for modelling the lightcurves of X-ray novae with fast rise and exponential decay (Lipunova and Malanchev 2017). With the help of `FREDDI` it is possible to describe the time-dependence of the accretion rate onto the black hole $\dot{M}(t)$ and to obtain lightcurves in various energy bands.

[6] http://xray.sai.msu.ru/~malanchev/freddi/.

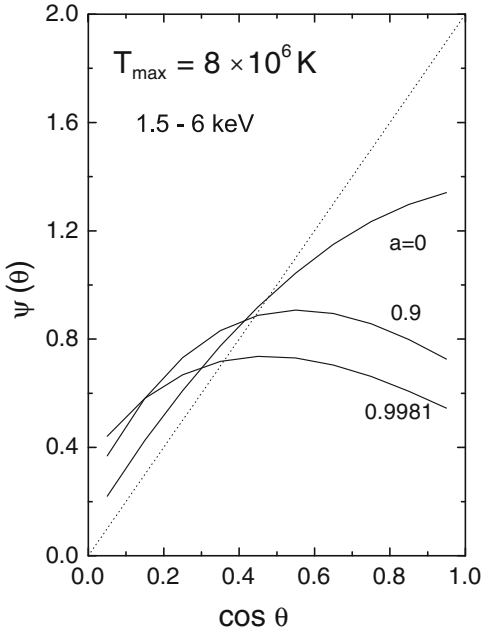

Fig. 1.23 Angular distribution $\Psi(\theta)$ of the intensity from a standard accretion disc around a Kerr black hole, integrated over 1.5–6 keV (from Suleimanov et al. 2008). The angle θ is the angle between the normal to the disc plane and the line of sight. $T_{\max}$ is the maximum effective temperature of the disc. The values of the dimensionless Kerr parameter a are indicated for the curves. The *dotted line* shows the angular distribution for a thin disc in the Newtonian approximation: $\Psi(\theta) = 2\cos(\theta)$. The observed flux can be found as $F = L\,\Psi(\theta)/(4\pi d)^2$, where L is the bolometric luminosity, d is the distance to the disc. The function $\Psi(\theta)$ is calculated using the code of Speith et al. (1995). The effects of limb-darkening are ignored here but are illustrated in Figure 9 in Suleimanov et al. (2007)

1.7.1 Solution to the Equations of Viscous Evolution

Let us examine the equation of viscous evolution of an accretion disc (1.123) obtained earlier in this chapter:

$$\frac{\partial \Sigma_0(h_{\rm K}, t)}{\partial t} = \frac{1}{4\pi}\frac{(GM)^2}{h_{\rm K}^3}\frac{\partial}{\partial h_{\rm K}}\left(\left[\frac{\partial h}{\partial h_{\rm K}}\right]^{-1}\frac{\partial F(h_{\rm K}, t)}{\partial h_{\rm K}}\right), \tag{1.196}$$

where t is the time, $h(r) = \omega(r)\,r$ is the specific angular momentum in the disc, $h_{\rm K} = \sqrt{GMr}$ is the Keplerian angular momentum, and $\Sigma_0(h, t)$ is the surface density of the disc and $F(h, t)$ the viscous torque, acting on a layer of the disc.

We will consider the case of Keplerian rotation, when $h_{\rm K} = h$. Rotation in a relativistic potential will complicate the computations and place restrictions on the choice of nodes for the radial coordinate h. For a Schwarzschild potential, in the

innermost regions of the disc, each following node must be located not further than twice as far from the centre as the previous one.

For a full set-up of the problem of viscous disc evolution, we need to give initial and boundary conditions. In the case of accretion onto a black hole, the boundary condition at the inner disc radius $R_{\rm in}$, corresponding to the innermost stable orbit (3.22), is given as the viscous torque F being equal to zero. If the accretion disc is limited by the magnetosphere of a neutron star or a young star, the inner boundary condition on the value of F is set by the conditions at the magnetospheric boundary. Thus, for a number of cases the inner boundary condition of the problem is a first (Dirichlet) type condition.

The type of outer boundary condition also depends on the astrophysical situation. In a binary system we may assume that angular momentum is removed only by tidal forces from the outer edge of the disc, corresponding to $h_{\rm out}$. Then, together with the assumption that matter flows into the accretion disc only through its outer boundary, we obtain a boundary condition of the second (Neumann) type: $\partial F/\partial h = \dot{M}_{\rm out}(t)$. In the more general case, if we take into account the radial distribution of tidal forces, removal of angular momentum from the disc surface through disc winds, capture of matter at a wide range of radii in the disc, etc., it becomes necessary to include additional terms in the original equation (1.196). If we consider the evolution of an infinite disc, for example a protoplanetary disc or a disc around a supermassive black hole in an active galactic nucleus, then from a mathematical point of view, a boundary condition at infinity is equivalent to the value and the derivative of the torque being equal to zero. However, from the point of view of numerical modelling, we cannot operate with infinite quantities of the specific angular momentum h. We may solve this problem in two ways. Firstly, we may limit the region of study to some value $h_{\rm out}$, to which, during the studied time-interval, no significant amount of matter will be able to reach, and there establish a boundary condition of the torque F being equal to zero. Secondly, we may replace the radial coordinate h with another coordinate, so that the infinite value h equals a finite value of the new coordinate, for example: $1/h$, $1-e^{-h}$ or $\mathrm{arcctg}\, h$. A change of the radial coordinate, however, complicates the original equation, and, as a consequence, place restrictions on the steps between the nodes for the new radial coordinate.

Equation (1.196) is written with respect to two unknown but related functions: $\Sigma_0(h,t)$ and $F(h,t)$. One of these quantities can be obtained for any value of the specific angular momentum h, and for any moment in time t, if the other quantity is known. Earlier in this chapter we studied the cases of linear and power-law relationships between $\Sigma_0(h)$ and $F(h)$, for which analytical solutions to Eq. (1.196) are possible. However, in the general case, the problem (1.196) has to be solved numerically. The problem is more convenient to solve with respect to the function $F(h,t)$, since the boundary conditions are set relative to this function. As we show below, using $F(h,t)$ as the unknown function is more convenient if we find the relationship between Σ_0 and F numerically from the equations of vertical structure. Thus we will express the surface density as a function of the radial coordinate and the torque: $\Sigma_0(F(h,t),\, h)$.

Note that the problem at hand is a specific case of the non-linear diffusion equation. Most often in physics, diffusion equations in which the non-linear diffusion coefficient is contained in the spatial derivative, are studied. As mentioned above, however, in our case it is more convenient to consider the problem with regard to the function $F(h, t)$. Then, the non-linear function $\Sigma_0(F(h, t),\ h)$ stands in the left part of Eq. (1.196). Below we will present a method of solving the equation, in which the non-linearity is included in the time-derivative. This method has a lot in common with the method studied in detail in the classical books on numerical methods, e.g., Press et al. (2002), used in the solution to diffusion equations with the non-linearity in the right part of the equation.

Let us consider the problem of evolution of an accretion disc in a binary system in the Newtonian potential, assuming that the removal of angular momentum is due to tidal forces from the outer edge of the disc only:

$$\begin{cases} \dfrac{\partial \Sigma_0(F(h,t),\ h)}{\partial t} = \dfrac{1}{4\pi}\dfrac{(GM)^2}{h^3}\dfrac{\partial^2 F(h,t)}{\partial h^2}, \\ F(h_{\rm in}, t) = F_{\rm in}(t), \\ \left.\dfrac{\partial F}{\partial h}\right|_{\rm out} = \dot{M}_{\rm out}(t), \\ F(h, 0) = F_0(h), \\ h \in [h_{\rm in}, h_{\rm out}], \\ t \in [0, t_{\rm fin}], \end{cases} \tag{1.197}$$

where $F_0(h)$ is the initial condition satisfying the boundary conditions and $t_{\rm fin}$ is the time interval for which the calculation is performed.

To construct a finite difference scheme we introduce an arbitrary collection of nodes h_n:

$$\begin{aligned} &h_1 < h_2 < \cdots < h_n < \cdots < h_{N-1} < h_N, \\ &\Delta h_n \equiv h_n - h_{n-1}, \\ &n = 1 \ldots N, \end{aligned} \tag{1.198}$$

where h_1 and h_N correspond to the values of the specific Keplerian angular momentum at the inner and outer radius, respectively. We will consider a solution to the equation at the time-interval between t_0, with already known values of the desired function, and $t_0 + \Delta t$, for which we need to determine these values.

We substitute the two functions with their corresponding grid functions and introduce the following designations:

$$\begin{array}{llll} F(h_n, t_0) & \Rightarrow F_n, & F(h_n, t_0 + \Delta t) & \Rightarrow \tilde{F}_n, \\ \Sigma_0(F(h_n, t_0), h_n) & \Rightarrow \Sigma_n, & \Sigma_0(F(h_n, t_0 + \Delta t), h_n) & \Rightarrow \tilde{\Sigma}_n, \\ F_{\rm in}(t_0) & \Rightarrow F_{\rm in}, & F_{\rm in}(t_0 + \Delta t) & \Rightarrow \tilde{F}_{\rm in}, \\ \dot{M}_{\rm out}(t) & \Rightarrow F'_{\rm out}, & \dot{M}_{\rm out}(t_0 + \Delta t) & \Rightarrow \tilde{F}'_{\rm out}. \end{array} \tag{1.199}$$

Let us start constructing the finite difference scheme. To begin with, we write down the difference equations for the boundary conditions. The inner boundary condition of the first kind is written in exact form as:

$$F_1 = F_{\rm in}. \tag{1.200}$$

To write down the outer boundary condition of the second kind, we expand $\tilde{F}_{N-1}$ in Taylor series around the point h_N:

$$\tilde{F}_{N-1} = \tilde{F}_N - \Delta h_N \left.\frac{\partial F}{\partial h}\right|_{h_N} + \frac{\Delta h_N^2}{2} \left.\frac{\partial^2 F}{\partial h^2}\right|_{h_N} + o(\Delta h_N^2). \tag{1.201}$$

Note that in all the expressions considered here and below for the derivatives with respect to h, we use the value of the torque at time $t_0 + \Delta t$. Thus constructed numerical scheme is called implicit. It is numerically stable. As opposed to an explicit scheme, in which the derivatives with respect to h would be written using the known value F_n at time t_0, an implicit scheme guarantees that the errors introduced in this step will not grow in the next steps.

Without going into details, we note that, in addition to the explicit and implicit methods, there is also a mixed (Crank–Nicolson) method in which the values for the function at t_0 and $t_0 + \Delta t$ are both used to calculate the derivative with respect to the spatial coordinate. In some cases, the Crank–Nicolson method gives a higher accuracy of the solution. The node stencils used in the various methods are shown in Fig. 1.24.

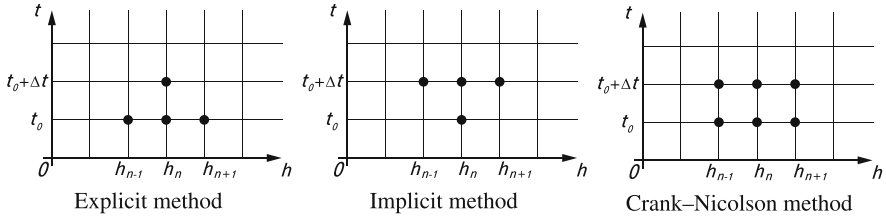

Fig. 1.24 Node stencils that are used for the n-th equation in the system (1.209) in different schemes. We use the implicit method stencil

Discarding the last term in (1.201), we obtain a simple expression for the numerical value of the first derivative of F with respect to h, with accuracy up to the first order of the expansion interval Δh_N:

$$\left.\frac{\partial F}{\partial h}\right|_{h_N} = \frac{\tilde{F}_N - \tilde{F}_{N-1}}{\Delta h_N} + o(\Delta h_N). \tag{1.202}$$

If we, however, in (1.201), substitute the value of the second derivative of F with respect to h, expressed from the original equation (1.197), we may increase the accuracy to the second order of Δh_N:

$$\left.\frac{\partial F}{\partial h}\right|_{h_N} = \frac{\tilde{F}_N - \tilde{F}_{N-1}}{\Delta h_N} + \Delta h_N \frac{2\pi h_N^3}{(GM)^2}\frac{\partial \Sigma_0(h_N)}{\partial t} + o(\Delta h_N^2), \tag{1.203}$$

where the expression for the derivative Σ_0 with respect to t by analogy with (1.202) takes the form:

$$\frac{\partial \Sigma_0(h_N)}{\partial t} = \frac{\tilde{\Sigma}_N - \Sigma_N}{\Delta t} + o(\Delta t). \tag{1.204}$$

In this way we obtain a final expression for the outer boundary condition:

$$\frac{\tilde{F}_N - \tilde{F}_{N-1}}{\Delta h_N} + \frac{\Delta h_N}{\Delta t}\frac{2\pi h_N^3}{(GM)^2}(\tilde{\Sigma}_N - \Sigma_N) + o(\Delta h_N^2) + o(\Delta t) = \tilde{F}'_{\text{out}}. \tag{1.205}$$

Now that we have equations for the values of the function at both ends of the interval over h, we obtain the difference form of the differential equation itself from (1.197). Let us write down the Taylor expansion for $\tilde{F}_{n-1}$ and $\tilde{F}_{n+1}$ around the point h_n:

$$\begin{aligned}
\tilde{F}_{n-1} &= \tilde{F}_n - \Delta h_n \left.\frac{\partial F}{\partial h}\right|_{h_n} + \frac{\Delta h_n^2}{2}\left.\frac{\partial^2 F}{\partial h^2}\right|_{h_n} + o(\Delta h_n^2), \\
\tilde{F}_{n+1} &= \tilde{F}_n + \Delta h_{n+1} \left.\frac{\partial F}{\partial h}\right|_{h_n} + \frac{\Delta h_{n+1}^2}{2}\left.\frac{\partial^2 F}{\partial h^2}\right|_{h_n} + o(\Delta h_{n+1}^2),
\end{aligned} \tag{1.206}$$

where $n = 2 \ldots N-1$.

For convenience we introduce the notation $\Delta h = \max(h_n)$, where $n = 2 \ldots N$. Then, we may change $o(\Delta h_n)$ to $o(\Delta h)$ everywhere.

The second derivative of F with respect to h may be expressed from (1.206):

$$\left.\frac{\partial^2 F}{\partial h^2}\right|_{h_n} = 2\frac{\tilde{F}_{n-1}\frac{\Delta h_{n+1}}{\Delta h_n + \Delta h_{n+1}} - \tilde{F}_n + \tilde{F}_{n+1}\frac{\Delta h_n}{\Delta h_n + \Delta h_{n+1}}}{\Delta h_n \Delta h_{n+1}} + o(\Delta h^2). \tag{1.207}$$

Note that when using a homogeneous grid with respect to h, that is for $\Delta h_n = \Delta h_{n+1} = \Delta h$, the last expression takes a simpler form:

$$\left.\frac{\partial^2 F}{\partial h^2}\right|_{h_n} = \frac{\tilde{F}_{n-1} - 2\tilde{F}_n + \tilde{F}_{n+1}}{\Delta h^2}. \tag{1.208}$$

Substituting the values of the derivatives (1.204) and (1.207) into the differential equation from (1.197) and replacing the boundary conditions in (1.197) by their difference analogues (1.200) and (1.205), we obtain a finite difference scheme for the problem:

$$\begin{cases} \dfrac{4\pi h_n^3}{(GM)^2}\dfrac{\tilde{\Sigma}_n - \Sigma_n}{\Delta t} = 2\dfrac{\tilde{F}_{n-1}\frac{\Delta h_{n+1}}{\Delta h_n + \Delta h_{n+1}} - \tilde{F}_n + \tilde{F}_{n+1}\frac{\Delta h_n}{\Delta h_n + \Delta h_{n+1}}}{\Delta h_n \Delta h_{n+1}}, \\ \tilde{F}_1 = \tilde{F}_{\text{in}}, \\ \dfrac{\tilde{F}_N - \tilde{F}_{N-1}}{\Delta h_N} + \dfrac{\Delta h_N}{\Delta t}\dfrac{2\pi h_N^3}{(GM)^2}(\tilde{\Sigma}_N - \Sigma_N) = \tilde{F}'_{\text{out}}, \\ n = 2 \ldots N - 1. \end{cases} \tag{1.209}$$

Note that the level of accuracy in the obtained system is $o(\Delta h^2) + o(\Delta t)$.

As a result, we have reduced the solution of the differential equations with boundary conditions (1.197) to a subsequent solution of the system of N algebraic equations (1.209) at each time-step between $t = 0$ and $t = t_{\text{fin}}$. This system is not linear, since Σ_n and F_n are related by the non-linear expression $\Sigma_n = \Sigma_0(F_n, h_n)$. One way to solve this system is to use the iterative root-finding algorithm for the value $\tilde{\Sigma}_n$. For this, some approximation to the value $\tilde{\Sigma}_n^{(1)}$ must first be chosen (the simplest variant is the value at the present time step Σ_n), and the system of linear algebraic equations is solved to find the intermediate value of $\tilde{\Sigma}_n^{(2)} = \Sigma_0(\tilde{F}_n^{(1)}, h_n)$ and then the system of linear algebraic equations is solved again. This simple iterative algorithm can be improved at the expense of extra memory usage; see Anderson (1965) for details.

One may think of a number of criteria to stop the integration. We will use one of them—the condition of small changes in the value for $\tilde{\Sigma}_n^{(s)}$ between two sequential iterations. We formalise this criterion:

$$\max_{n=2\ldots N}\left|\frac{\tilde{\Sigma}_n^{(s+1)} + \tilde{\Sigma}_n^{(s)}}{\tilde{\Sigma}_n^{(s+1)}}\right| < \epsilon, \tag{1.210}$$

where the top index in brackets refers to the number of performed iterations and ϵ is the dimensionless accuracy in the search for the value of $\tilde{\Sigma}_n$.

Note that in each iteration, the solution to the system of linear algebraic equations may be found by the tridiagonal matrix algorithm. The details of this algorithm can be found in textbooks on numerical methods, for example Press et al. (2002).

The described scheme (1.209) is implemented in the `FREDDI`[7] code. `FREDDI` is intended for modelling the lightcurves of X-ray novae with fast rise and exponential decay (Lipunova and Malanchev 2017). As initial conditions, we may choose either a quasi-stationary distribution (see Sect. 1.6.7), describing the radial structure of the disc after the peak in luminosity of the source, or the distribution corresponding to a dense torus far away from the central black hole.

1.7.2 Solving the Equations of Vertical Structure

In Sect. 1.5.2 we derived the equations for the vertical structure (1.93):

$$\begin{aligned}
\frac{1}{\rho}\frac{\mathrm{d}P}{\mathrm{d}z} &= -\omega_{\mathrm{K}}^2 z,\\
\frac{\mathrm{d}\Sigma}{\mathrm{d}z} &= \rho,\\
\frac{\mathrm{d}Q}{\mathrm{d}z} &= \frac{3}{2}\omega_{\mathrm{K}} w_{r\varphi},\\
\frac{c}{3\varkappa_{\mathrm{R}}\rho}\frac{\mathrm{d}(aT^4)}{\mathrm{d}z} &= -Q.
\end{aligned}$$

To solve these equations, we have to choose suitable boundary conditions. If we consider the surface density at a given radius as known, we have only three boundary conditions: $\Sigma(z = 0) = 0$, $\Sigma(z = z_0) = \Sigma_0/2$, and $Q(z = z_0) = 0$. On the other hand, if we consider the torque at a given radius as known, we may find the necessary number of boundary conditions to solve the system (1.211).

By analogy with the arguments in Sect. 1.5.2, we obtain the boundary condition for the pressure at the photosphere:

$$P(z = z_0) = \frac{2}{3}\frac{\omega_{\mathrm{K}}^2 z_0}{\varkappa_{\mathrm{R}}}. \tag{1.211}$$

If we assume that energy is released only in layers below the photosphere, the flux at the photosphere is determined by Eq. (1.73):

$$Q(z = z_0) = \frac{3}{8\pi}\frac{F\omega_{\mathrm{K}}}{r^2}. \tag{1.212}$$

[7] http://xray.sai.msu.ru/~malanchev/freddi/.

Due to symmetry, the flux is equal to zero in the plane of the disc:

$$Q(z=0)=0. \tag{1.213}$$

We consider the emitted spectrum to be that of a blackbody, so we may take the temperature in the photosphere to be equal to the effective temperature:

$$T(z=z_0)=\left(\frac{Q(z=z_0)}{\sigma_{\rm SB}}\right)^{1/4}. \tag{1.214}$$

The boundary condition $\Sigma=0$ may be set at the surface of the disc as well as in its symmetric plane. It turns out that in the symmetry plane there are only two boundary conditions, on the flux Q (1.186) and on the surface density. However, if we set Σ equal to zero at the disc surface and integrate the system towards the central plane, we can find the boundary values of all four unknown functions: the pressure P (1.211), the surface density Σ, the flux Q (1.213), and the temperature T (1.214). Thus, in what follows, we shall consider integration along the direction from the disc surface towards its symmetry plane.

While all four boundary conditions at the photosphere are known, we still do not know the disc half-thickness z_0. For convenience in integrating the system (1.211) from the photosphere to the symmetry plane, we rewrite it with aspect to the alternative vertical parameter $\hat{z}\equiv z_0-z$:

$$\frac{1}{\rho}\frac{{\rm d}P}{{\rm d}\hat{z}}=\omega_{\rm K}^2\,(z_0-\hat{z}), \tag{1.215}$$

$$\frac{{\rm d}\Sigma}{{\rm d}\hat{z}}=\rho, \tag{1.216}$$

$$\frac{{\rm d}Q}{{\rm d}\hat{z}}=-\frac{3}{2}\,\omega_{\rm K}\,w_{r\varphi}, \tag{1.217}$$

$$\frac{c}{3\varkappa_{\rm R}\rho}\frac{{\rm d}(aT^4)}{{\rm d}\hat{z}}=Q, \tag{1.218}$$

$$P(\hat{z}=0)=\frac{2}{3}\frac{\omega_{\rm K}^2 z_0}{\varkappa_{\rm R}}, \tag{1.219}$$

$$\hat{\Sigma}(\hat{z}=0)=0, \tag{1.220}$$

$$Q(\hat{z}=0)=\frac{3}{8\pi}\frac{F\omega_{\rm K}}{r^2}, \tag{1.221}$$

$$Q(\hat{z}=z_0)=0, \tag{1.222}$$

$$T(\hat{z}=0)=\left(\frac{Q(\hat{z}=0)}{\sigma_{\rm SB}}\right)^{1/4}, \tag{1.223}$$

where $\hat{\Sigma}(\hat{z})=\Sigma_0/2-\Sigma(\hat{z})$ is calculated in the direction from the disc surface.

This system consists of four equations, five boundary conditions and one unknown—z_0. We need to choose a value of z_0 such that when integrating the system (1.223) from $\hat{z} = 0$ to $\hat{z} = z_0$, the boundary condition $Q(\hat{z} = z_0) = 0$ is fulfilled. As an initial approximation, we can use values obtained analytically (see Sect. 1.5.3), and then search for z_0 using any method of root-finding.

1.7.2.1 Irradiation of the Accretion Disc

In X-ray binaries the outer parts of the disc with photospheric temperature of the order of 10^4 K may be irradiated by photons from the inner parts of the disc, direct or scattered in the corona, with temperatures of the order of 10^7 K. The surface of a neutron star may serve as an additional source of hard photons. The surface of protoplanetary discs, with temperatures of the order of 10^2 K, is irradiated by ultra violet radiation from a newly formed star.

Let us consider the case with irradiation by hard radiation incident on the disc surface at an angle $\arccos \zeta$. If the disc is illuminated by a point source located in its centre, and if the disc itself can be considered as thin, we may use the relation

$$\zeta = \frac{\mathrm{d}z_0}{\mathrm{d}r} - \frac{z_0}{r}. \tag{1.224}$$

Then the illuminating flux incident on the disc surface at radius r equals $\zeta L_\mathrm{x}/(4\pi r^2)$. If the source of the hard radiation is the disc itself, then the radiation pattern is not isotropic. Assuming that the central source is point-like, the flux may be written as $\zeta L_\mathrm{x}/(4\pi r^2) \times \Psi(\theta)$. The function $\Psi(\theta)$ is shown in Fig. 1.23, and θ is the angle measured from the vertical axis.

A detailed calculation of the effect of irradiation on the vertical structure of the disc is rather complicated, and was presented, e.g., in the work by Mescheryakov et al. (2011b). In a first approximation, we may limit ourselves to changing the boundary condition on the flux originating from the surface of the disc:

$$Q(\hat{z} = 0) = \frac{3}{8\pi} \frac{F\omega_\mathrm{K}}{r^2} + \zeta \frac{L_\mathrm{x}}{4\pi r^2} \Psi(\theta).$$

In order to explain the observed optical lightcurves from X-ray novae, the effective thickness of the disc for radiation interception in formula (1.224) needs to be twice as large as z_0 (Suleimanov et al. 2008). It is assumed in their calculations that the lower layers of the disc atmosphere above the photosphere are opaque to soft X-rays from the central parts of the disc. Furthermore, it was shown by Mescheryakov et al. (2011a), from modelling lightcurves of the illuminated stellar companion in the burster GS 1826-238, a low-mass X-ray binary with a neutron star, that the effective thickness of the disc for interception of X-rays is approximately twice as large as z_0.

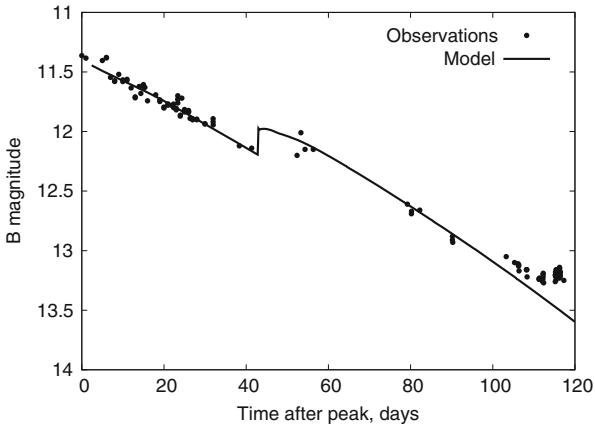

Fig. 1.25 Lightcurve of the X-ray nova A 0620-00 in the photometric B-band. Data from Duerbeck and Walter (1976), Lloyd et al. (1977) are shown with *filled circles*. The *solid line* shows our modelling of the lightcurve

1.7.3 Example Numerical Modelling of a FRED Lightcurve of an X-Ray Nova

Let us now turn to the numerical modelling of an outburst of X-ray nova A 0620-00. The following parameters of the binary system are used: mass of the compact object (a black hole) 6.6 $M_\odot$, mass of the optical companion 0.5 $M_\odot$, orbital period 0.323 days, inclination of the orbital plane to the line of sight 53.5°, and distance to the system 1.1 kpc. These parameters are observational results from analyses of the lightcurves of the system in quiescence (Cantrell et al. 2010; Gou et al. 2010).

In Figs. 1.25 and 1.26, lightcurves of the source after the peak of the outburst in 1975 in soft X-rays and in the B-band are shown. The lightcurve of this outburst is an example of a FRED-type lightcurve,[8] in which a fast rise in luminosity is followed by a quasi-exponential decay.

An interesting feature in most FRED-type lightcurves is the existence of a secondary peak. The nature of this secondary peak is currently not understood.

To reproduce the secondary peak, it has been suggested that a significant amount of matter was supplied to the disc by the donor star on the 43rd day after the peak. Within the framework of this model, this matter instantaneously increases the surface density of the disc in its outer parts, which leads to a jump in optical luminosity (Fig. 1.25).

Due to the increase in surface density in the outer regions of the disc, a gradual increase of the accretion rate takes place in the central regions of the disc. This leads to an increase in temperature and thereby X-ray luminosity of the disc. In this way, a local maximum shows up in the lightcurve (Fig. 1.26).

The maximal accretion rate $\dot{M}_{\max} \approx 0.2\,\dot{M}_{\rm Edd}$, and the α-parameter, ≈ 0.3, are determined from the part of the X-ray lightcurve before the secondary peak.

[8] Fast-rise exponential-decay.

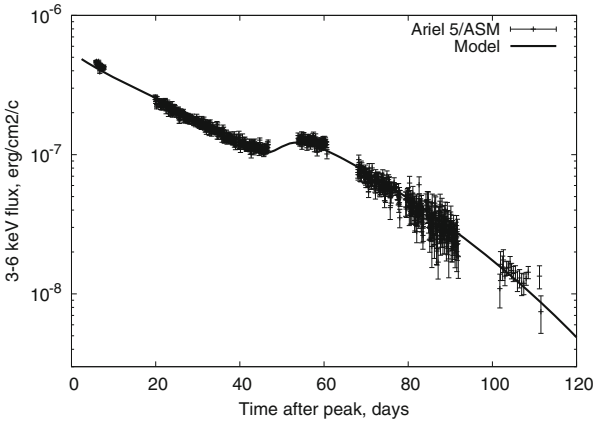

Fig. 1.26 Lightcurve of the X-ray nova A 0620-00 at 3–6 keV. The *vertical bars* show data with errors from Ariel 5 (Kaluzienski et al. 1977), and the *solid line* shows the model lightcurve

From the part of the optical lightcurve before the secondary peak, we estimate the effective thickness of the disc for X-ray radiation interception, which turns out to be $\approx 2\, z_0$ (Malanchev and Shakura 2015).

To model the lightcurve of an X-ray nova, one has to keep in mind that in general the disc is not physically uniform, but has a hot inner part with ionized matter (zones A, B and C; see Sect. 1.5) and a colder outer part with lower accretion rate. When the disc cools down to temperatures at which hydrogen recombines, the α-parameter decreases by approximately an order of magnitude (Smak 1984). In a first approximation, we may assume that accretion in the cold outer parts ceases. The boundary between the hot and cold parts gradually moves towards the centre following the hydrogen recombination front.

The open code `FREDDI` is provided by the authors to model FRED-type lightcurves of X-ray novae. This code calculates the disc evolution for a fully ionized disc, as well as for a disc with a cold front propagating inwards. Using this code, the outburst of the X-ray nova 4U 1543-47 in 2002, hosting a black hole, was modelled by Lipunova and Malanchev (2017).

Using `FREDDI`, estimates of α can be derived, which are more accurate than (1.149):

$$\alpha \approx 0.21 \left(\frac{R_{\rm hot}}{R_\odot}\right)^{25/16} \left(\frac{t_{\rm exp}}{30^{\rm d}}\right)^{-5/4} \left(\frac{\dot{M}_{\rm max}}{10^{18}\,{\rm g/s}}\right)^{-3/8} m_x^{5/16}\,, \tag{1.225}$$

for the Kramers opacity, and

$$\alpha \approx 0.20 \left(\frac{R_{\rm hot}}{R_\odot}\right)^{12/7} \left(\frac{t_{\rm exp}}{30^{\rm d}}\right)^{-9/7} \left(\frac{\dot{M}_{\rm max}}{10^{18}\,{\rm g/s}}\right)^{-3/7} m_x^{2/7} \tag{1.226}$$

for the OPAL approximation (Lipunova and Malanchev 2017). Here, $R_{\rm hot}$ is the radius of the hot zone of the disc at the peak of an outburst. Power indexes in the above expressions are obtained when substituting the thickness of the disk in (1.149) by its analytic expression from (1.104) or (1.110). The numerical factors in the expressions for α are found by fitting `FREDDI` results; their accuracy is around 5%.

References

Abramowicz MA (2016) Velocity, acceleration and gravity in Einstein's relativity. ArXiv e-prints 1608.07136

Abramowicz MA, Fragile PC (2013) Foundations of black hole accretion disk theory. Living Rev Relativ 16:1. https://doi.org/10.12942/lrr-2013-1. ArXiv 1104.5499

Anderson DG (1965) Iterative procedures for nonlinear integral equations. J ACM 12(4):547–560. https://doi.org/10.1145/321296.321305. http://doi.acm.org/10.1145/321296.321305

Balbus SA, Hawley JF (1991) A powerful local shear instability in weakly magnetized disks. I - Linear analysis. II - Nonlinear evolution. Astrophys J 376:214–233. https://doi.org/10.1086/170270

Balbus SA, Hawley JF (1998) Instability, turbulence, and enhanced transport in accretion disks. Rev Mod Phys 70:1–53. https://doi.org/10.1103/RevModPhys.70.1

Barenblatt GI (1996) Scaling, Self-similarity, and intermediate asymptotics: dimensional analysis and intermediate asymptotics. Cambridge texts in applied mathematics. Cambridge University Press, Cambridge

Barenblatt G (2003) Scaling. Cambridge texts in applied mathematics. Cambridge University Press, Cambridge. https://books.google.ru/books?id=05zBYET6tR0C

Bisikalo DV, Zhilkin AG, Boyarchuk AA (2013) Gaseous dynamic of close binary stars. FIZMATLIT (in Russian), Moscow

Bisnovatyi-Kogan GS, Blinnikov SI (1976) A hot corona around a black-hole accretion disk as a model for Cygnus X-1. Sov Astron Lett 2:191–193. ArXiv astro-ph/0003275

Bisnovatyi-Kogan GS, Lovelace RVE (2001) Advective accretion disks and related problems including magnetic fields. New Astron Rev 45:663–742. https://doi.org/10.1016/S1387-6473(01)00146-4. ArXiv astro-ph/0207625

Brandenburg A, Nordlund A, Stein RF, Torkelsson U (1996) The disk accretion rate for dynamo-generated turbulence. Astrophys J 458:L45. https://doi.org/10.1086/309913

Cannizzo JK (1992) Accretion disks in active galactic nuclei - vertically explicit models. Astrophys J 385:94–107. https://doi.org/10.1086/170918

Cannizzo JK (1998) The accretion disk limit cycle mechanism in the black hole x-ray binaries: toward an understanding of the systematic effects. Astrophys J 494:366. https://doi.org/10.1086/305210

Cannizzo JK, Lee HM, Goodman J (1990) The disk accretion of a tidally disrupted star onto a massive black hole. Astrophys J 351:38–46. https://doi.org/10.1086/168442

Cantrell AG, Bailyn CD, Orosz JA, McClintock JE, Remillard RA, Froning CS, Neilsen J, Gelino DM, Gou L (2010) The inclination of the soft x-ray transient A0620-00 and the mass of its black hole. Astrophys J 710:1127–1141. https://doi.org/10.1088/0004-637X/710/2/1127. ArXiv 1001.0261

Chandrasekhar S (1960) The stability of non-dissipative Couette flow in hydromagnetics. Proc Natl Acad Sci 46:253–257. https://doi.org/10.1073/pnas.46.2.253

Chen W, Shrader CR, Livio M (1997) The properties of x-ray and optical light curves of x-ray novae. Astrophys J 491:312. https://doi.org/10.1086/304921

Coroniti FV (1981) On the magnetic viscosity in Keplerian accretion disks. Astrophys J 244:587–599. https://doi.org/10.1086/158739
Deardorff JW (1970) A numerical study of three-dimensional turbulent channel flow at large Reynolds numbers. J Fluid Mech 41:453–480. https://doi.org/10.1017/S0022112070000691
Dubrulle B (1993) Differential rotation as a source of angular momentum transfer in the solar nebula. Icarus 106:59. https://doi.org/10.1006/icar.1993.1158
Dubus G, Lasota JP, Hameury JM, Charles P (1999) X-ray irradiation in low-mass binary systems. Mon Not R Astron Soc 303:139–147
Duerbeck HW, Walter K (1976) A periodic brightness variation of the optical counterpart of A 0620-00. NASA Spec Publ 389:343–345
Eardley DM, Lightman AP (1975) Magnetic viscosity in relativistic accretion disks. Astrophys J 200:187–203. https://doi.org/10.1086/153777
Favre AJ (1969) Statistical equations of turbulents gases. 231–267
Felten JE, Rees MJ (1972) Continuum radiative transfer in a hot plasma, with application to Scorpius X-l. Astron Astrophys 17:226
Ferguson JW, Alexander DR, Allard F, Barman T, Bodnarik JG, Hauschildt PH, Heffner-Wong A, Tamanai A (2005) Low-temperature opacities. Astrophys J 623:585–596. https://doi.org/10.1086/428642. ArXiv astro-ph/0502045
Filipov LG (1984) Self-similar problems of the time-dependant discs accretion and the nature of the temporary X-ray sources. Adv Space Res 3:305–313. https://doi.org/10.1016/0273-1177(84)90107-8
Frank J, King A, Raine DJ (2002) Accretion power in astrophysics, 3rd edn. Cambridge University Press, Cambridge
Fridman AM (1989) On the dynamics of a viscous differentially rotating gravitating medium. Sov Astron Lett 15:487
Galeev AA, Rosner R, Vaiana GS (1979) Structured coronae of accretion disks. Astrophys J 229:318–326. https://doi.org/10.1086/156957
Gorbatskii VG (1965) Disk-like envelopes in close binary systems and their effect on stellar spectra. Sov. Astron. 8:680
Gou L, McClintock JE, Steiner JF, Narayan R, Cantrell AG, Bailyn CD, Orosz JA (2010) The spin of the black hole in the soft x-ray transient A0620-00. Astrophys J 718:L122–L126. https://doi.org/10.1088/2041-8205/718/2/L122. ArXiv 1002.2211
Hameury JM, Lasota JP (2005) Tidal torques, disc radius variations, and instabilities in dwarf novae and soft X-ray transients. Astron Astrophys 443:283–289. https://doi.org/10.1051/0004-6361:20053691. ArXiv arXiv:astro-ph/0508509
Hameury JM, Menou K, Dubus G, Lasota JP, Hure JM (1998) Accretion disc outbursts: a new version of an old model. Mon Not R Astron Soc 298:1048–1060
Ichikawa S, Osaki Y (1994) Tidal torques on accretion disks in close binary systems. Publ Astron Soc Jpn 46:621–628
Iglesias CA, Rogers FJ (1996) Updated opal opacities. Astrophys J 464:943. https://doi.org/10.1086/177381
Ivanov PB, Papaloizou JCB, Polnarev AG (1999) The evolution of a supermassive binary caused by an accretion disc. Mon Not R Astron Soc 307:79–90. https://doi.org/10.1046/j.1365-8711.1999.02623.x. ArXiv astro-ph/9812198
Kaluzienski LJ, Holt SS, Boldt EA, Serlemitsos PJ (1977) All-Sky Monitor observations of the decay of A0620-00 /Nova Monocerotis 1975/. Astrophys J 212:203–210. https://doi.org/10.1086/155036
Kato S, Fukue J, Mineshige S (1998) Black-hole accretion disks. Kyoto University Press, Kyoto
Kato S, Fukue J, Mineshige S (2008) Black-hole accretion disks — towards a new paradigm —, 549 pp
Ketsaris NA, Shakura NI (1998) On the calculation of the vertical structure of accretion discs. Astron Astrophys Trans 15:193. https://doi.org/10.1080/10556799808201769
King AR, Ritter H (1998) The light curves of soft X-ray transients. Mon Not R Astron Soc 293:L42–L48

Kotko I, Lasota JP (2012) The viscosity parameter α and the properties of accretion disc outbursts in close binaries. Astron Astrophys 545:A115. https://doi.org/10.1051/0004-6361/201219618. ArXiv 1209.0017
Kurucz RL (1970) Atlas: a computer program for calculating model stellar atmospheres. SAO Special Report. Smithsonian Astrophysical Observatory, Cambridge
Kurucz R (1993) Kurucz CD-ROMs, Smithsonian Astrophysical Observatory, Cambridge
Landau LD, Lifshitz EM (1959) Fluid mechanics, Course of Theoretical Physics, vol 6
Landau LD, Lifshitz EM (1973) The classical theory of fields. Course of theoretical physics, vol 2, Sect. 88. Pergamon, Oxford
Lasota JP (2001) The disc instability model of dwarf novae and low-mass X-ray binary transients. New Astron Rev 45:449–508
Lasota JP (2015) Black hole accretion discs. ArXiv e-prints 1505.02172
Lightman AP, Eardley DM (1974) Black holes in binary systems: instability of disk accretion. Astrophys J 187:L1+
Lin DNC, Bodenheimer P (1982) On the evolution of convective accretion disk models of the primordial solar nebula. Astrophys J 262:768–779. https://doi.org/10.1086/160472
Lin DNC, Pringle JE (1987) A viscosity prescription for a self-gravitating accretion disc. Mon Not R Astron Soc 225:607–613
Lipunova GV (2015) Evolution of finite viscous disks with time-independent viscosity. Astrophys J 804:87. https://doi.org/10.1088/0004-637X/804/2/87. ArXiv 1503.09093
Lipunova GV, Malanchev KL (2017) Determination of the turbulent parameter in accretion discs: effects of self-irradiation in 4U 1543-47 during the 2002 outburst. Mon Not R Astron Soc 468:4735–4747. https://doi.org/10.1093/mnras/stx768. ArXiv 1610.01399
Lipunova GV, Shakura NI (2000) New solution to viscous evolution of accretion disks in binary systems. Astron Astrophys 356:363–372
Lipunova GV, Shakura NI (2002) Non-steady-state accretion disks in x-ray novae: outburst models for Nova Monocerotis 1975 and Nova Muscae 1991. Astron Rep 46:366–379
Lloyd C, Noble R, Penston MV (1977) The light curve of V616 Mon = A0620-00. Mon Not R Astron Soc 179:675–681. https://doi.org/10.1093/mnras/179.4.675
Lüst RZ (1952) Die Entwicklung einer um einen Zentralkörper rotierenden Gasmasse. I. Lösungen der hydrodynamischen Gleichungen mit turbulenter Reibung. Zeitschrift Naturforschung Teil A 7:87
Lynden-Bell D (1969) Galactic nuclei as collapsed old quasars. Nature 223:690
Lynden-Bell D, Pringle JE (1974) The evolution of viscous discs and the origin of the nebular variables. Mon Not R Astron Soc 168:603–637
Lyubarskij YE, Shakura NI (1987) Nonlinear self-similar problems of nonstationary disk accretion. Sov Astron Lett 13:386
MacRobert TM (1932) Fourier integrals. Proc R Soc Edinb 51:116–126
Malanchev KL, Shakura NI (2015) Vertical convection in turbulent accretion disks and light curves of the X-ray nova A0620-00 1975 outburst. Astron Lett 41:797–808. https://doi.org/10.1134/S1063773715120087. ArXiv 1511.02356
Marov M, Kolesnichenko A (2011) Turbulence and self-organization: modeling astrophysical objects. Astrophysics and Space Science Library, Springer, New York. https://books.google.ru/books?id=y1r2sgEACAAJ
Mescheryakov AV, Revnivtsev MG, Filippova EV (2011a) Parameters of irradiated accretion disks from optical and X-ray observations of GS 1826-238. Astron Lett 37:826–844. https://doi.org/10.1134/S1063773711120073
Mescheryakov AV, Shakura NI, Suleimanov VF (2011b) Vertical structure of the outer accretion disk in persistent low-mass X-ray binaries. Astron Lett 37:311–331. https://doi.org/10.1134/S1063773711050045. ArXiv 1108.4222
Meyer F, Meyer-Hofmeister E (1981) On the elusive cause of cataclysmic variable outbursts. Astron Astrophys 104:L10
Meyer F, Meyer-Hofmeister E (1982) Vertical structure of accretion disks. Astron Astrophys 106:34–42

Meyer F, Meyer-Hofmeister E (1984) HZ Her/Her X-1 - an alternative model for the 35d cycle? Astron Astrophys 140:L35–L38
Mihalas D (1978) Stellar atmospheres, 2nd edn. W. H. Freeman and Co., San Francisco
Mihalas D, Mihalas BW (1984) Foundations of radiation hydrodynamics. Courier Corporation, North Chelmsford
Monin A, Yaglom A (1971) Statistical fluid mechanics: mechanics of turbulence. vol 1. Peace Corps. https://books.google.ru/books?id=7BvYQwAACAAJ
Morozov AG, Khoperskov AV (2005) Physics of discs. Volgograd University Press, Volgograd (in Russian)
Nakao Y, Kato S (1995) Vertical dependence of the viscous heating in accretion disks. Publ Astron Soc Jpn 47:451–461
Novikov ID, Thorne KS (1973) Astrophysics of black holes. In: DeWitt C, DeWitt BS (eds) Black holes (Les Astres Occlus), Gordon and Breach, New York, pp 343–450
Ogilvie GI (1999) Time-dependent quasi-spherical accretion. Mon Not R Astron Soc 306:L9–L13
Paczynski B (1977) A model of accretion disks in close binaries. Astrophys J 216:822–826
Paczynski B, Bisnovatyi-Kogan G (1981) A model of a thin accretion disk around a Black Hole. Acta Astron. 31:283
Paczynsky B, Wiita PJ (1980) Thick accretion disks and supercritical luminosities. Astron Astrophys 88:23–31
Papaloizou J, Pringle JE (1977) Tidal torques on accretion discs in close binary systems. Mon Not R Astron Soc 181:441–454
Pletcher R, Tannehill J, Anderson D (1997) Computational fluid mechanics and heat transfer, 2nd edn. Series in computational and physical processes in mechanics and thermal sciences, Taylor & Francis. http://books.google.ru/books?id=ZJPbtHeilCgC
Prandtl L (1925) Bericht uber Untersuchungen zur ausgebildeten Turbulenz. Z Angew Math Mech 5:136–139. http://naca.central.cranfield.ac.uk/reports/1949/naca-tm-1231.pdf
Press WH, Teukolsky SA, Vetterling WT, Flannery BP (2002) Numerical recipes in C: the art of scientific computing, 2nd edn. Cambridge University Press, Cambridge
Pringle JE (1974) PhD thesis, University of Cambridge, 1974
Pringle JE (1991) The properties of external accretion discs. Mon Not R Astron Soc 248:754–759
Pringle JE, Rees MJ (1972) Accretion disc models for compact x-ray sources. Astron Astrophys 21:1
Rafikov RR (2013) Structure and evolution of circumbinary disks around supermassive black hole binaries. Astrophys J 774:144. https://doi.org/10.1088/0004-637X/774/2/144. ArXiv 1205.5017
Rafikov RR (2016) Generalized similarity for accretion/decretion disks. Astrophys J 830:7. https://doi.org/10.3847/0004-637X/830/1/7. ArXiv 1604.07439
Rayleigh L (1917) On the dynamics of revolving fluids. Proc R Soc Lond Ser A 93:148–154. https://doi.org/10.1098/rspa.1917.0010
Richard D, Zahn JP (1999) Turbulence in differentially rotating flows. What can be learned from the Couette-Taylor experiment. Astron Astrophys 347:734–738. ArXiv astro-ph/9903374
Shafee R, Narayan R, McClintock JE (2008) Viscous torque and dissipation in the inner regions of a thin accretion disk: implications for measuring black hole spin. Astrophys J 676:549–561. https://doi.org/10.1086/527346. ArXiv 0705.2244
Shakura NI (1973) Disk model of gas accretion on a relativistic star in a close binary system. Sov Astron 16:756
Shakura NI, Sunyaev RA (1973) Black holes in binary systems. Observational appearance. Astron Astrophys 24:337–355
Shakura NI, Sunyaev RA (1976) A theory of the instability of disk accretion on to black holes and the variability of binary X-ray sources, galactic nuclei and quasars. Mon Not R Astron Soc 175:613–632
Shakura NI, Sunyaev RA, Zilitinkevich SS (1978) On the turbulent energy transport in accretion discs. Astron Astrophys 62:179–187

Shapiro SL, Teukolsky SA (1983) Black holes, white dwarfs, and neutron stars: The physics of compact objects. Research supported by the National Science Foundation. Wiley-Interscience, New York, 663 pp

Shaviv G, Wehrse R (1986) The vertical temperature stratification and corona formation of accretion disc atmospheres. Astron Astrophys 159:L5–L7

Shibazaki N, Hōshi R (1975) Structure and stability of accretion-disk around a black-hole. Prog Theor Phys 54:706–718

Smak J (1984) Accretion in cataclysmic binaries. IV - Accretion disks in dwarf novae. Acta Astron 34:161–189

Sneddon IN (1951) Fourier transforms. International series in pure and applied mathematics. McGraw-Hill. http://books.google.ru/books?id=HRAJAQAAIAAJ

Sobolev VV (1969) Course in theoretical astrophysics, 1, vol. F-531. NASA, nasa technical translation 1

Speith R, Riffert H, Ruder H (1995) The photon transfer function for accretion disks around a Kerr black hole. Comput Phys Commun 88:109–120. https://doi.org/10.1016/0010-4655(95)00067-P

Suleimanov VF (1992) Modeling the accretion disks and spectra of cataclysmic variables - Part One - V603-AQUILAE. Sov Astron Lett 18:104–+

Suleimanov VF, Lipunova GV, Shakura NI (2007) The thickness of accretion α-disks: theory and observations. Astron Rep 51:549–562. https://doi.org/10.1134/S1063772907070049

Suleimanov VF, Lipunova GV, Shakura NI (2008) Modeling of non-stationary accretion disks in X-ray novae A 0620-00 and GRS 1124-68 during outburst. Astron Astrophys 491:267–277. https://doi.org/10.1051/0004-6361:200810155. ArXiv 0805.1001

Syunyaev RA, Shakura NI (1977) Disk reservoirs in binary systems and prospects for observing them. Sov Astron Lett 3:138–141

Tanaka T (2011) Exact time-dependent solutions for the thin accretion disc equation: boundary conditions at finite radius. Mon Not R Astron Soc 410:1007–1017. https://doi.org/10.1111/j.1365-2966.2010.17496.x. ArXiv 1007.4474

Tayler RJ (1980) Vertical energy transport in optically thick steady accretion discs. Mon Not R Astron Soc 191:135–150

Thorne KS, Price RH, MacDonald DA (1986) Black holes: the membrane paradigm. Yale University Press, New Haven

Tout CA, Pringle JE (1992) Accretion disc viscosity - a simple model for a magnetic dynamo. Mon Not R Astron Soc 259:604–612

Velikhov EP (1959) Stability of an ideally conducting liquid flowing between cylinders rotating in a magnetic field. Sov J Exp Theor Phys 9:995–998

Watson G (1944) A treatise on the theory of Bessel functions. Cambridge University Press. http://books.google.ru/books?id=WNoIAQAAIAAJ

Weizsäcker CFV (1948) Die Rotation kosmischer Gasmassen. Zeitschrift Naturforschung Teil A 3:524

Wood KS, Titarchuk L, Ray PS, Wolff MT, Lovellette MN, Bandyopadhyay RM (2001) Disk diffusion propagation model for the outburst of XTE J1118+480. Astrophys J 563:246–254. https://doi.org/10.1086/323768. ArXiv astro-ph/0108189

Zaitsev V, Polyanin A (2012) Handbook of exact solutions for ordinary differential equations. Taylor & Francis. http://books.google.ru/books?id=JjPDfRwOmAIC

Zdziarski AA, Kawabata R, Mineshige S (2009) Viscous propagation of mass flow variability in accretion discs. Mon Not R Astron Soc 399:1633–1640. https://doi.org/10.1111/j.1365-2966.2009.15386.x. ArXiv 0902.4530

Zeldovich YB (1981) On the friction of fluids between rotating cylinders. R Soc Lond Proc Ser 374:299–312. https://doi.org/10.1098/rspa.1981.0024

Zeldovich YB, Kompaneets AS (1950) Sbornik posvyashchennyy 70-leityu A. F. Ioffe (in: Collection of papers celebrating the seventieth birthday of A. F. Ioffe). AN SSSR, Moscow, in Russian

Zeldovich YB, Raizer YP (1967) Physics of shock waves and high-temperature hydrodynamic phenomena. Dover, New York
Zel'dovich YB, Shakura NI (1969) X-ray emission accompanying the accretion of gas by a neutron star. Sov Astron 13:175